SKEW CONFIGURATIONS OF LINES IN REAL DEL PEZZO SURFACES

A THESIS SUBMITTED TO
THE GRADUATE SCHOOL OF NATURAL AND APPLIED SCIENCES
OF
MIDDLE EAST TECHNICAL UNIVERSITY

BY

REMZİYE ARZU ZABUN

IN PARTIAL FULFILLMENT OF THE REQUIREMENTS
FOR
THE DEGREE OF DOCTOR OF PHILOSOPHY
IN
MATHEMATICS

SEPTEMBER 2014

Approval of the thesis:

SKEW CONFIGURATIONS OF LINES IN REAL DEL PEZZO SURFACES

submitted by **REMZİYE ARZU ZABUN** in partial fulfillment of the requirements for the degree of **Doctor of Philosophy in Mathematics Department, Middle East Technical University** by,

Prof. Dr. Canan Özgen
Dean, Graduate School of **Natural and Applied Sciences** _______________

Prof. Dr. Mustafa Korkmaz
Head of Department, **Mathematics** _______________

Prof. Dr. Sergey Finashin
Supervisor, **Mathematics Department, METU** _______________

Examining Committee Members:

Prof. Dr. Turgut Önder
Mathematics Department, METU _______________

Prof. Dr. Sergey Finashin
Mathematics Department, METU _______________

Assoc. Prof. Dr. Alexander Degtyarev
Mathematics Department, Bilkent University _______________

Prof. Dr. Yıldıray Ozan
Mathematics Department, METU _______________

Assoc. Prof. Dr. Mohan Lal Bhupal
Mathematics Department, METU _______________

Date: _______________

I hereby declare that all information in this document has been obtained and presented in accordance with academic rules and ethical conduct. I also declare that, as required by these rules and conduct, I have fully cited and referenced all material and results that are not original to this work.

Name, Last Name: REMZİYE ARZU ZABUN

Signature :

ABSTRACT

SKEW CONFIGURATIONS OF LINES IN REAL DEL PEZZO SURFACES

ZABUN, REMZİYE ARZU
Ph.D., Department of Mathematics
Supervisor : Prof. Dr. Sergey Finashin

September 2014, 135 pages

By blowing up $\mathbb{P}^2$ at $n \leq 8$ points which form a generic configuration, we obtain a del Pezzo surface X of degree $d = 9 - n$ with a configuration of n skew lines that are exceptional curves over the blown-up points. The anticanonical linear system maps X to $\mathbb{P}^d$, and the images of these exceptional curves form a configuration of n lines in $\mathbb{P}^d$. The subject of our research is the correspondence between the configurations of n generic points in $\mathbb{R}P^2$ and the configurations of n lines in $\mathbb{R}P^{9-n}$. This correspondence is nontrivial in the cases $n = 6$ and $n = 7$.

In the case of $n = 6$, there exist precisely 4 deformation classes of generic planar configurations of 6 points, and we describe the corresponding 4 deformation classes of configurations of 6 skew lines in $\mathbb{R}P^3$. In the case $n = 7$, there exist precisely 14 deformation classes of generic planar configurations of 7 points and we describe the corresponding 14 deformation classes of configurations of 7 bitangents to a quartic curve (such configurations are known in the literature as Aronhold sets).

Keywords: Planar configurations, real del Pezzo surfaces, configurations of lines on del Pezzo surfaces of degree 2 and 3, anti-canonical models

ÖZ

REEL DEL PEZZO UZAYLARI ÜZERİNDEKİ AYRIK DOĞRULARIN KONFİGÜRASYONLARI

ZABUN, REMZİYE ARZU
Doktora, Matematik Bölümü
Tez Yöneticisi : Prof. Dr. Sergey Finashin

Eylül 2014 , 135 sayfa

Projektif uzaydan $n \leq 8$ tane nokta alalım, öyle ki, bu noktaların kümesi dejenere olmamış bir konfigürasyon oluştursun. O zaman, bu noktaların patlatılması ile derecesi $d = 9 - n$ olan bir del Pezzo uzayı X elde edilir. Patlatılan her nokta bu uzay üzerinde bir doğruya karşılık gelir. Dolayısıyla, bu uzay üzerinde, ikişer ikişer birbirleri ile kesişmeyen n tane doğru içeren bir konfigürasyon elde edilir. X uzayının doğal olmayan bölenin lineer sistemi, X'ten $\mathbb{P}^{9-n}$'ye bir fonksiyon tanımlar. X üzerindeki bu özel n tane doğrunun bu fonksiyon altındaki görüntüsü d boyutlu projektif uzayda n tane doğrudur. Bu fonksiyonu reel zeminde ele alacağız, diğer bir deyişle, bu fonksiyon altında, reel projektif uzayda, n noktadan oluşan konfigürasyonların, d boyutlu reel projektif uzayda ki belirli n doğrudan oluşan konfigürasyonlara nasıl bağlı olduğunu inceleyeceğiz. Bu bağlantı $n = 6$ ve $n = 7$ durumlarında aşikar değildir.

Eğer $n = 6$ ise, dejenere olmamış 6 noktadan oluşan konfigürasyonların 4 tane deformasyon sınıfının var olduğunu gösterildi. Yukarıda belirtilen bağlantı incelenerek, 3 boyutlu reel projektif uzayda 6 doğrudan oluşan konfigürasyonların 4 farklı deformasyon sınıfı tasvir edildi. Eğer $n = 7$ ise, dejenere olmamış 7 noktadan oluşan konfigürasyonların 14 tane deformasyon sınıfının var olduğunu gösterildi ve böyle 7 noktadan oluşan konfigürasyonlar ile 2 boyutlu reel projektif uzayda iki noktada dördüncü dereceden eğriye teğet olan, 7 doğrudan oluşan konfigürasyonlar tasvir edildi (bu konfigürasyonlar literatürde Aronhold kümeleri olarak adlandırılır).

Anahtar Kelimeler: Düzlemsel konfigürasyonlar, reel del Pezzo uzayları, doğru konfigürasyonları, doğal olmayan bağlantı

To My Parents and to my best friend Sevgi Aydın

ACKNOWLEDGMENTS

I would like to thank my supervisor Professor Sergey Finashin for all his helps.

I thank the members of my thesis committee, Professors Alexander Degtyarev and Turgut Önder for inspiring remarks and moral support.

I would like to thank Professor Viatcheslav Kharlamov for inviting me to the Advanced Mathematics Research Institute (IRMA) in Strasbourg and for his valuable remark. I am grateful to the Mathematical Sciences Research Institute (MSRI) in Berkeley, to the Max Planck Institute for Mathematics (MPIM) in Bonn and to Bernoulli Center (EPFL) in Lausanne for their invitations and hospitality.

This work is also supported by TÜBİTAK-BİDEB PhD scholarship (2211).

TABLE OF CONTENTS

ABSTRACT v

ÖZ vi

ACKNOWLEDGMENTS ix

TABLE OF CONTENTS x

LIST OF TABLES xiv

LIST OF FIGURES xv

CHAPTERS

1 INTRODUCTION 1

1.1 The subject 1

1.2 The structure of the thesis and the main results 3

1.3 Conventions 4

2 CONFIGURATIONS OF POINTS IN $\mathbb{R}P^2$ 7

2.1 Linearly nondegenerate configurations 7

2.2 Affine realizations 9

2.3 Quadratically nondegenerate n-configurations for $n \leq 6$ . . . 18

2.4 Hexagonal augmentations of pentagonal configurations . . . 21

2.5 Quadratically nondegenerate 7-configurations: the statement of the main theorem 23

2.6 Heptagonal 7-configurations: dominancy indices 24

2.7 Heptagonal augmentations of hexagonal 6-configurations . . 28

2.8 The Q-deformation classes of heptagonal 7-configurations . . 31

2.9 Hexagonal 7-configurations 33

2.10 Pentagonal 7-configurations 41

2.11 Proof of Theorem 2.5.1 45

3 CONFIGURATIONS OF POINTS IN $\mathbb{R}P^1 \times \mathbb{R}P^1$ 47

3.1 Permutation diagrams 47

3.2 Bi-ordering 50

3.3 Linearly nondegenerate n-configurations on $\mathbb{R}P^1 \times \mathbb{R}P^1$ . . . 51

3.4 The real bidegree of real algebraic curves in $\mathbb{R}P^1 \times \mathbb{R}P^1$ . . . 54

3.5 Curves of bidegree $(1, 1)$ 55

3.6 Quadratically nondegenerate n-configurations on $\mathbb{R}P^1 \times \mathbb{R}P^1$ 55

3.7 Curves of bidegree $(1, 2)$ and bidegree $(2, 1)$ 56

3.8 A further project on Q-deformation classification of configurations of 5 points in $\mathbb{R}P^1 \times \mathbb{R}P^1$ 57

4 CREMONA TRANSFORMATION OF PLANE CONFIGURATIONS OF POINTS 61

4.1 Cremona transformations of 6-configurations 61

4.2 Cremona transformations of 7-configurations 65

5 CONFIGURATIONS OF LINES IN $\mathbb{R}P^3$ 67

5.1 Triple linking numbers 67

5.2 Derived configuration of lines and derivative trees 68

5.3 Deformations and coarse deformations of configurations of skew lines 70

5.4 Join configurations of $n \leq 6$ of skew lines 70

5.5 Classification of 6-configurations of lines 71

5.6 Derivative trees of join configurations 71

6 CONFIGURATIONS OF LINES ON REAL CUBIC SURFACES . . 77

6.1 Real lines on real cubic surfaces 77

6.2 The four types of real double sixes 79

6.3 Elliptic and hyperbolic lines on a blow-up model 81

7 REAL DEL PEZZO SURFACES 85

7.1 The marked real del Pezzo M-surfaces of degree 2 and 3 . . . 85

7.2 Combinatorial anti-canonical correspondence 85

7.3 Marking on anti-canonical models 87

8 ANTI-CANONICAL CORRESPONDENCE FOR REAL CUBIC SURFACES 91

8.1 CAC-correspondence for cubic surfaces 91

9 ANTI-CANONICAL MODELS OF REAL DEL PEZZO SURFACES OF DEGREE 2 99

9.1 CAC-correspondence for del Pezzo surfaces of degree 2 . . . 99

9.2 Lifting the bitangents to del Pezzo surfaces 101

9.3 Azygetic triples and Aronhold sets 103

10 ANTI-CANONICAL CORRESPONDENCE FOR REAL DEL PEZZO SURFACES OF DEGREE 2 107

10.1 Complementary 7-configurations 107

10.2 The 14 real Aronhold sets representing the 14 Q-deformation classes of planar 7-configurations 108

10.3 Proof of Theorem 10.2.1 113

11 APPLICATIONS: COMBINATORIAL PENCILS OF REAL RATIONAL CUBIC CURVES PASSING THROUGH SIX POINTS 115

11.1 Partitioned orders 115

11.2 Combinatorial pencils of rational cubics passing through 6 points 116

APPENDICES

A THE MODIFICATIONS OF ELLIPTIC AND HYPERBOLIC LINES UNDER CREMONA TRASFORMATIONS 121

A.1 Elliptic and hyperbolic lines corresponding to a 6-configuration in QC^6 121

B ANTI-CANONICAL CORRESPONDENCE BETWEEN CONFIGURATIONS IN QC^7 AND ARONHOLD SETS 125

B.1 Aronhold sets obtained by Cremona transformations based at triple of bitangent lines of the heptagonal Aronhold set 125

REFERENCES 133

CURRICULUM VITAE 135

LIST OF TABLES

TABLES

Table 2.1 The spectra and derivative codes for LC^7-deformation classes 12

Table 2.2 The six D_5-orbits representing the four L-deformation classes in LC^6 15

Table 2.3 The ten D_6-orbits representing the eight L-deformation classes of 7-configurations with $R_1 > 0$ in LC^7 16

Table 2.4 The seven D_5-orbits representing the four Q-deformation classes in QC^6 23

Table 2.5 The positions of $p_i, p_j \in \mathcal{P} \in QC^7_{(7,0,0,0)}$ with respect to the conic $Q_{i,j}$. 30

Table 2.6 The dominancy indices of points of a 7-configuration $\mathcal{P} \in QC^7_{(7,0,0,0)}$ 31

Table 2.7 The seven D_3-orbits on $\Lambda_Q(\mathcal{P})$ for $\mathcal{P} \in QC^6_1$ representing the seven Q-deformation classes in QC^7 39

Table 2.8 The position of p_i, p_j of a hexagonal configuration $\mathcal{P} \in QC^7$ with respect to the conics $Q_{i,j}$ 39

Table 2.9 The five D_3-orbits on $\Lambda_Q(\mathcal{P})$ for $\mathcal{P} \in QC^6_1$ representing three Q-deformation classes in QC^7 44

Table 8.1 The derivative codes of 6-configurations of skew lines in $\mathbb{R}P^3$ with total linking code $(10, 10)$. 96

Table 8.2 The derivative codes of 6-configurations of skew lines in $\mathbb{R}P^3$ with total linking code $(12, 8)$. 96

Table 8.3 The derivative codes of 6-configurations of skew lines in $\mathbb{R}P^3$ with the total linking code $(8, 12)$. 96

Table 8.4 Total triple number and the derivative linking code of $\mathcal{L}_{\mathcal{P}}$ for any $\mathcal{P} \in QC^6$. 97

LIST OF FIGURES

FIGURES

Figure 2.1 One L-deformation class in LC^5 and four L-deformation classes in LC^6. 8

Figure 2.2 The eleven L-deformation classes in LC^7: 1 of the 11 deformation classes is heptagonal, 5 ones are hexagonal, and the remaining six are pentagonal. 10

Figure 2.3 A cyclically numerated configuration $\mathcal{P} \in LC^n$ 11

Figure 2.4 The six L-polygons representing the six D_5-orbits for pentagonal configurations in LC^5 13

Figure 2.5 The L-polygons representing the ten D_6-orbits for hexagonal configurations in LC^6 14

Figure 2.6 The eleven configurations of seven lines from the eleven deformation classes in LL^7 17

Figure 2.7 The region F^t for the dominant point $p_0^t \in \mathcal{P}^t \in QC_1^6$, $t \in [\frac{1}{2}, 1]$. . . . 20

Figure 2.8 The four Q-deformation classes in QC^6 21

Figure 2.9 The seven Q-regions associated to any pentagonal configuration in QC^5. 22

Figure 2.10 The dominancy indices of two neighbors of a non-extremal point of a heptagonal configuration in $QC^7_{(7,0,0,0)}$ 25

Figure 2.11 The arc of an ellipse $Q_{1,j}$ sketched on the figure contains an extra intersection point. 27

Figure 2.12 The Q-regions associated to a hexagonal configuration in QC_1^6 . . . 29

Figure 2.13 Three types of decorations of edges in $\Gamma(\mathcal{P})$ for $\mathcal{P} \in QC^7_{(7,0,0,0)}$. . . . 32

Figure 2.14 The e-decorated adjacency graphs of $\mathcal{P} \in QC^7_{(7,0,0,0)}$ 33

Figure 2.15 The six D_6-orbits on internal Q-regions associated to a hexagonal configuration in QC^6. 34

Figure 2.16 The seven D_3-orbits on internal Q-regions associated to a hexagonal configuration in QC^7. 35

Figure 2.17 A pair of hexagonal 6-configurations with the same diagonal. . . . 37

Figure 2.18 37

Figure 2.19 The seven Q-deformation classes for hexagonal configurations in QC^7 40

Figure 2.20 The five D_3-orbits on Q-regions associated to a pentagonal configurations in QC^7 with $R_1 = 1$ 43

Figure 2.21 The three Q-deformation classes for pentagonal 7-configurations with $R_1 = 1$ in QC^7. 44

Figure 3.1 The permutation and coarse permutation class diagrams for $\sigma \in S_4$ 48

Figure 3.2 The permutation and coarse permutation class diagrams for $\sigma \in S_5$ 48

Figure 3.3 The permutation diagram $Z_{(3142)}$ 49

Figure 3.4 58

Figure 3.5 The eight cyclic orders coming from $A^1_{\mathcal{P}}$ with $deg_{\mathbb{R}}(A^1_{\mathcal{P}}) = (1, 0)$ . . 58

Figure 4.1 The images of a hexagonal configuration in QC^6_1 under quadratic Cremona transformations 62

Figure 4.2 The images of a heptagonal configuration in QC^7 under quadratic Cremona transformations 66

Figure 5.1 The configurations of 4 and 5 skew lines in $\mathbb{R}P^3$, together with their derivative trees of degree 2. 69

Figure 5.2 Two 6-configurations of skew lines in $\mathbb{R}P^3$, M and L. 72

Figure 5.3 The derivative tree of (1234) 73

Figure 5.4 The derivative tree of (123654) 74

Figure 5.5 The L-deformation classes of n-configurations of skew lines, $n \le 5$. 74

Figure 5.6 The 19 L-deformation classes of 6-configurations of skew lines in $\mathbb{R}P^3$. 75

Figure 6.1 A double six $(\mathcal{L}, \mathcal{L}')$, where $\mathcal{L} = \{L_1, \ldots, L_6\}$, $\mathcal{L}' = \{L'_1, \ldots, L'_6\}$ in $\mathbb{R}P^3$. By the black points on these lines, we show the chosen 19 points to construct a cubic surface. 79

Figure 6.2 The labeled vertices represent double sixes corresponding to QC_i^6, $i = 1, 2, 3, 6$ 80

Figure 6.3 The points $q_t, q_t^{'}$ of the intersection $\Omega_t \cap L$, $t \in [0, 1]$, where L, Ω_t are as introduced above. 81

Figure 6.4 The finite loop O and infinite loop $\mathcal{J}$ of a nodal cubic A. 82

Figure 6.5 The degeneration of a nodal cubic with empty loop to a cubic with a solitary node 83

Figure 6.6 The examples of hyperbolic and elliptic lines on $X_{\mathcal{P}}$ for $\mathcal{P} \in QC_1^6$, which are the proper images of lines L_{ij}, L_{jk}, and L_{il}. 84

Figure 6.7 The examples of hyperbolic and elliptic lines on $X_{\mathcal{P}}$ for $\mathcal{P} \in QC_1^6$, which are the proper images of conics Q_i, Q_j. 84

Figure 7.1 The commutative diagram. 86

Figure 7.2 The anti-canonical and the combinatorial anti-canonical correspondences 87

Figure 7.3 The correspondence between 6-configurations and their complementary 6-configurations in QC^6 88

Figure 7.4 The modifications of the exceptional curves E_i, $\widetilde{Q_i} \subset X_{\mathcal{P}}$, $i \in \{1, \ldots, 6\}$, under $Cr_{123} \circ Cr_{456} \circ Cr_{123}$. 89

Figure 7.5 The modification of a 6-configuration from each of the classes QC_i^6, $i = 1, 2, 3, 6$, under $Cr_{123} \circ Cr_{456} \circ Cr_{123}$. 89

Figure 8.1 The CAC-correspondence between Q-deformation classes in QC^6 and L-deformation classes of 6-configuration of skew lines in $\mathbb{R}P^3$. 91

Figure 8.2 The join configuration $J(\sigma)$ for some $\sigma \in S_4$. 92

Figure 8.3 Triple linking numbers of lines of $\mathcal{L}_{\mathcal{P}}$ for $\mathcal{P} \in QC_6^6$ 93

Figure 8.4 Triple linking numbers of lines of $\mathcal{L}_{\mathcal{P}}$ for $\mathcal{P} \in QC_2^6$ 95

Figure 8.5 Triple linking numbers of lines of $\mathcal{L}_{\mathcal{P}}$ for $\mathcal{P} \in QC_3^6$ 95

Figure 9.1 A decoration of the preimage of a bitangent line. 103

Figure 9.2 Two decorated bitangents to a quartic C whose corresponding liftings in X_C are skew lines. 103

Figure 9.3 An example of the syzygetic and azygetic triples 104

Figure 9.4 The k-gon whose edges are formed by the bitangent lines $L^1, \ldots, L^k$. 105

Figure 10.1 The correspondence between 7-configurations and their complementary 7-configurations in QC^7 107

Figure 10.2 The CAC-correspondence between the Aronhold set and the heptagonal configuration in QC^7 109

Figure 10.3 110

Figure 10.4 The image $\pi(f_C^{-1}(L))$ of the line L as shown in Figure 10.3. 111

Figure 10.5 The seven nodal cubics A_i based at $\mathcal{P} \in QC^7$ 112

Figure 10.6 The arc of an ellipse $Q_{1,j}$ sketched on the figure contains two extra intersection points. 112

Figure 10.7 The arc of an ellipse $Q_{1,2}$ sketched on the figure contains two extra intersection points. 113

Figure 11.1 The combinatorial pencil CP_1°. This figure shows the case, where $\mathcal{P} \in QC_1^6$, and $p_1 \in \mathcal{P}$ is subdominant. 117

Figure 11.2 The combinatorial pencils associated to a hexagonal configuration in QC^6 118

Figure 11.3 The associated graphs for the seven combinatorial pencils for all 6-configurations of QC^6. 119

Figure 11.4 The number of points on the finite loops of five combinatorial $(\mathcal{P}, p)$-based nodal cubics 120

Figure A.1 121

Figure B.1 125

CHAPTER 1

INTRODUCTION

1.1 The subject

A (non-singular) *del Pezzo surface* is defined as a smooth projective surface whose anti-canonical divisor $-K$ is ample. The degree d of a del Pezzo surface is the self intersection index of $-K$. Such degree is known to take values between 1 and 9.

It is well known that a complex del Pezzo surface of degree d is isomorphic either to $\mathbb{P}^1 \times \mathbb{P}^1$, or to $\mathbb{P}^2$ blown up at $n = 9 - d$ points in general position where $1 \leq d \leq 9$ (see Yu. I. Manin [Man]). In the latter case, such an isomorphism is called *a blow-up model* of a del Pezzo surface.

Let $p_1, \ldots, p_n$ be n points of $\mathbb{P}^2$ in general position where $n \leq 8$ and let X be the del Pezzo surface which is the blow-up of $\mathbb{P}^2$ at these n points. The *anti-canonical map* $\psi : X \to \mathbb{P}^d$ defined by the linear system $|-K|$ of the space X is an embedding for $d > 2$, and by the *anti-canonical model* of X we mean isomorphism $X \to \psi(X) \subset \mathbb{P}^d$. In the case $d = 2$, ψ is known to be a double covering over $\mathbb{P}^2$ ramified along a nonsingular quartic, and by the anti-canonical model of X we mean an isomorphism with the total space of this covering. If we denote by $E_1, \ldots, E_n$ the exceptional curves in X for the blow-up model, and if we let $H \subset X$ denote a proper transform of a general line in $\mathbb{P}^2$, then we can write $-K = 3H - \sum_{i=1}^{n} E_i$. The images $\psi(E_1), \ldots, \psi(E_n)$ form a configuration of lines in $\mathbb{P}^d$, and for $n < 7$ these lines are skew. We call the correspondence between the quadratically nondegenerate planar n-configurations and the associated n-configuration of lines as mentioned above the *anti-canonical correspondence*. We study this correspondence in the real setting, that is, how the configuration of lines $\psi(E_1), \ldots, \psi(E_n)$ in $\mathbb{R}P^d$ depends on the configuration of the n blown up points in $\mathbb{R}P^2$. For $n = 8$, the question in such a form is trivial since $\mathbb{R}P^d = \mathbb{R}P^1$. The case $n \leq 5$ is also not interesting, since there is only one deformation class of n-configurations. So, we restrict ourselves to studying the cases $n = 6, 7$.

In the case $n = 6$, the del Pezzo surface X has degree 3 and its anti-canonical model X is presented as a cubic surface in $\mathbb{P}^3$. In the real setting, if we blow up six real point in $\mathbb{R}P^2$, this cubic is an M-surface (see Section 1.3 for the definition), that is its real locus is homeomorphic to the connected sum of 7 copies of $\mathbb{R}P^2$. Our task in this case is to describe the correspondence between the deformation classes of quadratically nondegenerate configurations of six points in $\mathbb{R}P^2$ and the deformation classes of configurations of six skew lines in $\mathbb{R}P^3$. In particular, we give a criterion for a configuration of six skew lines to lie on a cubic surface.

The deformation classification of configurations of ≤ 5 skew lines in $\mathbb{R}P^3$ is due to Oleg Viro [VV]. F. Mazurovskii classified 6-configurations of skew lines in $\mathbb{R}P^3$ and showed that there are 11 coarse deformation classes of such configurations in $\mathbb{R}P^3$ in [M1] (by a coarse deformation equivalence relation, we mean a composition of a usual deformation with the projective equivalence). These results motivated us to give an answer to the following question: which ones among these 12 coarse deformation classes can be realized on a real nonsingular cubic M-surface? We show that there are 4 such coarse deformation classes corresponding to the four deformation classes of 6-configurations (see Figure 8.1).

In the case of $n = 7$, the del Pezzo surface X has degree 2, and its anti-canonical model presents X as a double covering $X \to \mathbb{P}^2$ ramified along a nonsingular quartic curve. The surface X contains 56 exceptional curves (called *lines* on X) which are projected into 28 lines in $\mathbb{P}^2$ bitangent to the ramification quartic. In the real setting, if the seven blown up points are real, the quartic is a real curve whose real locus $\mathbb{R}C$ has 4 connected components (see Theorem 2.3.5). For real M-quartics, all the 28 bitangents are real and each bitangent is covered by two real exceptional curves in X. We show that there are 14 deformation classes of quadratically nondegenerate 7-configurations of points in $\mathbb{R}P^2$ (see Theorem 2.5.1), and that the anti-canonical correspondence associates each quadratically nondegenerate planar 7-configuration with a real Aronhold set that is a configuration of 7 bitangents whose lifting are pairwise disjoint on the del Pezzo surface (see Theorem 10.2.1). We describe the deformations of real Aronhold sets resulting from deformations of real 7-configurations of points, and find the 14 deformation classes of real Aronhold sets corresponding to the 14 deformation classes of 7-configurations of points in Appendix B.

1.2 The structure of the thesis and the main results

In Chapter 2, we classify quadratically nondegenerate configurations of 6 and 7 points in $\mathbb{R}P^2$ up to deformations. Namely, we show in Theorem 2.3.5 that there are 4 deformation classes of quadratically nondegenerate 6-configurations and in Theorem 2.5.1 that there are 14 deformation classes of quadratically nondegenerate 7-configurations in $\mathbb{R}P^2$.

In Chapter 3, we study, similarly, the linearly and quadratically nondegenerate configurations of 5 points in a nonsingular real quadric M-surface (that is a one-sheeted hyperboloid in $\mathbb{R}P^3$) up to deformations . In particular, we showed that there are precisely four deformation classes of linearly nondegenerate 5-configurations of points in $\mathbb{R}P^1 \times \mathbb{R}P^1$ (see Theorem 3.3.4). The deformation classification of quadratically nondegenerate 5-configurations of points in $\mathbb{R}P^1 \times \mathbb{R}P^1$ will be investigated in a further study. In addition, we introduce a notion of the coarse permutation classes, and define their invariant, namely, coarse permutation class diagram, characterizing these classes. Coarse permutation classes appear in three different situations: in Chapter 3 to characterize the configurations on a hyperboloid, in Chapter 5 to characterize the join configurations and in Chapter 8 to characterize the skew configurations of 6 lines on a real cubic surface.

In Chapter 4, we show how the deformation classes of quadratically nondegenerate planar 6-configurations and 7-configurations in convex position change under Cremona transformations based on some triples of points in these configurations.

Chapter 5 is a preparatory one in which we recall some results and fix some terminology and notation (that will be used in Chapter 6) related to configurations of skew lines in $\mathbb{R}P^3$.

In Chapter 6 we associate a deformation class of quadratically nondegenerate planar 6-configurations to a given double six on a nonsingular real cubic M-surface, so we determine the types of all 36 double sixes on any nonsingular real cubic M-surface. We determine ellipticity and hyperbolicity (in the sense of B. Segre [Se]) of lines in the anti-canonical model of a del Pezzo surface of degree 3 (i.e., a real cubic surface) depending on the 6-configuration of blown up points (see Appendix A).

In Chapter 7 we give definitions and preliminary information on marked real del Pezzo surfaces of degree 2 and 3, and on the combinatorial anti-canonical correspondence between the deformation classes of configurations of 6 (respectively 7) points and the deformation classes of configurations of 6 (respectively 7) lines in the corresponding anti-canonical model.

In Chapter 8 we study the anti-canonical correspondence between 6-configurations and marked real cubic M-surfaces. We describe the 4 deformation classes of configurations of 6 skew lines in $\mathbb{R}P^3$ for each of the 4 deformation classes of quadratically nondegenerate planar 6-configurations (see Theorem 8.1.1).

In Chapter 9 we introduce and discuss the combinatorial anti-canonical correspondence for del Pezzo surfaces of degree 2. In addition, we introduce the notions of Aronhold sets and azygetic triples, and relate them to our studies of configurations.

In Chapter 10, we study the anti-canonical model of del Pezzo surface of degree 2, namely, we describe the 14 Aronhold sets of 7 bitangents of lines for each of the 14 deformation classes of quadratically nondegenerate planar 7-configurations (see Theorem 10.2.1).

In Chapter 11, we present a certain application of the results of Chapters 6 and 7, which was partially motivated by the work of S. Fiedler-Le Touzé [T2] and [T3].

1.3 Conventions

- For some $n \in \mathbb{Z}^+$, $\{1, \ldots, \hat{i}, \ldots, n\}$ means that i is omitted.

- We denote the complex projective n-space by $\mathbb{P}^n$, and the real projective n-space by $\mathbb{R}P^n$.

- A complex variety (surface, curve, etc.) X is called *real* if X is equipped with a real structure (i.e. an anti-holomorphic involution), and we denote by $\mathbb{R}X$ the fixed point set of the real structure. A real variety X is called an *M-variety* (M-surface, M-curves, etc.) if X satisfies the equality $b_*(X, \mathbb{Z}_2) = b_*(\mathbb{R}X, \mathbb{Z}_2)$ where $b_*(X, \mathbb{Z}_2)$ and $b_*(\mathbb{R}X, \mathbb{Z}_2)$ are the sums of all Betti numbers of X and $\mathbb{R}X$ with coefficients in $\mathbb{Z}_2$, respectively.

- Given $I_n = \{1, 2, \ldots, n\}$ the symmetric group S_n of degree n consists of all bijections $\sigma : I_n \to I_n$. Such a bijection is called a permutation of I_n and we denote a permutation sending $k \in I_n$ to $i_k \in I_n$ either by

$$\sigma = \begin{pmatrix} 1 & 2 & \cdots & n-1 & n \\ i_1 & i_2 & \cdots & i_{n-1} & i_n \end{pmatrix} \in S_n,$$

  or (abuse of the notation if it does not lead to a confusion) by $(i_1\ i_2\ \ldots\ i_{n-1}\ i_n)$. We multiply permutations σ_1, σ_2 by composing them as maps, i.e., $\sigma_1\sigma_2(i) = \sigma_1(\sigma_2(i))$.

CHAPTER 2

CONFIGURATIONS OF POINTS IN $\mathbb{R}P^2$

The aim of this chapter is to classify up to deformation quadratically nondegenerate 6 and 7-configurations. We need it to classify real marked del Pezzo M-surfaces of degrees 3 and 2, that is, del Pezzo surfaces of degrees 3 and 2 with a maximal family of real skew lines up to deformation. The classification of linearly non-degenerate deformation classes of 6 and 7-configurations is given in [F], so we shall determine how many quadratically non-degenerate deformation classes of 6 and 7-configurations exist for each of the linearly non-degenerate deformation classes of 6 and 7-configurations.

2.1 Linearly nondegenerate configurations

By an *n-configuration* in a projective surface X, we mean a set of n distinct points of X. We denote the space of all n-configurations in X by $C^n(X)$. When $X = \mathbb{P}^2$, an n-configuration in $C^n(X)$ is called *planar*.

A planar n-configuration is called *linearly nondegenerate* if no three points among the n points is collinear. Let $L\Delta^n$ denote the space of *linearly degenerate* planar n-configurations (i.e., those for which three of the n points lie on a line). Then, the space of linearly nondegenerate planar n-configurations is $C^n(\mathbb{R}P^2) \smallsetminus L\Delta^n$, and it is denoted by LC^n. It is easy to see that the space LC^n is a Zariski open subset of the algebraic variety $C^n(\mathbb{R}P^2)$.

An *L-deformation* between two n-configurations $\mathcal{P}^0, \mathcal{P}^1 \in LC^n$ is a path $\{\mathcal{P}^t\}_{t\in[0,1]}$

between $\mathcal{P}^0$ and $\mathcal{P}^1$ in the space LC^n. Given two n-configurations $\mathcal{P}^0, \mathcal{P}^1 \in LC^n$, we say they are *L-deformation equivalent*, or of the same *L-deformation type* if there exists an *L-deformation* between $\mathcal{P}^0$ and $\mathcal{P}^1$. The relation between n-configurations in LC^n of being L-deformation equivalent is an equivalence relation since two n-configurations $\mathcal{P}^0, \mathcal{P}^1 \in LC^n$ are L-deformation equivalent if they are in the same connected components of the space LC^n.

It is easily seen that the space LC^n is connected for $n \leq 5$. The space LC^6 has 4 connected components (see ([F])).

Following ([F]), for a given n-configuration $\mathcal{P} \in LC^n$ for $n \geq 4$, we construct a graph embedded in $\mathbb{R}P^2$ whose vertices are the points of the configuration $\mathcal{P}$ and whose edges are linear segments (i.e., each of which is just one of the two segments connecting each pair of points in $\mathcal{P}$), which are not crossed by any of the lines determined by each pair of the remaining $n-2$ points of $\mathcal{P}$. We call this graph the *adjacency graph* and denote it by $\Gamma(\mathcal{P})$.

The adjacency graphs representing all the L-deformation classes of configurations of n points in LC^n for $n = 5, 6$ are shown in Figure 2.1.

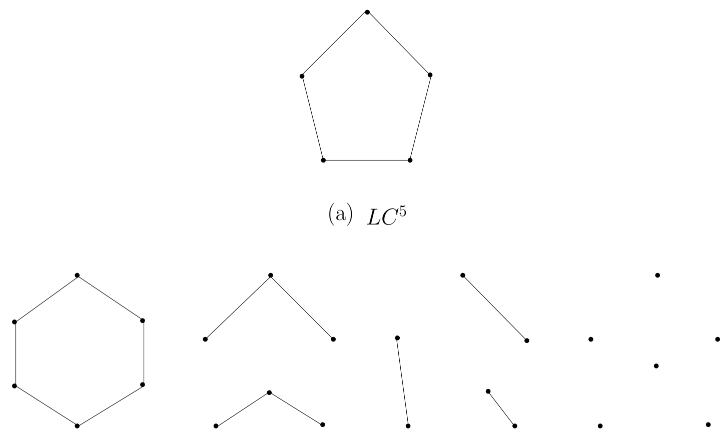

(a) LC^5

(b) LC^6_1 (c) LC^6_2 (d) LC^6_3 (e) LC^6_6

Figure 2.1: One L-deformation class in LC^5 and four L-deformation classes in LC^6.

The number of connected components (i.e, $1, 2, 3$, and 6) of adjacency graphs are complete invariants for the L-deformation classes of 6-configurations in LC^6, that is to say, this number distinguishes the four L-deformation classes. These

L-deformation classes are denoted LC^6_i, $i = 1, 2, 3, 6$ (see Figure 2.1).

Removing a point $p_i \in \mathcal{P}$ from a 7-configuration $\mathcal{P} = \{p_1, \dots, p_7\} \in LC^7$ we obtain a 6-configuration denoted by $\mathcal{P}_{\hat{i}}$ that we call a *derivative of* $\mathcal{P}$. We label the point p_i with an index $d \in \{1, 2, 3, 6\}$ if $\mathcal{P}_{\hat{i}} \in LC^6_d$, and obtain in this way a function $d_{\mathcal{P}} : \mathcal{P} \to \{1, 2, 3, 6\}$. It is trivial to see that $d_{\mathcal{P}}$ takes the same values on the connected components of the adjacency graph $\Gamma(\mathcal{P})$. The induced map $d_{\Gamma(\mathcal{P})}$ on the set of these connected components is called the *d-decoration* of the adjacency graph $\Gamma(\mathcal{P})$. The adjacency graph $\Gamma(\mathcal{P})$ together with the d-decoration, i.e., the pair $(\Gamma(\mathcal{P}), d_{\Gamma(\mathcal{P})})$ is called the *d-decorated adjacency graph* of $\mathcal{P}$.

Lemma 2.1.1. *If $\mathcal{P} \in LC^7$ and $p_i, p_j \in \mathcal{P}$ belong to the same connected component of the adjacency graph $\Gamma(\mathcal{P})$, then the configurations $\mathcal{P}_{\hat{i}}, \mathcal{P}_{\hat{j}} \in LC^6$ are L-deformation equivalent.* □

Theorem 2.1.2. [F]. *The space LC^7 has 11 connected components (i.e., 11 L-deformation classes).* □

Adjacency graphs (cf.[F]) of 7-configurations in LC^7 representing these eleven L-deformation classes are shown in Figure 2.2. In this figure we provide these adjacency graphs with the d-decorations.

For $d_{\mathcal{P}} : \mathcal{P} \to \{1, 2, 3, 6\}$, with $\mathcal{P} \in LC^7$, and a value $k \in \{1, 2, 3, 6\}$, we define R_k to be the number of points in $d^{-1}_{\mathcal{P}}(k)$. Given a 7-configuration $\mathcal{P} \in LC^7$, we call the quadruple $R(\mathcal{P}) = (R_1, R_2, R_3, R_6)$ the *derivative code* of $\mathcal{P}$. The derivative codes are complete invariants for the L-deformation classes of 7-configurations in LC^7, i.e., they distinguish the 11 L-deformation classes LC^7_σ where σ denote derivative codes of such configurations (see Figure 2.2).

2.2 Affine realizations

An *affine realization* $\mathcal{P}_L$ of a configuration $\mathcal{P} \in C^n(\mathbb{R}P^2)$ is the restriction of $\mathcal{P}$ to an affine plane $\mathbb{R}^2 = \mathbb{R}P^2 \setminus L$ where L is a line in $\mathbb{R}P^2 \setminus \mathcal{P}$.

Given an n-configuration $\mathcal{P} \in LC^n$ and a line $L \subset \mathbb{R}P^2 \setminus \mathcal{P}$, let $F_{\mathcal{P},L}$ denote the

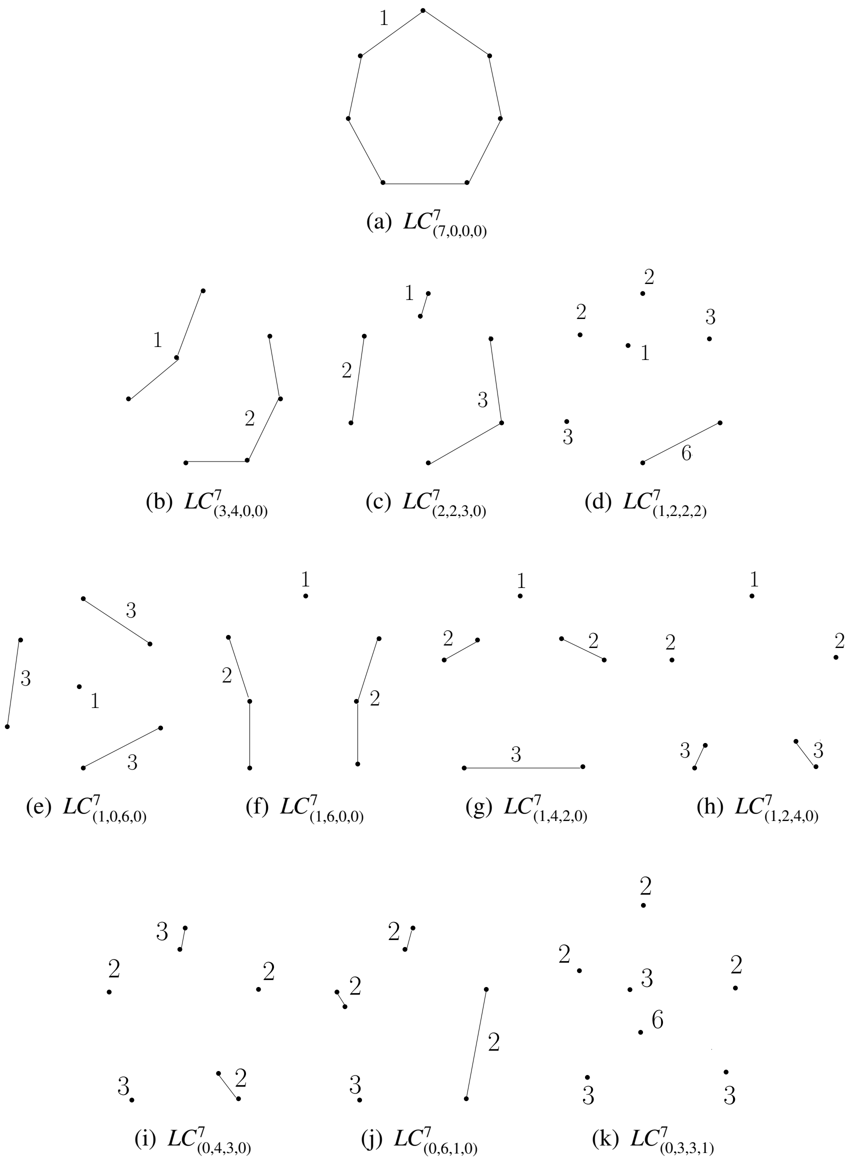

Figure 2.2: The eleven L-deformation classes in LC^7: 1 of the 11 deformation classes is heptagonal, 5 ones are hexagonal, and the remaining six are pentagonal.

convex hull of $\mathcal{P}$ in the affine plane $\mathbb{R}P^2 \setminus L$, and $|F_{\mathcal{P},L}|$ be the number of sides of $F_{\mathcal{P},L}$.

We say that an n-configuration $\mathcal{P} \in LC^n$ is *m-gonal* if m is the maximum of $|F_{\mathcal{P},L}|$ for all lines $L \subset \mathbb{R}P^2 \setminus \mathcal{P}$. In particular, an n-configuration $\mathcal{P}$ is *n-gonal* if there exists an affine realization of $\mathcal{P}$ such that all of its points form a convex n-gon $F_{\mathcal{P},L}$ for some line L in the affine plane $\mathbb{R}P^2 \setminus \mathcal{P}$. In fact as it follows form Lemma 2.2.1 that in the case $n \geq 5$, the n-gon $F_{\mathcal{P},L}$ is unique, i.e., it does not depend on the choice of a line L such that points of $\mathcal{P}$ form an n-gon in $\mathbb{R}P^2 \setminus L$. Hence, for an n-gonal configuration $\mathcal{P} \in LC^n$, we use the notation $F_{\mathcal{P}}$ to denote the convex hull of $\mathcal{P}$ and call it the *principle n-gon*.

The numeration of the points $p_1, \ldots, p_n$ of an n-gonal configuration $\mathcal{P} \in LC^n$, $n \geq 5$, is called *cyclic* if the vertices, i.e., $p_1, \ldots, p_n$ of the principle n-gon go in a cyclic order (clockwise or counterclockwise if we fix some orientation of the plane) as in Figure 2.3. We say that points of an n-gonal configuration $\mathcal{P}$ are *cyclically numerated* if they are denoted by $p_1, p_2, \ldots, p_n$ following a cyclic order of the vertices on the principle n-gon $F_{\mathcal{P}}$.

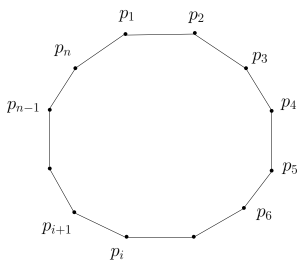

Figure 2.3: A cyclically numerated configuration $\mathcal{P} \in LC^n$

Passing to the dual plane $\widehat{\mathbb{R}P^2}$, an n-configuration $\mathcal{P} \in LC^n$ is represented by a configuration $\widehat{\mathcal{P}}$ of n lines such that no three lines of $\widehat{\mathcal{P}}$ are concurrent. We call the configuration $\widehat{\mathcal{P}}$ the *dual configuration* of $\mathcal{P}$. We can easily see that $\mathcal{P}$ is m-gonal if m is the maximal number of sides of the subdivision polygons associated to $\mathcal{P}$, i.e., the connected components of $\widehat{\mathbb{R}P^2} \setminus \widehat{\mathcal{P}}$. It is trivial to observe that $5 \leq |F_{\mathcal{P},L}| \leq n$ for all lines $L \subset \mathbb{R}P^2 \setminus \mathcal{P}$ if $\mathcal{P} \in LC^n$ for $n \geq 5$. For instance, for $n = 7$, the configuration $\mathcal{P}$ can be heptagonal, hexagonal or pentagonal.

For a given configuration $\mathcal{P} \in LC^7$, by the *spectrum* we mean the 5-tuple $S(\mathcal{P}) = (S_3, \ldots, S_7)$ where S_τ denote the number of τ-gons in the subdivision polygons associated to $\mathcal{P}$. The spectra and derivative codes representing the eleven L-deformation classes of 7-configurations in LC^7 are shown in Table 2.1.

Lemma 2.2.1. *An affine realization $\mathcal{P}_L$ of $\mathcal{P} \in C^n(\mathbb{R}P^2)$ for some line L is m-gonal if and only if $\widehat{L} \in \widehat{\mathbb{R}P^2}$ lies inside a subdivision m-gon of $\widehat{\mathcal{P}}$.* □

Corollary 2.2.2. *A heptagonal configuration in LC^7 has a unique affine realization up to L-deformation. Similarly, a hexagonal configuration in LC^7 has a unique affine realization.*

Table 2.1: The spectra and derivative codes for LC^7-deformation classes

$\mathcal{P} \in LC^7$	(R_1, R_2, R_3, R_6)	$(S_3, S_4, S_5, S_6, S_7)$
Heptagonal	$(7, 0, 0, 0)$	$(7, 14, 0, 0, 1)$
Hexagonal	$(3, 4, 0, 0)$	$(7, 13, 1, 1, 0)$
	$(2, 2, 3, 0)$	$(8, 11, 2, 1, 0)$
	$(1, 2, 2, 2)$	$(11, 5, 5, 1, 0)$
	$(1, 0, 6, 0)$	$(9, 9, 3, 1, 0)$
Pentagonal with $R_1 = 1$	$(1, 6, 0, 0)$	$(7, 12, 3, 0, 0)$
	$(1, 4, 2, 0)$	$(8, 10, 4, 0, 0)$
	$(1, 2, 4, 0)$	$(9, 8, 5, 0, 0)$
Pentagonal with $R_1 = 0$	$(0, 4, 3, 0)$	$(8, 10, 4, 0, 0)$
	$(0, 6, 1, 0)$	$(7, 12, 3, 0, 0)$
	$(0, 3, 3, 1)$	$(10, 6, 6, 0, 0)$

Proof. The result follows from Lemma 2.2.1 since $S_7 = 1$ for all heptagonal configurations $\mathcal{P} \in QC^7$, and $S_6 = 1$ for all hexagonal configurations $\mathcal{P} \in QC^7$ (see Table 2.1). □

For a given n-configuration $\mathcal{P} \in LC^n$ where $n \geq 3$, the lines passing through all pairs of points of $\mathcal{P}$ divide $\mathbb{R}P^2$ into a finite number of polygons which are called *L-polygons* associated to $\mathcal{P}$. We denoted by $\Lambda_L(\mathcal{P})$ the set of all L-polygons associated to $\mathcal{P}$. The conics passing through all 5-tuples of points of $\mathcal{P}$ divide these L-polygons into regions called *Q-regions* associated to $\mathcal{P}$. We denoted by $\Lambda_Q(\mathcal{P})$ the set of all Q-regions associated to $\mathcal{P}$. If $\mathcal{P}$ is an n-gonal configuration in LC^n, then an L-polygon in $\Lambda_L(\mathcal{P})$ and a Q-region in $\Lambda_Q(\mathcal{P})$ are called *internal* if they are inside the principle n-gon $F_{\mathcal{P}}$ of $\mathcal{P}$. Otherwise, they are called *external*.

The dihedral group D_n acts on the vertices of the principle n-gon $F_{\mathcal{P}}$ for a given n-gonal configuration $\mathcal{P} \in LC^n$ where $n \geq 3$. When $n = 5, 6$, this action induces actions on $\Lambda_L(\mathcal{P})$ and $\Lambda_Q(\mathcal{P})$. We denote by $[M]^L_n$ and $[N]^Q_n$ the orbits of an L-polygon M and a Q-region N with respect to this action, respectively.

Example 2.2.3. As $\mathcal{P}$, we can take, for example, a pentagonal configuration $\mathcal{P}$ in LC^5, and choose the cyclic numeration of points $p_1, \dots, p_5 \in \mathcal{P}$. It is easily confirmed that the quotient space of the D_5-action on $\Lambda_L(\mathcal{P})$ has six distinct D_5-orbits. We shall denote by A, B, C, D, E, and F the L-polygons representing the six D_5-orbits (see Figure 2.4).

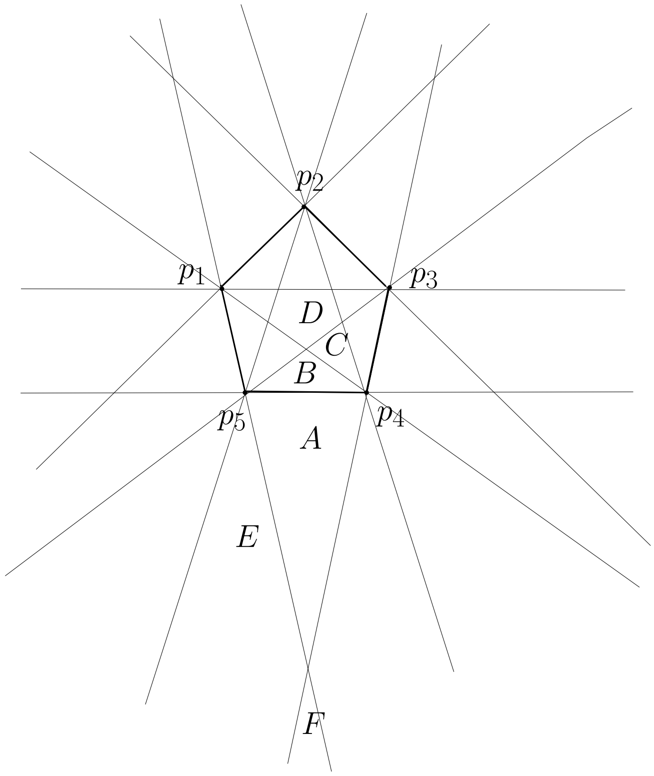

Figure 2.4: Three internal L-polygons B, C, D and three external L-polygons A, E, F representing the six D_5-orbits for pentagonal configurations in LC^5.

Example 2.2.4. As $\mathcal{P}$, let us take a hexagonal configuration $\mathcal{P}$ in LC^6, and choose the cyclic numeration of points $p_1, \ldots, p_6 \in \mathcal{P}$. It is easily confirmed that the quotient space of the D_6-action on $\Lambda_L(\mathcal{P})$ has ten distinct D_6-orbits. We shall denote by A, B, C, D, E, F, G, H, I, and J the L-polygons representing the ten D_6-orbits (see Figure 2.5). In particular, the L-polygon E is called the *central triangle*.

Let $\{\mathcal{P}^t\}_{t\in[0,1]}$ be an L-deformation between two n-configurations $\mathcal{P}^0, \mathcal{P}^1 \in LC^n$, and M^0 be one of the L-polygons associated to $\mathcal{P}^0$. We denote by $\{M^t\}_{t\in[0,1]}$ the continuous family of L-polygons associated to $\mathcal{P}^t$ for any $t \in [0, 1]$ such that these L-polygons are obtained from M^0 by the L-deformation $\{\mathcal{P}^t\}_{t\in[0,1]}$. We call this family the *L-deformation of* M^0. Take a point $p^0 \in \mathbb{R}P^2$ lying inside M^0, and let us denote by $\{p^t\}_{t\in[0,1]}$ the continuous family of points lying inside the

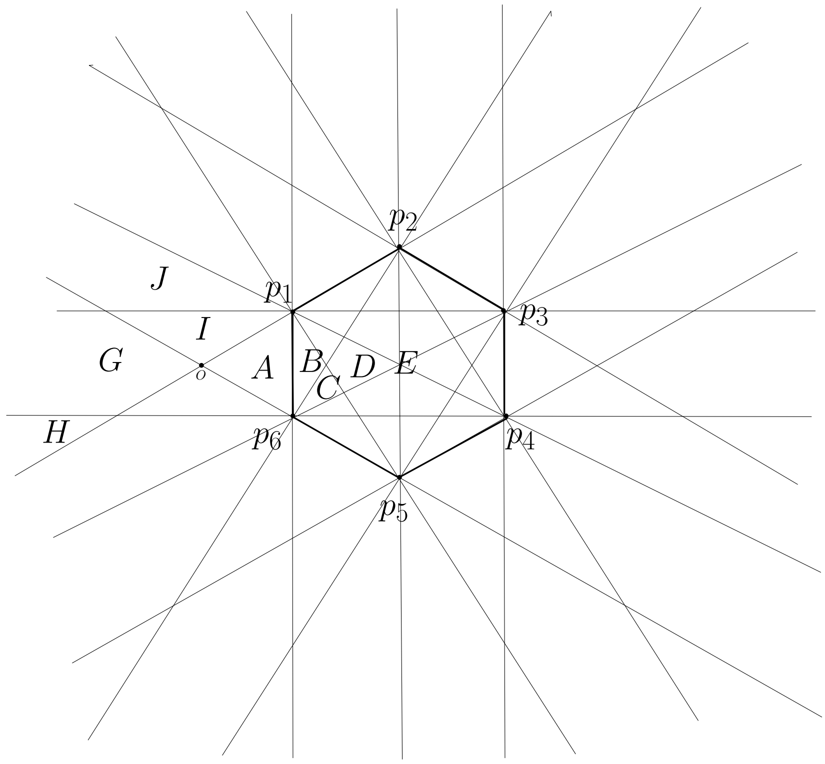

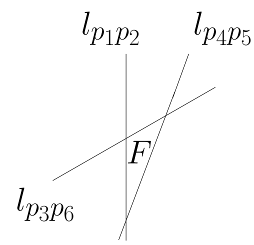

Figure 2.5: Four internal L-polygons B, C, D, E and six external L-polygons A, F, G, H, I, J representing the ten D_6-orbits for hexagonal configurations in LC^6.

L-polygons M^t, $t \in [0,1]$, in the L-deformation of M^0 such that these points are obtained from p^0 by the L-deformation $\{\mathcal{P}^t\}_{t\in[0,1]}$. We call this family the *L-deformation of p^0*.

We say that an L-polygon M associated to an n-configuration in LC^n *collapses* during an L-deformation in LC^n if the L-deformation of M contains an L-polygon which consists of just one point.

Given an n-gonal configuration $\mathcal{P} \in LC^n$, any permutation of D_n which acts on the vertices of the principle n-gon $F_{\mathcal{P}}$ can be realized as an L-deformation of

$\mathcal{P}$. During this L-deformation, some of the L-polygons in $\Lambda_L(\mathcal{P})$ can collapse. If such an L-polygon M does not collapse we can extend the L-deformation to an L-deformation of a configuration $\mathcal{P}' = \mathcal{P} \cup \{p\} \in LC^{n+1}$ obtained from $\mathcal{P}$ by adding one additional point $p \in \mathbb{R}P^2$ to M. We say that the configuration $\mathcal{P}'$ is obtained by the *augmentation of* $\mathcal{P}$ *inside* M.

Finashin gave the following statement about when an L-deformation $\{\mathcal{P}^t\}_{t\in I}$ between two n-gonal configurations $\mathcal{P}^0, \mathcal{P}^1 \in LC^n$ can be extended to an L-deformation between some augmented configurations in LC^{n+1}.

Proposition 2.2.5. ([F]) *Let* $\{\mathcal{P}^t\}_{t\in[0,1]}$ *be an L-deformation between two n-gonal configurations* $\mathcal{P}^0$, $\mathcal{P}^1 \in LC^n$, *and* M^0 *be one of the L-polygon associated to the configuration* $\mathcal{P}^0$ *and* $\{p^t_{n+1}\}_{t\in[0,1]}$ *be the L-deformation of a point* $p^0_{n+1} \in \mathbb{R}P^2$ *lying inside* M^0. *Assume, in addition, that the polygon* M^0 *does not collapse during the L-deformation* $\{\mathcal{P}^t\}_{t\in[0,1]}$. *Then* $\{\mathcal{P}^t \cup \{p^t_{n+1}\}\}_{t\in[0,1]}$ *is an L-deformation between the augmented configurations* $\mathcal{P}^0 \cup \{p^0_{n+1}\}$ *and* $\mathcal{P}^1 \cup \{p^1_{n+1}\}$. □

The next statement is immediate consequence of Proposition 2.2.5.

Corollary 2.2.6. *Let* $\mathcal{P}$ *be an n-gonal configuration in* LC^n, *and* $p_i \in \mathbb{R}P^2$ *lies in an L-polygon* F_i *associated to* $\mathcal{P}$ *where* $i \in \{0, 1\}$. *Assume, in addition, that* M_0, M_1 *belong to the same orbit of the* D_n*-action on* $\Lambda_L(\mathcal{P})$. *Then the augmented configuration* $\mathcal{P} \cup \{p_0\} \in LC^{n+1}$ *is L-deformation equivalent to the augmented configuration* $\mathcal{P} \cup \{p_1\} \in LC^{n+1}$. □

Table 2.2: The six D_5-orbits in $\Lambda_L(\mathcal{P})$ for any pentagonal 5-configuration $\mathcal{P} \in LC^5$, representing the four L-deformation classes in LC^6.

D_5-orbits	LC^6_σ
$[A]^L_5$	LC^6_1
$[B]^L_5$, $[E]^L_5$	LC^6_2
$[C]^L_5$, $[F]^L_5$	LC^6_3
$[D]^L_5$	LC^6_6

By Proposition 2.2.5 and Corollary 2.2.6, we obtain Tables 2.2 and 2.3. These tables show the correspondence between D_n-orbits in $\Lambda_L(\mathcal{P})/D_n$ where $\mathcal{P} \in LC^n$,

$n = 5, 6$, is an n-gonal configuration and L-deformation classes of augmented configurations in LC^{n+1} (i.e., each of them is obtained from $\mathcal{P}$ by adding just one point of $\mathbb{R}P^2$ to one of the L-polygons in $\Lambda_L(\mathcal{P})$).

Table 2.3: The ten D_6-orbits in $\Lambda_L(\mathcal{P})$ for any hexagonal 5-configuration $\mathcal{P} \in LC^6$, representing the eight L-deformation classes of 7-configurations with $R_1 > 0$ in LC^7.

D_6-orbits	LC^7_σ
$[A]^L_6$	$LC^7_{(7,0,0,0)}$
$[B]^L_6$, $[I]^L_6$	$LC^7_{(3,4,0,0)}$
$[C]^L_6$, $[J]^L_6$	$LC^7_{(2,2,3,0)}$
$[D]^L_6$	$LC^7_{(1,2,2,2)}$
$[E]^L_6$	$LC^7_{(1,0,6,0)}$
$[F]^L_6$	$LC^7_{(1,6,0,0)}$
$[G]^L_6$	$LC^7_{(1,4,2,0)}$
$[H]^L_6$	$LC^7_{(1,2,4,0)}$

We say that a configuration (i.e., a set) of seven lines in $\mathbb{R}P^2$ is *linearly nondegenerate* if no three lines of the configuration is concurrent. Let us denote by LL^7 the space of linearly nondegenerate configurations of seven lines in $\mathbb{R}P^2$.

Two configurations of seven lines, $\mathcal{L}^0, \mathcal{L}^1 \in LL^7$, are said to be *L-deformation equivalent* if they can be joined by a continuous family of configurations of seven lines, $\mathcal{L}^t \subset \mathbb{R}P^2$, $t \in [0, 1]$, and *coarse L-deformation equivalent* if one of these configurations is L-deformation equivalent to the projective transformation of the other. In other words, $\mathcal{L}^0, \mathcal{L}^1$ belong to the same connected component of $LL^7/PGL(3, \mathbb{R})$ if they are coarse L-deformation equivalent. In fact, since $PGL(3, \mathbb{R})$ is connected there is no difference between L-deformation classes and coarse deformation classes in $LL^7/PGL(3, \mathbb{R})$.

Since the space LL^7 is the polar dual of the space LC^7 of linearly nondegenerate 7-configurations LL^7 has 11 connected components (i.e., 11 L-deformation classes). The linearly nondegenerate configurations of 7 lines in LL^7 representing these deformation classes are as shown in Figure 2.6. It will be convenient to use the notations LL^7_σ for these deformation classes where σ are the derivative codes for configurations in LC^7.

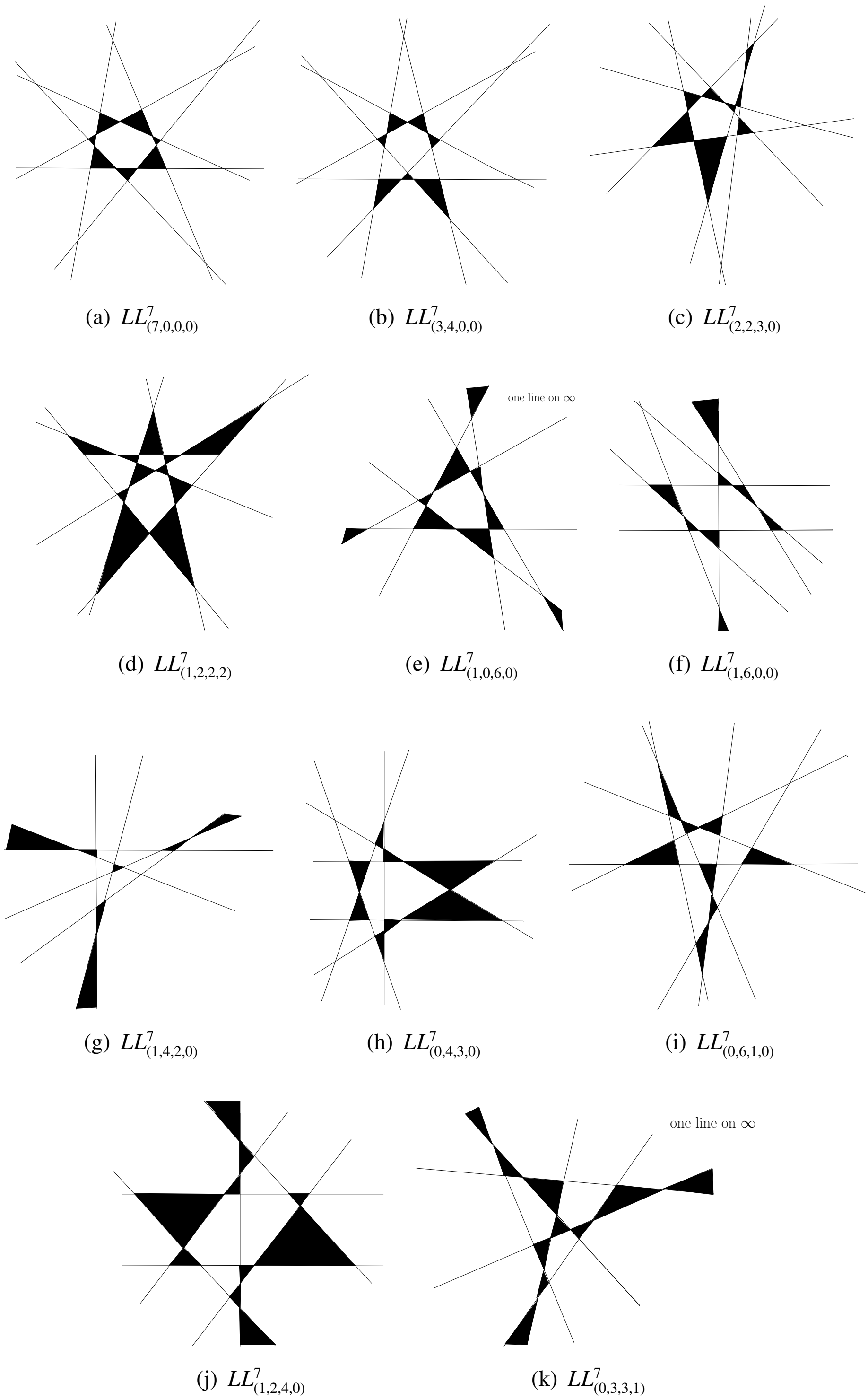

Figure 2.6: The eleven configurations of seven lines from the eleven deformation classes in LL^7. We shaded only triangles in their subdivision polygons.

2.3 Quadratically nondegenerate n-configurations for $n \leq 6$

An n-configuration in $C^n(\mathbb{R}P^2)$ is called *quadratically nondegenerate* if no tree points lies on a line and no six points of the configuration lies on a conic. Let $Q\Delta^n$ denote the space of *quadratically degenerate* planar n-configurations (i.e., those for which three of the n points lie on a line or six of the n points lie on a conic). Then, the space of quadratically nondegenerate n-configurations is $QC^n = C^n(\mathbb{R}P^2) \setminus (L\Delta^n \cup Q\Delta^n) = LC^n \setminus Q\Delta^n$, where $L\Delta^n$ is the space of linearly degenerate planar n-configurations. Note that the space QC^n is a Zariski open subset of LC^n.

A *Q-deformation* between two configurations $\mathcal{P}, \mathcal{P}' \in QC^n$ is a path $\{\mathcal{P}^t\}_{t\in[0,1]}$ between $\mathcal{P}^0$ and $\mathcal{P}^1$ in the space QC^n. We say that two n-configurations $\mathcal{P}^0, \mathcal{P}^1 \in QC^n$ are *Q-deformation equivalent*, or of the same *Q-deformation class* if there exist an *Q-deformation* between $\mathcal{P}$ and $\mathcal{P}'$. Notice that the relation between configurations in QC^n of being Q-deformation equivalent is an equivalence relation since two n-configurations $\mathcal{P}, \mathcal{P}' \in QC^n$ are *Q-deformation equivalent* if they are in the same connected components of the space QC^n.

It follows immediately from the definition that $Q\Delta^n = \emptyset$ for $n < 6$, so we obtain the following.

Proposition 2.3.1. *If $n \leq 5$, then $LC^n = QC^n$.* □

Recall that the space LC^6 has four L-deformation classes LC^6_σ, where $\sigma \in \{1, 2, 3, 6\}$ (see Figure 2.1(b)-(e)). For each $\sigma \in \{1, 2, 3, 6\}$, let QC^6_σ denote the complement $LC^6_\sigma \setminus Q\Delta^6$.

Lemma 2.3.2. *Assume that $\sigma \in \{2, 3, 6\}$. Then, $LC^6_\sigma = QC^6_\sigma$. From this, it follows that QC^6_σ is connected for any $\sigma \in \{2, 3, 6\}$.*

Proof. Any 6-configurations in $Q\Delta^6$ have to be in a convex position since their points lie on some conics, thus $Q\Delta^6 \subset LC^6_1$, and so, $LC^6_\sigma \cap Q\Delta^6$ is empty for $\sigma \in \{2, 3, 6\}$. □

For any n-configurations $\mathcal{P} \in QC^n$ for $n \geq 5$, let $S_\mathcal{P}$ denote the set of $\binom{n}{5}$ conics passing through all 5-tuples of points of $\mathcal{P}$.

Given an n-configuration $\mathcal{P} \in QC^n$, the complement of a conic $Q \in \mathcal{S}_{\mathcal{P}}$ in $\mathbb{R}P^2$ has two components, one of which is homeomorphic to a disk and the other is homeomorphic to Möbius band. The former is called the *interior* of the conic Q and the latter is called the *exterior* of the conic Q. Each of the remaining $n-5$ points of $\mathcal{P}$ lies in either the interior or the exterior of the conic Q. If a point $p \in \mathcal{P}$ lies in the interior of the conic Q, then it is called *subdominant* with respect to the conic Q. Otherwise, it is called *dominant* with respect to the conic Q. In particular, for $\mathcal{P} = \{p_1, \dots, p_6\} \in QC^6$, let Q_i, $i = 1, \dots, 6$, denote the unique conic passing through the five points $p_1, \dots, \widehat{p_i}, \dots, p_6$ of $\mathcal{P}$, where a hat over a point of $\mathcal{P}$ shows that the point is omitted.

Proposition 2.3.3. *Let $\mathcal{P}^0, \mathcal{P}^1 \in QC^6_1$ (i.e., hexagonal 6-configurations), and assume that p^i_0 is a dominant point of $\mathcal{P}^i$, where $i \in \{0, 1\}$. Then, there is a Q-deformation $\{\mathcal{P}^t\}_{t\in[0,1]}$ between $\mathcal{P}^0$ and $\mathcal{P}^1$ which takes p^0_0 to p^1_0.*

Proof. Let $p^i_1, p^i_2, p^i_3, p^i_4, p^i_5 \in \mathcal{P}^i$, $i = 0, 1$, denote the remaining five points of $\mathcal{P}^i$ different from p^i_0. We assume that the points of $\mathcal{P}^i$, $i = 0, 1$, are cyclically numerated as it is shown on Figure 2.3. Consider conics Q^i, $i \in \{0, 1\}$, passing through the five points of $\mathcal{P}^i$ other than p^i_0. There exists a real projective transformation $\phi : \mathbb{R}P^2 \to \mathbb{R}P^2$ sending Q^0 to Q^1. Let $\mathcal{P}^{\frac{1}{2}} = \{p^{\frac{1}{2}}_0, p^{\frac{1}{2}}_1, p^{\frac{1}{2}}_2, p^{\frac{1}{2}}_3, p^{\frac{1}{2}}_4, p^{\frac{1}{2}}_5\}$ denote the image $\phi(\mathcal{P}^0)$, and $p^{\frac{1}{2}}_0$ denote the image $\phi(p^0_0)$. Since any pair of 5-configuration whose points lie on the same conic can be obviously connected by a Q-deformation $\mathcal{P}^{\frac{1}{2}}_{\hat{0}} = \{p^{\frac{1}{2}}_1, \dots, p^{\frac{1}{2}}_5\}$ and $\mathcal{P}^1_{\hat{0}} = \{p^1_1, \dots, p^1_5\}$ are Q-deformation equivalent. Let $\mathcal{P}^t_{\hat{0}}$, $t \in [\frac{1}{2}, 1]$, denote a Q-deformation between $\mathcal{P}^{\frac{1}{2}}_{\hat{0}}$ and $\mathcal{P}^1_{\hat{0}}$. The points p^t_0 lie inside the shaded region F^t for $t \in [\frac{1}{2}, 1]$ shown in Figure 2.7. The region F^t is connected and does not contract to a point as t varies, so the deformation $\mathcal{P}^t_{\hat{0}}$, $t \in [\frac{1}{2}, 1]$, can be extended to a Q-deformation $\mathcal{P}^t$, $t \in [\frac{1}{2}, 1]$. The composition $\mathcal{P}^t \circ \phi$ is the required Q-deformation between $\mathcal{P}^0$ and $\mathcal{P}^1$ taking p^0 to p^1. $\square$

The next statement follows immediately from Proposition 2.3.3 and the fact that any 6-configuration $\mathcal{P} \in QC^6_1$ has a dominant point (in fact, exactly three

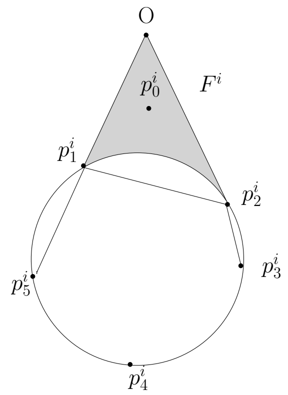

Figure 2.7: The region F^t for the dominant point $p_0^t \in \mathcal{P}^t \in QC_1^6$, $t \in [\frac{1}{2}, 1]$.

such points).

Proposition 2.3.4. *Any pair of* 6*-configurations in QC_1^6 are Q-deformation equivalent. That is, the space QC_1^6 is connected.* □

Proposition 2.3.4 shows that there is one and only one deformation class of hexagonal configurations in the space QC_1^6. Together with Proposition 2.3.2 it gives the next result.

Theorem 2.3.5. *Each of the four existing connected components LC_1^6, LC_2^6, LC_3^6 and LC_6^6 of the space LC^6 contains exactly one connected component $QC_\sigma^6 = LC_\sigma^6 \cap QC^6$ of QC^6, and so, the space QC^6 has four connected components QC_1^6, QC_2^6, QC_3^6 and QC_6^6 (i.e., four Q-deformation classes).* □

A *υ-decoration* of the adjacency graph $\Gamma(\mathcal{P})$ for a given configuration $\mathcal{P} \in QC^6$ is the map $\upsilon_{\mathcal{P}}$ from the set of vertices of $\Gamma(\mathcal{P})$, i.e $\mathcal{P}$, into the set $\{\bullet, \circ\}$ defined by $\upsilon_{\mathcal{P}}(p) = \bullet$ if the point $p \in \mathcal{P}$ is dominant with respect to the conic $Q_{\widehat{p}}$ passing through five points of $\mathcal{P}$ other than p and $\upsilon_{\mathcal{P}}(p) = \circ$ if the point $p \in \mathcal{P}$ is subdominant with respect to the conic $Q_{\widehat{p}}$. The pair $(\Gamma(\mathcal{P}), \upsilon_{\mathcal{P}})$ is called the *υ-decorated adjacency graph* of $\mathcal{P}$.

The υ-decorated adjacency graphs representing the four Q-deformation classes QC_1^6, QC_2^6, QC_3^6 and QC_6^6 in QC^6 are as shown in Figure 2.8.

In the hexagonal case, to show that the colors of vertices (i.e., white and black) are cyclically alternating (see Figure 2.8(a)), we can make the following simple

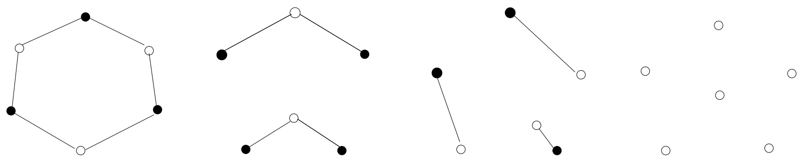

(a) QC^6_1 (b) QC^6_2 (c) QC^6_3 (d) QC^6_6

Figure 2.8: The four Q-deformation classes in QC^6. We color in black the dominant points of configurations and in white the subdominant ones.

observation.

Lemma 2.3.6. *Let $\mathcal{P} \in QC^6$, and assume that two points of $\mathcal{P}$ are joined by an edge in $\Gamma_L(\mathcal{P})$. Then, if one of the two points is subdominant then the other one is dominant and vice versa.*

Proof. It follows from analysis of the pencil of conics passing through the 4 remaining points since this pencil cannot contain a singular conic intersecting an edge of the adjacency graph. □

2.4 Hexagonal augmentations of pentagonal configurations

Given a pentagonal configuration $\mathcal{P} \in QC^5$, the conic passing through five points of $\mathcal{P}$ divides the L-polygon A (see Figure 2.4) into two Q-regions which are denoted by A_1 and A_2 as shown in Figure 2.9, but it does not intersect with other L-polygons lying in D_5-orbits other than $[A]^L_5$. Thus, the quotient space of the D_5-action on $\Lambda_Q(\mathcal{P})$ has seven distinct D_5-orbits. The Q-regions A_1, A_2 B, C, D, E, and F representing the seven D_5-orbits are as shown in Figure 2.9. Note that $[X]^L_5 = [X]^Q_5$ for any $X = B, C, D, E, F$, and $[A]^L_5 = [A_1]^Q_5 \cup [A_2]^Q_5$.

Let $\{\mathcal{P}^t\}_{t\in[0,1]}$ be a Q-deformation between two n-configurations $\mathcal{P}^0, \mathcal{P}^1 \in QC^n$, and M^0 is one of the Q-regions associated to $\mathcal{P}^0$. We denote by $\{M^t\}_{t\in[0,1]}$ the continuous family of Q-regions associated to $\mathcal{P}^t$ for any $t \in [0, 1]$ such that these Q-regions are obtained from M^0 by this deformation. We call $\{M^t\}_{t\in[0,1]}$ the *Q-deformation of M^0*. Take a point $p^0 \in \mathbb{R}P^2$ lying inside M^0, and let us denote by $\{p^t\}_{t\in[0,1]}$ the continuous family of points lying inside Q-regions M^t,

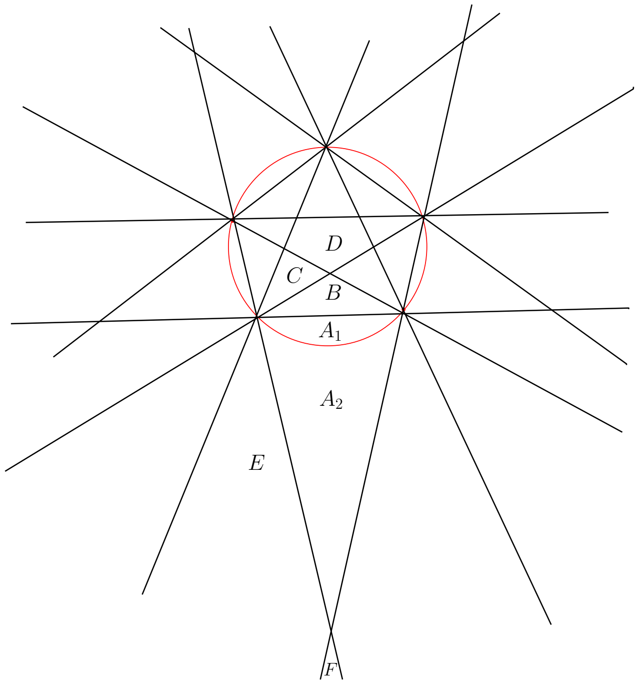

Figure 2.9: The seven Q-regions associated to any pentagonal configuration in QC^5.

$t \in [0, 1]$, in the Q-deformation of M^0 such that these points are obtained from p^0 by the Q-deformation $\{\mathcal{P}^t\}_{t\in[0,1]}$. We call $\{p^t\}_{t\in[0,1]}$ the *Q-deformation of* p^0.

As in the case of L-polygons, we say that a Q-region M^0 associated to an n-configuration $\mathcal{P} \in QC^n$ *collapses* during a Q-deformation of $\mathcal{P}$ if $\{M^t\}_{t\in[0,1]}$ contains a Q-region which consists of just one point. The following statement is immediately obtained.

Lemma 2.4.1. *None of the seven Q-regions A_1, A_2 B, C ,D, E, F associated to any pentagonal configuration $\mathcal{P} \in QC^5$ can collapse during any Q-deformation.*

□

Lemma 2.4.2. *Let $\mathcal{P} \in QC^5$ be a pentagonal configuration, and assume that M_i, $i = 1, 2$, is a Q-region associated to $\mathcal{P}$ lying in the orbit ${}^{Q}[A_i]_5$ and that we take a point $p_i \in \mathbb{R}P^2$ from the interior of M_i. Then, $\mathcal{P} \cup \{p_1\}$ is Q-deformation equivalent to $\mathcal{P} \cup \{p_2\}$.*

Proof. By Proposition 2.3.4 and Lemma 2.4.1, $\mathcal{P} \cup \{p_1\}$ is Q-deformation equivalent to $\mathcal{P} \cup \{p_2\}$ since $\mathcal{P} \cup \{p_1\}$ and $\mathcal{P} \cup \{p_2\}$ are heptagonal configurations in QC^6. □

Recall from Section 2.2 that there are six D_5-orbits (those of representing to L-deformation classes in LC^6 as shown in Figure 2.2) of the D_5-action on $\Lambda_L(\mathcal{P})$ for any pentagonal configuration $\mathcal{P} \in LC^5$, and from Proposition 2.3.1 in Section 2.3 that $LC^5 = QC^5$. The seven orbits in $\Lambda_Q(\mathcal{P})/D_5$ representing the four Q-deformation classes QC^6_1, QC^6_2, QC^6_3 and QC^6_6 in QC^6 are as shown in Table 2.4.

Table 2.4: The seven D_5-orbits in $\Lambda_Q(\mathcal{P})$ for any $\mathcal{P} \in QC^5$ representing the four Q-deformation classes in QC^6.

D_5-orbits	QC^6_σ
$[A_1]^Q_5$, $[A_2]^Q_5$	QC^6_1
$[B]^Q_5$, $[E]^Q_5$	QC^6_2
$[C]^Q_5$, $[F]^Q_5$	QC^6_3
$[D]^Q_5$	QC^6_6

2.5 Quadratically nondegenerate 7-configurations: the statement of the main theorem

Our aim in the rest of Chapter 2 is to show that the space QC^7 contains 14 connected components.

Theorem 2.5.1. (see Section 2.11.) *The space QC^7 has 14 connected components. More precisely, $LC^7_{(2,2,3,0)}$ contains three connected components of QC^7, $LC^7_{(3,4,0,0)}$ contains two connected components of QC^7 and each of the remaining 9 connected components of LC^7 contains one connected component of QC^7.*

For the proof of the theorem, the first step is to analyze Q-deformation classes of heptagonal, hexagonal and pentagonal configurations in QC^7 separately. Then, we show (see Section 2.11) that the theorem is obtained as a consequence of the results in Proposition 2.8.2, Proposition 2.9.1, Proposition 2.10.1(a) and (b).

2.6 Heptagonal 7-configurations: dominancy indices

Combinatorial classification of heptagonal configurations (taking into account the mutual position of their points with respect to the 21 conics passing through all 5-tuples of them) were obtained by S. Fiedler-Le Touzé [T2]. Here we refine this result and obtain a classification of such configurations up to Q-deformations. In turn, we give an alternative proof of the combinatorial result of Fiedler-Le Touzé.

Recall from Section 2.3 that we denote by $\mathcal{S}_{\mathcal{P}}$ the set of conics passing through all 5-tuples of points of $\mathcal{P} \in QC^n$ for any $n \geq 5$. Let $\mathcal{P} \in QC^7$ and $p \in \mathcal{P}$. We define a map $\mathrm{ind}_p : \mathcal{S}_{\mathcal{P}_{\widehat{p}}} \to \{0, 1\}$ by $\mathrm{ind}_p(Q) = 1$ if p is dominant with respect to Q or $\mathrm{ind}_p(Q) = 0$ if p is subdominant with respect to Q for any $Q \in \mathcal{S}_{\mathcal{P}_{\widehat{p}}}$ where $\mathcal{P}_{\widehat{p}} = \mathcal{P} \setminus \{p\}$ and $Q \in \mathcal{S}_{\mathcal{P}_{\widehat{p}}}$. For a conic $Q \in \mathcal{S}_{\mathcal{P}_{\widehat{p}}}$, the image $\mathrm{ind}_p(Q)$ is called the *index* of the point p with respect to Q. We define the *dominancy index* $d(p)$ of a point $p \in \mathcal{P}$ to be the number of conics in $S_{\mathcal{P}_{\widehat{p}}}$ for which p lies in the exterior region of $\mathbb{R}P^2$ or, equivalently,

$$d(p) = \sum_{Q \in \mathcal{S}_{\mathcal{P}_{\widehat{p}}}} \mathrm{ind}_p(Q).$$

An *outer (inner) point* of $\mathcal{P}$ is a one that lies in the exterior (interior) region with respect to every conic in $S_{\mathcal{P}_{\widehat{p}}}$. In particular, for heptagonal configurations in $QC^7_{(7,0,0,0)}$ outer (inner) points are the ones with dominancy index 6 (respectively 0). Other points whose dominancy indices are neither 0 nor 6 are called *non-extremal* points.

Lemma 2.6.1. *A heptagonal configuration in $QC^7_{(7,0,0,0)}$ can not have more than one outer and more than one inner point.*

Proof. Let $\mathcal{P}$ be a heptagonal configuration in $QC^7_{(7,0,0,0)}$ and $p \in \mathcal{P}$. We assume that $\mathcal{P}$ has two outer points. After removing the point p from $\mathcal{P}$ we obtain a hexagonal configuration in QC^6_1, in which both outer points should be dominant. Hence, these points should have the same parity, i.e., dominant or subdominant with respect to the cyclic numeration on $\mathcal{P} \setminus \{p\}$. However, one can choose the point that we remove in such a way that the parity of these two given points on the initial heptagon becomes different on the hexagon. We get a contradiction. The case of two inner points is similar. $\square$

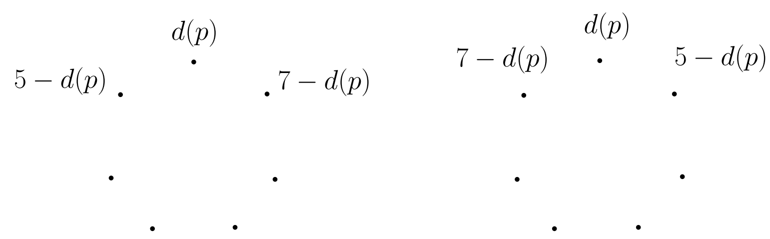

Figure 2.10: Two possibilities for the dominancy indices of two neighbors of a non-extremal point p of $\mathcal{P} \in QC^7_{(7,0,0,0)}$.

For a 7-configuration $\mathcal{P} = \{p_1, \ldots, p_7\} \in QC^7$, let $Q_{i,j} = Q_{j,i}$ denote one of the 21 conics passing through the five points of $\mathcal{P}$ other than p_i, p_j, where $i, j \in \{1, \ldots, 7\}$ and $i \neq j$.

Proposition 2.6.2. *Assume that $\mathcal{P} \in QC^7_{(7,0,0,0)}$ and that p is a non-extremal point of $\mathcal{P}$. Then, one of the two neighbors of p (with respect to the cyclic order of the heptagon vertices) has dominancy index $5 - d(p)$ and the other neighbor has dominancy index $7 - d(p)$ (see Figure 2.10).*

Proof. Let $\mathcal{P} \in QC^7_{(7,0,0,0)}$, and choose the cyclic numeration $p_1, \ldots, p_7$ of points of $\mathcal{P}$ such that p_1 is a non-extremal point. Here, the points p_2 and p_7 are two neighbors of the point p_1. We will show that

$$\{d(p_1) + d(p_2), d(p_1) + d(p_7)\} = \{5, 7\}.$$

For each $i \in \{1, 2, \ldots, 7\}$, the dominancy index of the point p_i is

$$d(p_i) = \sum_{\substack{1 \leq j \leq 7 \\ j \neq i}} \mathrm{ind}_{p_i}(Q_{i,j}).$$

Then,

$$\begin{aligned} d(p_1)+d(p_2) &= \sum_{\substack{1\le j\le 7\\ j\neq 1}} \mathrm{ind}_{p_1}(Q_{1,j}) + \sum_{\substack{1\le j\le 7\\ j\neq 2}} \mathrm{ind}_{p_2}(Q_{2,j}) \\ &= \sum_{\substack{1\le j\le 7\\ j\neq 1,2}} \Big(\mathrm{ind}_{p_1}(Q_{1,j}) + \mathrm{ind}_{p_2}(Q_{2,j})\Big) + \mathrm{ind}_{p_1}(Q_{1,2}) + \mathrm{ind}_{p_2}(Q_{1,2}). \end{aligned}$$

First, we shall prove the following statements:

Lemma 2.6.3. *Consider $\mathcal{P} \in QC^7_{(7,0,0,0)}$, and assume that the points $p_1, \ldots, p_7$ of $\mathcal{P}$ are cyclically numerated. Then, the following statements holds:*

(a) If $p_i \in \mathcal{P}$ such that $\mathrm{ind}_{p_i}(Q_{i,j}) = 1$ for some $j \in \{1,\ldots,7\} - \{i, i+1\}$, then $\mathrm{ind}_{p_{i+1}}(Q_{i+1,j}) = 0$. Also, if $p_i \in \mathcal{P}$ such that $\mathrm{ind}_{p_i}(Q_{i,j}) = 0$ for some $j \in \{1,\ldots,7\} - \{i, i+1\}$, then $\mathrm{ind}_{p_{i+1}}(Q_{i+1,j}) = 1$.

(b) If $p_i \in \mathcal{P}$ is non-extremal point for some $i \in \{1,\ldots,7\}$, then both of the indices $\mathrm{ind}_{p_i}(Q_{i,i+1}), \mathrm{ind}_{p_{i+1}}(Q_{i,i+1})$ are equal to either 1 or 0.

(c) For any 3 consecutive vertices p_{i-1}, p_i, p_{i+1} in a heptagonal configuration, such that p_i is not extremal, if one edge, $[p_{i-1}p_i]$ is inside (i.e., $\mathrm{ind}_{p_{i-1}}(Q_{i,i-1}) = \mathrm{ind}_{p_i}(Q_{i,i-1}) = 0$) then the other one, $[p_ip_{i+1}]$ is outside (i.e., $\mathrm{ind}_{p_i}(Q_{i,i+1}) = \mathrm{ind}_{p_{i+1}}(Q_{i,i+1}) = 1$), and vice versa.

Proof of Lemma 2.6.3. The proof of the first statement of the lemma follows from analysis of the pencil of conics passing through the four points of $\mathcal{P}$ other than p_i, p_{i+1}, p_j since this pencil cannot contain a singular conic intersecting an edge of the adjacency graph. For the proof of the second statement, we assume that $\mathrm{ind}_{p_i}(Q_{i,i+1}) = 1$ and $\mathrm{ind}_{p_{i+1}}(Q_{i,i+1}) = 0$ (the case in which $\mathrm{ind}_{p_i}(Q_{i,i+1}) = 0$ and $\mathrm{ind}_{p_{i+1}}(Q_{i,i+1}) = 1$ is similar). Since the point p_i is a non-extremal point of $\mathcal{P}$ there exists a conic $Q_{i,j}$ for some $j \in \{1,\ldots,7\} \setminus \{i, i+1\}$ such that $\mathrm{ind}_{p_i}(Q_{i,j}) = 0$. Looking at the mutual positions of the conic $Q_{i,i+1}$ and $Q_{i,j}$ we find a contradiction to Bezout's theorem. In fact it is enough to sketch a piece of $Q_{i,j}$, and so wee see that the conics $Q_{i,i+1}$ and $Q_{i,j}$ intersect at least one additional point different than the four common points, namely, $\{p_1,\ldots,p_7\} \setminus \{p_i, p_{i+1}, p_j\}$. (See Figure 2.11 in which p_1 is a non-extremal point with $\mathrm{ind}_{p_1}(Q_{1,2}) = 1$, $\mathrm{ind}_{p_2}(Q_{1,2}) = 0$.) Removing p_i from $\mathcal{P}$, we obtain a hexagonal 6-configuration in which points p_{i-1} and p_{i+1} become consecutive, and thus, are connected by an edge. Then, for the proof of the third statement, it is enough to apply Lemma 2.3.6 to this edge.

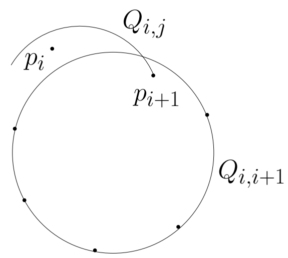

Figure 2.11: The arc of an ellipse $Q_{1,j}$ sketched on the figure contains an extra intersection point.

□

Corollary 2.6.4. *If a side of a heptagon is crossed by the conic passing through the other* 5 *points (i.e., vertices) of the hexagon, then the endpoints of these edge are extremal: one of them is outer vertex, and the other one is inner.*

Proof of Corollary 2.6.4. Let $\mathcal{P} \in QC^7_{(7,0,0,0)}$ be a heptagonal configuration, and assume that the numeration of points $p_1, \ldots, p_7$ of $\mathcal{P}$ is cyclic. By Lemma 2.6.3 (b), if an edge $[p_i, p_{i+1}]$ is crossed by the conic $Q_{i,i+1}$, then p_i can not be a non-extremal point of $\mathcal{P}$. On the other hand, p_{i+1} can not be non-extremal, because you could apply Lemma 2.6.3(b) to another numeration (in the opposite direction). By Lemma 2.6.1, since both p_i and p_{i+1} are extremal, then one of them is outer and another one is inner. □

The index $\mathrm{ind}_{p_1}(Q_{1,2})$ is either 1 or 0. We assume $\mathrm{ind}_{p_1}(Q_{1,2}) = 1$ (the case $\mathrm{ind}_{p_1}(Q_{1,2}) = 0$ is similar). By Lemma 2.6.3(b), $\mathrm{ind}_{p_2}(Q_{1,2}) = 1$, and so $\mathrm{ind}_{p_1}(Q_{1,2}) + \mathrm{ind}_{p_2}(Q_{1,2}) = 2$. By Lemma 2.6.3(a), if $\mathrm{ind}_{p_1}(Q_{1,j}) = 1$ for some $j \in \{3,4,5,6,7\}$, then $\mathrm{ind}_{p_2}(Q_{2,j}) = 0$, and in addition, if $\mathrm{ind}_{p_1}(Q_{1,j}) = 0$ for some $j \in \{3,4,5,6,7\}$, then $\mathrm{ind}_{p_2}(Q_{2,j}) = 1$. Then,

$$\sum_{\substack{1 \le j \le 7 \\ j \ne 1,\,2}} \Big(\mathrm{ind}_{p_1}(Q_{1,j}) + \mathrm{ind}_{p_2}(Q_{2,j}) \Big) = 5.$$

Hence, we obtain $d(p_1) + d(p_2) = 7$. Similarly, we have

$$
\begin{aligned}
d(p_1) + d(p_7) &= \sum_{\substack{1 \le j \le 7 \\ j \ne 1}} \mathrm{ind}_{p_1}(Q_{1,j}) + \sum_{\substack{1 \le j \le 7 \\ j \ne 7}} \mathrm{ind}_{p_7}(Q_{7,j}) \\
&= \sum_{\substack{1 \le j \le 7 \\ j \ne 1,7}} \Big(\mathrm{ind}_{p_1}(Q_{1,j}) + \mathrm{ind}_{p_7}(Q_{7,j}) \Big) + \mathrm{ind}_{p_1}(Q_{1,7}) + \mathrm{ind}_{p_7}(Q_{1,7}).
\end{aligned}
$$

If $\mathrm{ind}_{p_1}(Q_{1,2}) = 1$, then $\mathrm{ind}_{p_1}(Q_{1,7}) = 0$ by Lemma 2.6.3(c). Thus, by Lemma 2.6.3(b), $\mathrm{ind}_{p_7}(Q_{1,7}) = 0$, and so $\mathrm{ind}_{p_1}(Q_{1,7}) + \mathrm{ind}_{p_7}(Q_{1,7}) = 0$. By similar reasons as given above, we get

$$
\sum_{\substack{1 \le j \le 7 \\ j \ne 1,7}} \Big(\mathrm{ind}_{p_1}(Q_{1,j}) + \mathrm{ind}_{p_7}(Q_{7,j}) \Big) = 5.
$$

Thus, we obtain $d(p_1) + d(p_7) = 5$.

Therefore, we complete the proof. □

Proposition 2.6.5. *The dominancy indices of points of any heptagonal configurations in $QC^7_{(7,0,0,0)}$ go in the following cyclic order (with respect to the cyclic numeration of vertices of the principle hexagon, see Figure 2.3):* $6, 1, 4, 3, 2, 5, 0$.

Proof. Let $\mathcal{P} \in QC^7_{(7,0,0,0)}$ be a heptagonal configuration. By Lemma 2.6.1, this configuration should have a non-extremal point, say p_2, with respect to some cyclic numeration on $\mathcal{P}$. Then, $d(p_2) = k$ for some $k \in \{1, 2, 3, 4, 5\}$. If $d(p_2) = 1$ then either $d(p_3) = 4$, $d(p_1) = 6$ or $d(p_3) = 6$, $d(p_1) = 4$ by Proposition 2.6.2. Firstly, we assume that $d(p_3) = 4$, $d(p_1) = 6$. Applying Proposition 2.6.2 successively we get $d(p_4) = 3$, $d(p_5) = 2$, $d(p_6) = 5$, and $d(p_7) = 0$. Then, the cyclic numeration of vertices of the principle hexagon is $6, 1, 4, 3, 2, 5, 0$. If $d(p_3) = 6$, $d(p_1) = 4$ we could apply Proposition 2.6.2 to another numeration (in the opposite direction). For the other cases $k = 2, 3, 4, 5$, we apply Proposition 2.6.2 to another numeration. This completes the proof. □

2.7 Heptagonal augmentations of hexagonal 6-configurations

Let $\mathcal{P} \in QC^6_1$ be a hexagonal configuration, and assume that the numeration of points $p_1, \ldots, p_6$ of $\mathcal{P}$ is cyclic such that p_6 is dominant point. The six conics Q_i,

$i = 1, \ldots, 6$, which are passing through the five points of $\mathcal{P}$ other than p_i divide the L-polygon $p_1 O p_6$ (see Figure 2.5) into either six Q-regions R_j, $j = 1, \ldots, 6$, or seven Q-regions R_j, $j = 0, 1, \ldots, 6$ as it is shown in Figure 2.12.

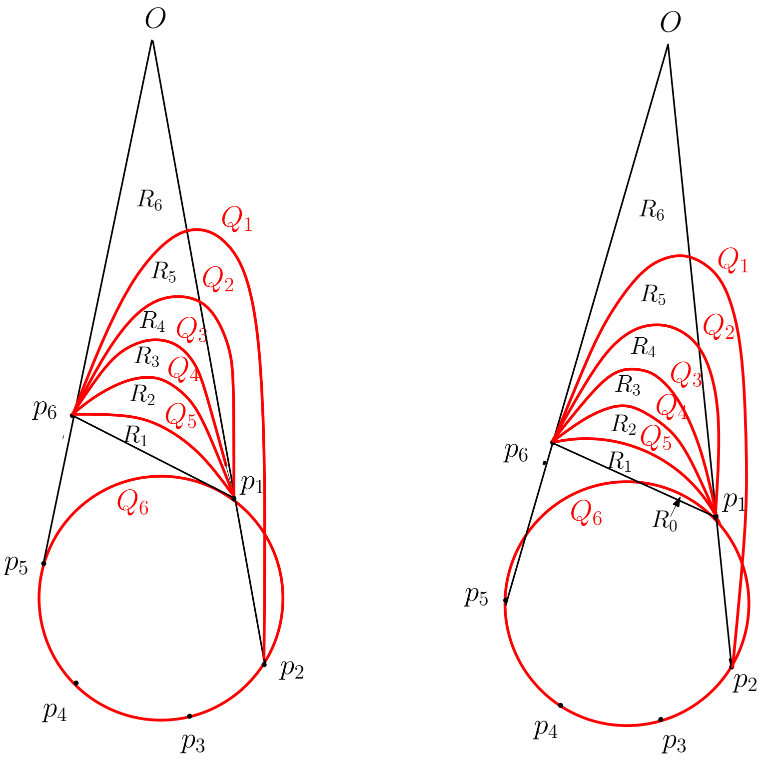

(a) the case of six Q-regions (b) the case of seven Q-regions

Figure 2.12: The Q-region R_{6-i}, $i = 1, \ldots, 5$, associated to a hexagonal configuration in QC_1^6 is the region between two conics Q_i and Q_{i+1} lying inside the triangle $p_1 O p_6$. The Q-regions R_6 and R_0 are the exterior of the conic Q_1 and the interior of the conic Q_6 lying inside $p_1 O p_6$, respectively.

Proposition 2.7.1. *Let $\mathcal{P}^t$, $t \in [0, 1]$, be a Q-deformation such that $\mathcal{P}^t \in QC^6$ are hexagonal configurations for all t. Let the numeration of points $p_1^0, \ldots, p_6^0$ of $\mathcal{P}^0$ be cyclic such that the point p_6^0 is dominant, and let R_i^0, $i = 0, 1, \ldots, 6$ be Q-regions associated to $\mathcal{P}^0$ as above. We assume that $\{R_i^t\}_{t\in[0,1]}$ is the Q-deformation of R_i^0 for some $i \in \{0, 1, \ldots, 6\}$. Choose a point $p^0 \in \mathbb{R}P^2$ from the interior of R_i^0, and assume, in addition, that $\{p^t\}_{t\in[0,1]}$ is the Q-deformation of p^0. Then the heptagonal augmentation $\mathcal{P}^t \cup \{p^t\}$ (i.e., $\mathcal{P}^t \cup \{p^t\} \in QC^7_{(7,0,0,0)}$ for all t) is also Q-deformation. Moreover, the dominancy index of the point $p^t \in \tilde{\mathcal{P}}^t$ is equal to the index i of the region $R_i^t \ni p^t$.*

Proof. The proof of the first part is obvious since neither lines containing three points of the heptagonal augmented configuration $\mathcal{P}^t \cup \{p^t\}$ nor conics passing through six points of $\mathcal{P}^t \cup \{p^t\}$ for each $t \in [0,1]$ occurs. The proof of the second part follows from the facts that the dominancy index of p_0^0 is zero if the point p_0^0 lies inside the Q-region R_0^0 (see Figure 2.12). More generally, if the point p_0^0 lies inside the Q-region R_i^0, $i = 1, \dots, 6$, then the dominancy index of p_0^0 is increasing by i since in this case, it lies in the interior of the $6 - i$ number of conics. □

Table 2.5: In this figure, "in" (respectively, "out") means that $p_i \in \mathcal{P}$, $i = 1, \dots, 7$, lies in the interior (respectively, the exterior) of the conics $Q_{i,j}$ for any $j \in \{1, \dots, \hat{i}, \dots, 7\}$ if $p^0 = p_7$ lies in the Q-region R_i, $i = 0, 1, \dots, 6$, associated to a heptagonal 7-configuration $\mathcal{P}$ as below.

$Q_{i,j}$	p_7 in R_5	p_7 in R_4	p_7 in R_3	p_7 in R_2	p_7 in R_1	p_7 in R_0	p_7 in R_6
$Q_{1,2}$	p_1 in, p_2 out	p_1 , p_2 out	p_1 , p_2 out	p_1 , p_2 out	p_1 , p_2 out	p_1 , p_2 out	p_1 , p_2 in
$Q_{1,3}$	p_1 , p_3 in	p_1 , p_3 in	p_1 out, p_3 in	p_1 out, p_3 in	p_1 out, p_3 in	p_1 out, p_3 in	p_1 in, p_3 out
$Q_{1,4}$	p_1 in, p_4 out	p_1 in, p_4 out	p_1 in, p_4 out	p_1 , p_4 out	p_1 , p_4 out	p_1 , p_4 out	p_1 , p_4 in
$Q_{1,5}$	p_1, p_5 in	p_1 , p_5 in	p_1 , p_5 in	p_1 ,p_5 in	p_1 out, p_5 in	p_1 out, p_5 in	p_1 in, p_5 out
$Q_{1,6}$	p_1 in, p_6 out	p_1 in, p_6 out	p_1 in, p_6 out	p_1 in, p_6 out	p_1 in, p_6 out	p_1 , p_6 out	p_1 , p_6 in
$Q_{1,7}$	p_1 , p_7 in	p_1 , p_7 in	p_1 , p_7 in	p_1 , p_7 in	p_1 , p_7 in	p_1 , p_7 in	p_1 in, p_7 out
$Q_{2,3}$	p_2 , p_3 out	p_2 out, p_3 in	p_2 , p_3 in	p_2 , p_3 in	p_2 , p_3 in	p_2 , p_3 in	p_2 , p_3 out
$Q_{2,4}$	p_2 out, p_4 in	p_2 , p_4 out	p_2 , p_4 out	p_2 in, p_4 out	p_2 in, p_4 out	p_2 in, p_4 out	p_2 out, p_4 in
$Q_{2,5}$	p_2 , p_5 out	p_2 out, p_5 in	p_2 out, p_5 in	p_2 out, p_5 in	p_2 , p_5 in	p_2 , p_5 in	p_2 , p_5 out
$Q_{2,6}$	p_2 out, p_6 in	p_2 , p_6 out	p_2 , p_6 out	p_2 , p_6 out	p_2 , p_6 out	p_2 in, p_6 out	p_2 out, p_6 in
$Q_{2,7}$	p_2 , p_7 out	p_2 out, p_7 in	p_2 out, p_7 in	p_2 out, p_7 in	p_2 out, p_7 in	p_2 out, p_7 in	p_2 , p_7 out
$Q_{3,4}$	p_3 , p_4 in	p_3 , p_4 in	p_3 in, p_4 out	p_3 , p_4 out	p_3 , p_4 out	p_3 , p_4 out	p_3 , p_4 in
$Q_{3,5}$	p_3 in, p_5 out	p_3 in, p_5 out	p_3 , p_5 in	p_3 , p_5 in	p_3 out, p_5 in	p_3 out, p_5 in	p_3 in, p_5 out
$Q_{3,6}$	p_3 , p_6 in	p_3 , p_6 in	p_3 in, p_6 out	p_3 in, p_6 out	p_3 in, p_6 out	p_3 , p_6 out	p_3 , p_6 in
$Q_{3,7}$	p_3 in, p_7 out	p_3 in, p_7 out	p_3 , p_7 in	p_3 , p_7 in	p_3 , p_7 in	p_3 , p_7 in	p_3 in, p_7 out
$Q_{4,5}$	p_4 , p_5 out	p_4 , p_5 out	p_4, p_5 out	p_4 out, p_5 in	p_4 , p_5 in	p_4 , p_5 in	p_4 , p_5 out
$Q_{4,6}$	p_4 out, p_6 in	p_4 out, p_6 in	p_4 out, p_6 in	p_4 , p_6 out	p_4 , p_6 out	p_4 in, p_6 out	p_4 out, p_6 in
$Q_{4,7}$	p_4 , p_7 out	p_4 , p_7 out	p_4 , p_7 out	p_4 out, p_7 in	p_4 out, p_7 in	p_4 out, p_7 in	p_4 , p_7 out
$Q_{5,6}$	p_5 , p_6 in	p_5 , p_6 in	p_5 , p_6 in	p_5 , p_6 in	p_5 in, p_6 out	p_5 , p_6 out	p_5 , p_6 in
$Q_{5,7}$	p_5 in, 7out	p_5 in, p_7 out	p_5 in, p_7 out	p_5 in, p_7 out	p_5 , p_7 in	p_5 , p_7 in	p_5 in, p_7 out
$Q_{6,7}$	p_6 , p_7 out	p_6 , p_7 out	p_6 , p_7 out	p_6 , p_7 out	p_6 , p_7 out	p_6 out, p_7 in	p_6 , p_7 out

Remark 2.7.2. Let $\mathcal{P} \in QC^7_{(7,0,0,0)}$, and choose a cyclic numeration of the points $p_1, \dots, p_7$ of $\mathcal{P}$ such that p_6 is dominant with respect to the conic $Q_{6,7}$ passing through five points of $\mathcal{P}$ other than p_6 and p_7. Consider the hexagonal configuration $\mathcal{P}_{\hat{7}} = \mathcal{P} \setminus \{p_7\}$, and its associated Q-regions R_i, $i = 0, \dots, 6$, which are the sections of the L-polygon p_1Op_6 divided by the six conics Q_i, $i = 1, \dots, 6$, which are passing through the five points of $\mathcal{P}_{\hat{7}}$ other than p_i as shown in Figure 2.12. Notice that the point p_7 have to lie inside one of these regions. Then, by straightforward computation, we get Table 2.5, in which each

column shows the position of each pair of points $p_j, p_k \in \mathcal{P}$ with respect to the conics $Q_{j,k}$, where $1 \le j < k \le 7$, when the point $p^0 = p_7$ lies in the region $R_i = R_i^0$, $0 \le i \le 6$. This table is equivalent to the table given by S. Fiedler-Le Touzé [T2].

Making use of the results in Table 2.5, we get the following Table 2.6 whose columns show the dominancy indices of points of $\mathcal{P}$ where $p_7 \in \mathcal{P}$ lies in R_i, $i = 0, 1, \ldots, 6$.

Table 2.6: The dominancy indices of points of a 7-configuration $\mathcal{P} \in QC^7_{(7,0,0,0)}$ as above, when $p_7 \in \mathcal{P}$ lies in the regions R_i, $i = 0, 1, \ldots, 6$.

	p_7 in R_0	p_7 in R_1	p_7 in R_2	p_7 in R_3	p_7 in R_4	p_7 in R_5	p_7 in R_6
$d(p_1)$	5	4	3	2	1	0	0
$d(p_2)$	2	3	4	5	6	6	5
$d(p_3)$	3	2	1	0	0	1	2
$d(p_4)$	4	5	6	6	5	4	3
$d(p_5)$	1	0	0	1	2	3	4
$d(p_6)$	6	6	5	4	3	2	1
$d(p_7)$	0	1	2	3	4	5	6
The outer point of $\mathcal{P}$	p_6	p_6	p_4	p_4	p_2	p_2	p_7

2.8 The Q-deformation classes of heptagonal 7-configurations

In this section we study Q-deformation classes of heptagonal 7-configurations (that form subset $QC^7_{(7,0,0,0)}$).

For a given heptagonal configuration $\mathcal{P} \in QC^7_{(7,0,0,0)}$, we say that the cyclic numeration of points $p_1, \ldots, p_7$ of $\mathcal{P}$ is *canonical* if $d(p_1) = 6$ and $d(p_7) = 0$.

Proposition 2.8.1. *Let $\mathcal{P}^0, \mathcal{P}^1 \in QC^7_{(7,0,0,0)}$, assume that p^i_0 is the outer point of $\mathcal{P}^i$, where $i \in \{0, 1\}$. Then, there is a Q-deformation $\{\mathcal{P}^t\}_{t\in[0,1]}$ between $\mathcal{P}^0$ and $\mathcal{P}^1$ which takes p^0_0 to p^1_0.*

Proof. We assume that the numeration of the points $p^i_0, p^i_1, p^i_2, \ldots, p^i_6$ of $\mathcal{P}^i$, $i = 0, 1$, is cyclic such that p^i_0 and p^i_6 are outer and inner points of $\mathcal{P}^i$, respectively. Consider the hexagonal configurations $\mathcal{P}^i_{\widehat{0}} \in QC^6_1$, $i = 0, 1$, obtained from $\mathcal{P}^i$ by removing p^i_0. By Lemma 2.3.6, the point $p^i_1 \in \mathcal{P}^i_{\widehat{0}}$, $i = 0, 1$, is dominant since the point $p^i_6 \in \mathcal{P}^i_{\widehat{0}}$ is subdominant. By Proposition 2.3.3, there is a Q-deformation

$\{\mathcal{P}^t_{\widehat{0}}\}$, $t \in [0,1]$, sending p^0_1 to p^1_1. Since p^i_0, $i = 0, 1$, is outer point of $\mathcal{P}^i$ it must lie in the Q-region R^i_6 which are the divisions of the L-polygon $p^i_1 O^i p^i_6$ associated to $\mathcal{P}^i_{\widehat{0}}$ by the conics Q^i_j, $j = 1, \ldots, 6$, passing through five points of $\mathcal{P}^i_{\widehat{0}}$ other than p^i_j. Let $\{R^t_6\}$ and $\{p^t_0\}$, $t \in [0,1]$, be the Q-deformations of R^0_6 and p^0_0 under the Q-deformation $\{\mathcal{P}^t_{\widehat{0}}\}$. The Q-regions R^t_6 are connected and they do not contract to a point as t varies, so the deformation $\mathcal{P}^t_{\widehat{0}}$ can be extended to a Q-deformation $\mathcal{P}^t = \mathcal{P}^t_{\widehat{0}} \cup \{p^t_0\}$, $t \in [0,1]$. □

Since any heptagonal configuration $\mathcal{P} \in QC^7_{(7,0,0,0)}$ has a unique outer (and, a unique inner) point by Proposition 2.6.1, we get the following statement.

Proposition 2.8.2. *The space $QC^7_{(7,0,0,0)}$ of quadratically nondegenerate heptagonal configurations of seven points is connected.* □

We decorate edges of the adjacency graph $\Gamma(\mathcal{P})$ for a given heptagonal configuration $\mathcal{P} \in QC^7_{(7,0,0,0)}$ in such a way that an edge is illustrated by bold or thin if two end points of the edge are both dominant or both subdominant with respect to the conic passing through remaining five points of $\mathcal{P}$, respectively, or by a dotted edge with an arrow from the dominant point to the subdominant point if one of the end points of the edge is dominant and the other is subdominant. (See Figure 2.13). We call this decoration the *e-decoration* of $\Gamma(\mathcal{P})$. The adjacency graph $\Gamma(\mathcal{P})$ together with the e-decoration is called the *e-decorated adjacency graph* of $\mathcal{P}$.

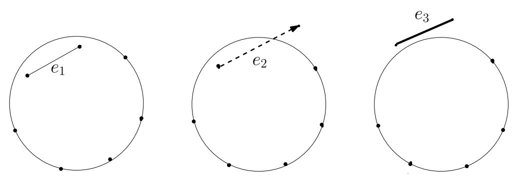

Figure 2.13: Three types of decorations of edges in $\Gamma(\mathcal{P})$ for $\mathcal{P} \in QC^7_{(7,0,0,0)}$.

The cyclic numeration of points $p_1, \ldots, p_7$ of a given heptagonal configuration $\mathcal{P} \in QC^7_{(7,0,0,0)}$ is called the *canonical numeration* if $d(p_1) = 6$ and $d(p_7) = 0$.

Proposition 2.8.3. *All heptagonal configurations in $QC^7_{(7,0,0,0)}$ have topologically the same e-decorated adjacency graph as shown in Figure 2.14.*

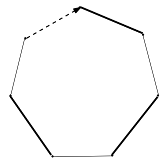

Figure 2.14: The e-decorated adjacency graphs of $\mathcal{P} \in QC^7_{(7,0,0,0)}$ in which the direction of the arrow from the inner point to the outer point.

Proof of Proposition 2.8.3. The uniqueness immediately follows from Proposition 2.8.2. The e-decoration of adjacency graphs for any heptagonal configurations in $QC^7_{(7,0,0,0)}$ follows form Lemma 2.6.3 and Proposition 2.6.5. In addition, this decoration can be also obtained by using the table 2.5. □

2.9 Hexagonal 7-configurations

Let $\mathcal{P} \in QC^6$ be a hexagonal configuration, and assume that the numeration of points $p_1, \ldots, p_6$ of $\mathcal{P}$ is cyclic such that p_1 is dominant with respect to the conic Q_1 passing through five points of $\mathcal{P}$ other than p_1. The conics Q_i, $i = 1, \ldots, 6$, divide the internal L-polygons (i.e., those of lying inside the principle hexagon $F_{\mathcal{P}}$, see Figure 2.5) into finite number of Q-regions. It is easily seen that the quotient space of D_6-action on the internal Q-regions have six distinct D_6-orbits. We shall denote by B_1, B_2, C_1, C_2, D, and E the Q-regions representing the six D_6-orbits as shown in Figure 2.15.

For a hexagonal configuration $\mathcal{P} \in QC^7$, we say that a point p of $\mathcal{P}$ is *h-interior* if it lies inside the principle hexagon (see Section 2.2) of the hexagonal configuration $\mathcal{P}_{\widehat{p}} = \mathcal{P} \setminus \{p\} \in QC^6_1$. Any hexagonal configuration $\mathcal{P} \in QC^7$ has one and only one h-interior point since $S_6(\mathcal{P}) = 1$ (see Table 2.1).

Proposition 2.9.1. *The following statements hold:*

(a) The space $LC^7_{(3,4,0,0)}$ contains two connected components of QC^7, and these components are denoted by $QC^7_{(3,4,0,0)_1}$ and $QC^7_{(3,4,0,0)_2}$ (see Figure 2.19(a) and (b)).

(b) The space $LC^7_{(2,2,3,0)}$ contains three connected components of QC^7, and

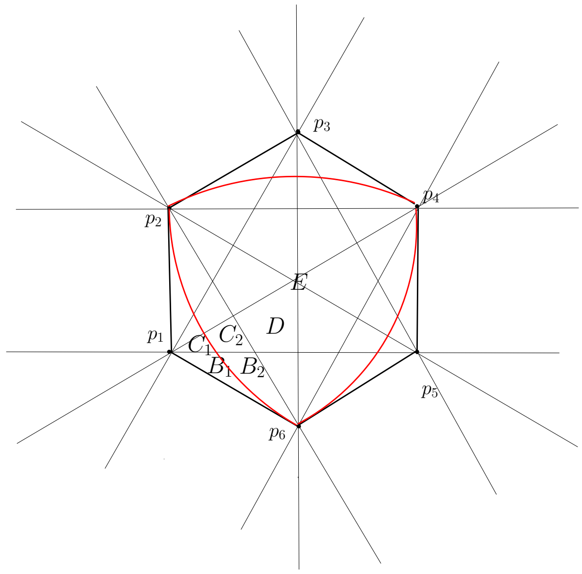

Figure 2.15: The six D_6-orbits on internal Q-regions associated to a hexagonal configuration in QC^6.

these components are denoted by $QC^7_{(2,2,3,0)_i}$ *for each* $i \in \{1,2,3\}$ *(see Figure 2.19(c), (d) and (e)).*

(c) The spaces LC^7_σ*, for* $\sigma = (1,0,6,0), (1,2,2,2)$ *are contained in* QC^7 *and thus, each of these spaces contains one connected component of* QC^7 *(i.e.,* $QC^7_\sigma = LC^7_\sigma$ *see 2.19(f) and (g)).*

Hence, the space of hexagonal configurations in QC^7 *has* 7 *connected components as introduced in items (a), (b), and (c).*

Proof. Let $\mathcal{P} \in QC^7$ be a hexagonal configuration, and p_7 be the h-interior point of $\mathcal{P}$. Assume that the numeration of points $p_1, \ldots, p_6$ of the hexagonal 6-configuration $\mathcal{P}_{\hat{7}} = \mathcal{P} \setminus \{p_7\}$ is cyclic such that p_1 is dominant. All permutations of D_6 which preserve the colors of the six points of $\mathcal{P}_{\hat{7}}$ (i.e., black for dominant points and white for subdominant points) form the subgroup D_3, and these color preserving permutations induce an action on $\Lambda_Q(\mathcal{P}_{\hat{7}})$. We call this action the D_3-*action* on $\Lambda_Q(\mathcal{P}_{\hat{7}})$. We denote by $[M]^Q_3$ the orbit of a Q-region M with respect to this action. The quotient space of the D_3-action on internal Q-regions associated to $\mathcal{P}_{\hat{7}}$ have seven distinct D_3-orbits. We shall denote by B_1, B_2, C_1, C_2, C_3, D, and E the Q-regions representing the seven D_3-orbits on the internal

Q-regions as shown in Figure 2.16. Note that there is one more D_3-orbit on internal Q-regions than in the case of D_6-orbits (see Figures 2.15 and 2.16).

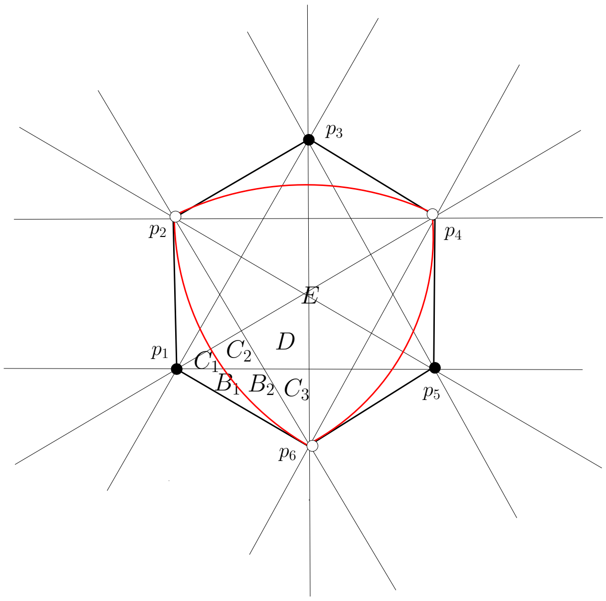

Figure 2.16: The seven D_3-orbits on internal Q-regions associated to a hexagonal configuration in QC^7.

Recall from Section 2.1 that there are four L-deformation classes of hexagonal 7-configurations in LC^7 and the adjacency graphs representing these classes are shown in Figure 2.2(b)-(e). Table 2.3 shows which D_6 orbits on L-polygons associated to a hexagonal configuration in LC^7 correspond to each L-deformation class of hexagonal 7-configurations in LC^7. By definition $QC^7_\sigma = LC^7_\sigma \setminus Q\Delta^7$ (see Section 2.3). It is equivalent to say that $QC^7_{(1,0,6,0)}$ and $QC^7_{(1,2,2,2)}$ are the subspaces of QC^7 consisting of hexagonal 7-configurations whose h-interior points lie in their associated Q-regions D and E, respectively. We denote by $QC^7_{(3,4,0,0)_i}$ $(i = 1, 2)$ and $QC^7_{(2,2,3,0)_i}$ $(i = 1, 2, 3)$ the subspaces of QC^7 consisting of hexagonal 7-configurations whose h-interior points lie in their associated Q-regions B_i and C_i, respectively.

The connectedness of $PGL(3, \mathbb{R})$ implies there exits a Q-deformation of $\mathcal{P}_{\widehat{7}}$ induced by a given permutation in D_3. If the Q-region associated to $\mathcal{P}_{\widehat{7}}$ containing the point p_7 is not collapsing under this Q-deformation, then this deformation can be extended to a Q-deformation of the augmented 7-configuration $\mathcal{P}$.

For the continuation of this proof we need the following two lemmas.

Lemma 2.9.2. *Assume that $\mathcal{P}^0 \in QC^6$ is a hexagonal configuration, and that $\mathcal{P}^t$, $[0,1]$, is a Q-deformation. Then, no internal Q-regions associated to $\mathcal{P}^0$ different from the central triangle can collapse.*

Proof of Lemma 2.9.2. An internal Q-region associated to $\mathcal{P}$ does not collapse if it contains a vertex of the principle hexagon of $\mathcal{P}$ and some angle $\angle ABC$, where $A, B, C \in \mathcal{P}$. In addition, there can not be exist a convex hexagon with triple intersection point of the diagonals unless they are the three big diagonals. □

The following result is the immediate consequence of Lemma 2.9.2.

Corollary 2.9.3. *Assume that $\mathcal{P}^i \in QC^7$, $i = 0, 1$, are two hexagonal configurations, and that $p^i_7 \in \mathcal{P}^i$ is h-interior point which lies in an internal Q-region M^i associated to $\mathcal{P}^i_{\bar{7}}$ other than central triangles. If, in addition, M^0, M^1 belong to the same type D_3-orbit, then $\mathcal{P}^0$ is Q-deformation equivalent to $\mathcal{P}^1$.* □

Lemma 2.9.4. *Assume that $\mathcal{P}^i \in QC^6_1$, $i = 0, 1$ are hexagonal configurations, and that the central triangles E^i associated to $\mathcal{P}^i$ do not degenerate to a point (i.e., their big diagonals are not concurrent). Then, there exists a Q-deformation $\{\mathcal{P}^t\}_{t\in[0,1]}$ such that central triangles E^t, $t \in [0, 1]$, associated to $\mathcal{P}^t$ do not collapse during this Q-deformation.*

Proof of Lemma 2.9.4. Assume that the numerations of points $p^i_0, \dots, p^i_5$ of $\mathcal{P}^i$, $i = 0, 1$, are cyclic such that p^0_j, p^1_j are dominant for j odd and subdominant for j even. Without loss of generality we can assume that

(1) the lines $L_{p^i_0 p^i_3}$,$L_{p^i_1 p^i_4}$ and $L_{p^i_2 p^i_5}$ containing to big diagonals of the principle hexagons of $\mathcal{P}^i$, $i = 0, 1$, are the same.
(2) the central triangles are the same.

We can find a projective transformation between these configurations sending the central triangle of $\mathcal{P}^0$ to the central triangle of $\mathcal{P}^1$ such that each of these diagonals contains same type points as shown in Figure 2.17.

For a given triangle $ABC \subset \mathbb{R}P^2$, let us denote by QC^6_{ABC} the subspace of QC^6_1 consisting of convex hexagonal 6-configurations (i.e. those of convex in $\mathbb{R}P^2 \setminus L$

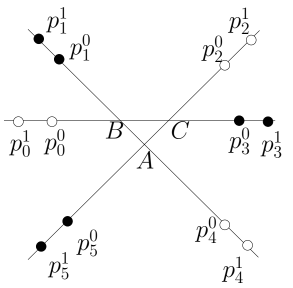

Figure 2.17: A pair of hexagonal 6-configurations with the same diagonal.

for a line L) having the central triangle ABC.

The following proposition is crucial for continuation of the proof of Lemma 2.9.4.

Proposition 2.9.5. *Given a triangle $ABC \subset \mathbb{R}P^2$, the space QC^6_{ABC} is connected.*

Proof of Proposition 2.9.5. Note that the central triangle of a given convex hexagon is contained in each subpentagon of this hexagon, and so it is also contained inside the conics passing through all 5-tuples of vertices of this hexagon. For the proof of this proposition, we need the following lemma.

Let S_{ABC} be the set of pairs (Q, D), where Q is a conic containing the triangle ABC inside, and $D \in \mathbb{R}P^2$ is a point which lies in one of the three boundary lines L_{AB}, L_{AC} and L_{BC} of the triangle, and at the same time outside Q such that it forms a convex hexagon together with an arbitrary 5-tuple from the six intersection points of $Q \cap (L_{AB} \cup L_{AC} \cup L_{BC})$ (for example, see Figure 2.18). Define a map α from S_{ABC} to QC^6_{ABC} by $\alpha(Q, D) = (p_0, p_1, p_2, p_3, p_4, p_5)$, where $p_0 = D$ and the five other points are the intersections of Q and the three boundary lines L_{AB}, L_{AC} and L_{BC}. By definition of this map, the following lemma is trivial.

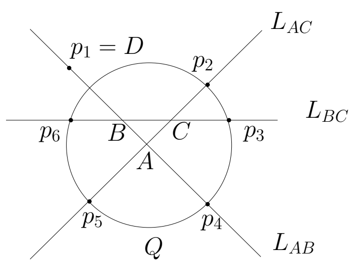

Figure 2.18

Lemma 2.9.6. *The map $\alpha : (Q, D) \mapsto (p_0, p_1, p_2, p_3, p_4, p_5)$ as above establishes one-to-one correspondence between S_{ABC} and QC^6_{ABC} for a given triangle $ABC \subset \mathbb{R}P^2$.* $\square$

It is trivial and well-known fact that the space of conics containing given a central triangle ABC inside is connected since this space is homotopically equivalent to the space of conics containing given a point. The map

$$S_{ABC} \to \{Q : Q \text{ conics containing a given triangle } ABC \text{ inside}\}$$

is a fibration with a fiber interval, so the total space of all pairs S_{ABC} is connected. $\square$

By Proposition 2.9.5 the proof of Lemma 2.9.4 is completed. $\square$

The next statement is an immediate consequence of the Lemma 2.9.4.

Corollary 2.9.7. *Let $\mathcal{P}^i \in QC^7$, $i = 0, 1$, be two hexagonal configurations, and assume that $p^i_7 \in \mathcal{P}^i$ is h-interior point which lies in central triangles E^i associated to $\mathcal{P}^i_{\bar{7}}$. Then $\mathcal{P}^0$ is Q-deformation equivalent to $\mathcal{P}^1$.* $\square$

Form Corollaries 2.9.3 and 2.9.7, we obtain that the spaces $QC^7_{(3,4,0,0)_i}$, $i = 1, 2$, $QC^7_{(2,2,3,0)_i}$, $i = 1, 2, 3$, $QC^7_{(1,0,6,0)}$, and $QC^7_{(1,2,2,2)}$ are connected. This completes the proof of Proposition 2.9.1. $\square$

By Proposition 2.9.1, we obtain Table 2.7. This table shows the correspondence between D_3-orbits in $\Lambda_Q(\mathcal{P})$, where $\mathcal{P} \in QC^6$ is a hexagonal configuration and Q-deformation classes of augmented configurations in QC^7 (i.e., each of them is obtained from $\mathcal{P}$ by adding just one point of $\mathbb{R}P^2$ to one of the Q-regions in $\Lambda_Q(\mathcal{P})$).

Let $\mathcal{P} \in QC^7$ be a hexagonal configuration, and p_7 be its h-interior point. Assume that the numeration of six points $p_1, \ldots, p_6$ of $\mathcal{P}$ other than p_7 is cyclic such that p_1 is dominant and p_7 lies inside one of the seven Q-regions associated to $\mathcal{P}_{\bar{7}}$ as shown in Figure 2.16. Then, by straightforward computation yields

Table 2.7: The seven D_3-orbits of Q-regions associated to a hexagonal configuration in QC^6 representing the seven Q-deformation classes of hexagonal configurations in QC^7.

D_3-orbits	Q-deformation classes in QC^7
$[B_1]_3^Q$	$QC^7_{(3,4,0,0)_1}$
$[B_2]_3^Q$	$QC^7_{(3,4,0,0)_2}$
$[C_1]_3^Q$	$QC^7_{(2,2,3,0)_1}$
$[C_2]_3^Q$	$QC^7_{(2,2,3,0)_2}$
$[C_3]_3^Q$	$QC^7_{(2,2,3,0)_3}$
$[D]_3^Q$	$QC^7_{(1,2,2,2)}$
$[E]_3^Q$	$QC^7_{(1,0,6,0)}$

Table 2.8: In this figure, "in" (respectively, "out") means that $p_i \in \mathcal{P}$, $i = 1, \ldots, 7$ lie in the interior (respectively, the exterior) of the conics $Q_{i,j}$, where $j \neq i$ and $j \in \{1, \ldots, 7\}$, depending on the position of the h-interior point p_7 of a hexagonal configuration $\mathcal{P} \in QC^7$ as below.

$Q_{i,j}$	$p_7 \in B_1$	$p_7 \in B_2$	$p_7 \in C_1$	$p_7 \in C_2$	$p_7 \in C_3$	$p_7 \in D$	$p_7 \in E$
$Q_{1,2}$	p_1 out, p_2 in	p_1 , p_2 out	p_1 out, p_2 in	p_1 , p_2 out	p_1 , p_2 out	p_1 , p_2 out	p_1 , p_2 out
$Q_{1,3}$	p_1 , p_3 out	p_1 out, p_3 in	p_1 , p_3 out	p_1 out, p_3 in	p_1 in, p_3 out	p_1 in, p_3 out	p_1 out, p_3 in
$Q_{1,4}$	p_1 out, p_4 in	p_1 , p_4 out	p_1 out, p_4 in	p_1 , p_4 out	p_1 , p_4 in	p_1 , p_4 in	p_1 , p_4 out
$Q_{1,5}$	p_1, p_5 out	p_1 out, p_5 in	p_1 , p_5 out	p_1 out,p_5 in	p_1 out, p_5 in	p_1 in, p_5 out	p_1 out, p_5 in
$Q_{1,6}$	p_1 out, p_6 in	p_1 , p_6 out	p_1 out, p_6 in	p_1 , p_6 out	p_1 , p_6 out	p_1 , p_6 out	p_1 , p_6 in
$Q_{1,7}$	p_1 , p_7 out	p_1 out, p_7 in	p_1 , p_7 out	p_1 out, p_7 in	p_1 out, p_7 in	p_1 out, p_7 in	p_1 out, p_7 in
$Q_{2,3}$	p_2 , p_3 out	p_2 , p_3 out	p_2 , p_3 out	p_2 , p_3 in	p_2 , p_3 out	p_2 , p_3 in	p_2 , p_3 in
$Q_{2,4}$	p_2 out, p_4 in	p_2 out, p_4 in	p_2 out, p_4 in	p_2 in, p_4 out	p_2 out, p_4 in	p_2 in, p_4 out	p_2 in, p_4 out
$Q_{2,5}$	p_2 , p_5 out	p_2 , p_5 out	p_2 , p_5 out	p_2 , p_5 out	p_2 , p_5 out	p_2 , p_5 out	p_2 , p_5 out
$Q_{2,6}$	p_2 in, p_6 out	p_2 in, p_6 out	p_2 out, p_6 in	p_2 out, p_6 in	p_2 in, p_6 out	p_2 out, p_6 in	p_2 out, p_6 in
$Q_{2,7}$	p_2 , p_7 in	p_2 , p_7 in	p_2 , p_7 in	p_2 , p_7 in	p_2 , p_7 in	p_2 , p_7 in	p_2 , p_7 in
$Q_{3,4}$	p_3 , p_4 in	p_3 , p_4 in	p_3 , p_4 out	p_3 , p_4 out	p_3 , p_4 out	p_3 , p_4 in	p_3 , p_4 out
$Q_{3,5}$	p_3 in, p_5 out	p_3 in, p_5 out	p_3 in, p_5 out	p_3 in, p_5 out	p_3 out, p_5 in	p_3 in, p_5 out	p_3 out, p_5 in
$Q_{3,6}$	p_3 , p_6 out	p_3 , p_6 out	p_3 , p_6 in	p_3 , p_6 in	p_3 , p_6 out	p_3 , p_6 in	p_3 , p_6 out
$Q_{3,7}$	p_3 out, p_7 in	p_3 out, p_7 in	p_3 out, p_7 in	p_3 out, p_7 in	p_3 out, p_7 in	p_3 out, p_7 in	p_3 out, p_7 in
$Q_{4,5}$	p_4 , p_5 out	p_4 , p_5 out	p_4 , p_5 out	p_4 , p_5 out	p_4 , p_5 in	p_4 , p_5 in	p_4 , p_5 in
$Q_{4,6}$	p_4 in, p_6 out	p_4 in, p_6 out	p_4 out, p_6 in	p_4 out, p_6 in	p_4 in, p_6 out	p_4 out, p_6 in	p_4 in, p_6 out
$Q_{4,7}$	p_4 , p_7 in	p_4 , p_7 in	p_4 , p_7 in	p_4 , p_7 in	p_4 , p_7 in	p_4 , p_7 in	p_4 , p_7 in
$Q_{5,6}$	p_5 , p_6 out	p_5 , p_6 out	p_5 , p_6 out	p_5 , p_6 out	p_5 , p_6 out	p_5 , p_6 out	p_5 , p_6 out
$Q_{5,7}$	p_5 out, 7in	p_5 out, p_7 in	p_5 out, p_7 in	p_5 out, p_7 in	p_5 out, p_7 in	p_5 out, p_7 in	p_5 out, p_7 in
$Q_{6,7}$	p_6 , p_7 in	p_6 , p_7 in	p_6 , p_7 in	p_6 , p_7 in	p_6 , p_7 in	p_6 , p_7 in	p_6 , p_7 in

Table 2.8, in which each column shows the position of each pair of points $p_i, p_j \in \mathcal{P}$ with respect to the conics $Q_{i,j}$, where $1 \leq i < j \leq 7$ provided that p_7 lies one of the seven Q-regions associated to $\mathcal{P}_{\widehat{7}}$.

Let $\mathcal{P}$ be a hexagonal configuration in QC^7, and p_7 is its h-interior point. The quadruple $\left(\Gamma(\mathcal{P}), d_{\mathcal{P}}, \upsilon_{\mathcal{P}_{\widehat{7}}}, e^1_{\mathcal{P}}\right)$ is called the *dev-decorated adjacency graph* of $\mathcal{P}$, where $d_{\mathcal{P}}$ is the d-decoration of $\Gamma(\mathcal{P})$ (see Section 2.1, $\upsilon_{\mathcal{P}_{\widehat{7}}}$ is the υ-decoration of $\mathcal{P}_{\widetilde{7}}$ (see Section 2.3), and $e^1_{\mathcal{P}}$ is the induced decoration of the e-decoration of $\Gamma(\mathcal{P})$ on the edges of $\Gamma(\mathcal{P})$ with labeled by 1 (see Section 2.8).

The dev-decorated adjacency graphs representing the seven Q-deformation classes of hexagonal configurations in QC^7 are shown in Figure 2.19.

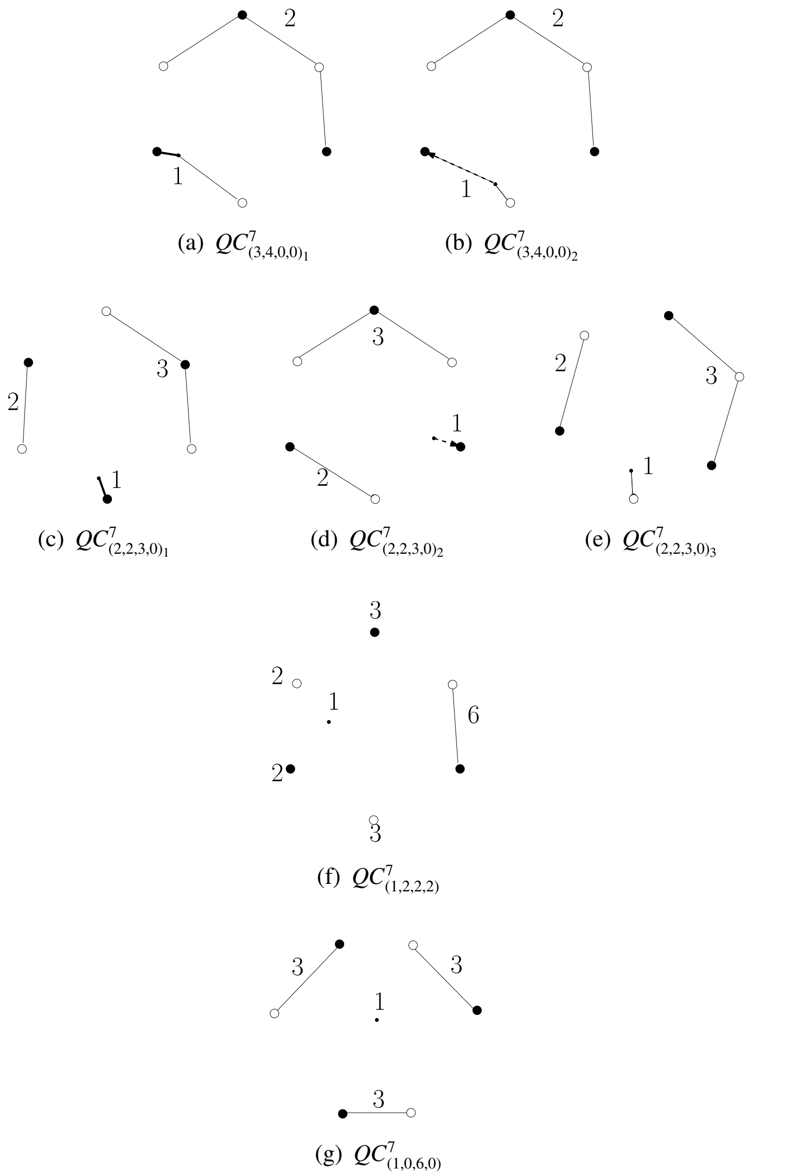

(a) $QC^7_{(3,4,0,0)_1}$ (b) $QC^7_{(3,4,0,0)_2}$

(c) $QC^7_{(2,2,3,0)_1}$ (d) $QC^7_{(2,2,3,0)_2}$ (e) $QC^7_{(2,2,3,0)_3}$

(f) $QC^7_{(1,2,2,2)}$

(g) $QC^7_{(1,0,6,0)}$

Figure 2.19: The seven Q-deformation classes for hexagonal configurations in QC^7

2.10 Pentagonal 7-configurations

Proposition 2.10.1. *The following statements hold:*

(a) $QC^7_\sigma = LC^7_\sigma$ *if* $\sigma \in \{(0,4,3,0),(0,6,1,0),(0,3,3,1)\}$.

(b) The space QC^7_σ *is connected for each* $\sigma \in \{(1,6,0,0),(1,4,2,0),(1,2,4,0)\}$.

Hence, the space of pentagonal configurations in QC^7 *has* 6 *connected components as introduced in items (a) and (b).*

Proof. For item (a), consider the L-deformation classes LC^7_σ consisting of pentagonal 7-configurations with $R_1 = 0$ for $\sigma \in \{(0,4,3,0),(0,6,1,0),(0,3,3,1)\}$ (see Table 2.1). In these cases of σ, $LC^7_\sigma \cap Q\Delta^7 = \emptyset$ since $R_1 = 0$ (that is, there are no 7-configurations in LC^7_σ such that some six points lie on a conic). This proves item (a).

To prove item (b), consider a pentagonal configuration $\mathcal{P} \in QC^7$. If the first entry of the derivative codes of $\mathcal{P}$ (see Section 2.1) is equal to 1, i.e. $R_1 = 1$, then there is a point of $\mathcal{P}$, say p_7, such that $\mathcal{P}_{\hat{7}} \in QC^6$ is a hexagonal configuration, i.e. $\mathcal{P}_{\hat{7}} \in QC^6_1$. Let us assume that the numeration of points $p_1, \dots, p_6$ of $\mathcal{P}_{\hat{7}}$ is cyclic such that p_6 is dominant. The L-polygons associated to $\mathcal{P}_{\hat{7}}$ are as shown in Figure 2.5. Since the configuration $\mathcal{P}$ is pentagonal configuration with $R_1 = 1$, the point p_7 should lie in one of the external L-polygons representing the L-deformation classes $LC^7_{(1,6,0,0)}$, $LC^7_{(1,4,2,0)}$, and $LC^7_{(1,2,4,0)}$, respectively (see Figure 2.5 and Table 2.1).

For the continuation of this proof we need the following lemma.

Lemma 2.10.2. *Assume that* $\mathcal{P} \in QC^7$ *is a pentagonal configuration such that the first entry of its derivative code is equal to* 1*, i.e.* $R_1 = 1$*, and that* $p_7 \in \mathcal{P}$ *is a point such that* $\mathcal{P}_{\hat{7}} \in QC^6_1$ *is hexagonal configuration. Then, the six conics* $Q_{i,7}$ *passing through five points of* $\mathcal{P}$ *other than* p_i *and* p_7 *do not cross external L-polygons associated to* $\mathcal{P}_{\hat{7}}$ *representing the L-deformation classes* $LC^7_{(1,6,0,0)}$, $LC^7_{(1,4,2,0)}$*, and* $LC^7_{(1,2,4,0)}$ *(see Table 2.3).*

Proof of Lemma 2.10.2. Let us assume that the numeration of points $p_1, \dots, p_6$ of $\mathcal{P}_{\hat{7}}$ is cyclic such that p_6 is dominant. By Figures 2.5 and 2.12, we observe that the six conics $Q_{i,7}$ cross only external L-polygons representing the L-deformation classes $LC^7_{(3,4,0,0)}$, $LC^7_{(2,2,3,0)}$ consisting of hexagonal 7-configurations (see Table 2.3). $\square$

The next statement is an immediate consequence of Lemma 2.10.2.

Corollary 2.10.3. *The external Q-regions and external L-polygons associated to a pentagonal configuration with $R_1 = 1$ are the same.* $\square$

The quotient space with respect to the D_3-action (i.e., the induced action of permutations of D_6 preserving colors of points of $\mathcal{P}_{\hat{7}}$) on the external Q-regions associated to $\mathcal{P}_{\hat{7}}$ has five distinct D_3-orbits. We denote by F_1, F_2, G, H_1, and H_2 the external Q-regions representing the five D_3-orbits as shown in Figure 2.20.

We denote by $QC^7_{(1,4,2,0)}$ the subspace of QC^7 consisting of pentagonal configurations with $R_1 = 1$, each of which has a point, after removing it from this 7-configuration we get a hexagonal 6-configuration, lying in its associated Q-region G. Besides, we denote by $QC^7_{(1,2,4,0)_i}$ and $QC^7_{(1,6,0,0)_i}$, $i = 1, 2$, the subspaces of QC^7 consisting of pentagonal 7-configurations with $R_1 = 1$, each configuration having a point lying in its associated Q-regions H_i and F_i, respectively. After the removal of this point from the corresponding 7-configuration we get a hexagonal 6-configuration.

To show the connectedness of these subspace we need the following observation:

Lemma 2.10.4. *Let $\mathcal{P}^i \in QC^7$, $i = 0, 1$, be two pentagonal configurations with $R_1 = 1$, and p^i_7 be a point of $\mathcal{P}^i$ such that $\mathcal{P}^i_{\hat{7}} = \mathcal{P}^i \setminus \{p^i_7\} \in QC^6_1$. Assume that for each $i = 0, 1$, F^i_j, $j = 1, 2$, are the external Q-regions associated to $\mathcal{P}^i$ as introduced above. If, in addition, p^i_7 lies in either F^i_1 or F^i_2 then $\mathcal{P}^0$ is Q-deformation equivalent to $\mathcal{P}^1$. Besides, assume that for each $i = 0, 1$, H^i_j, $j = 1, 2$, are the external Q-regions associated to $\mathcal{P}^i$ as introduced above. If, in addition, p^i_7 lies in either H^i_1 or H^i_2, then $\mathcal{P}^0$ is Q-deformation equivalent to $\mathcal{P}^1$.*

Proof of Lemma 2.10.4. We assume that the numerations of six points $p^i_1, p^i_2,$

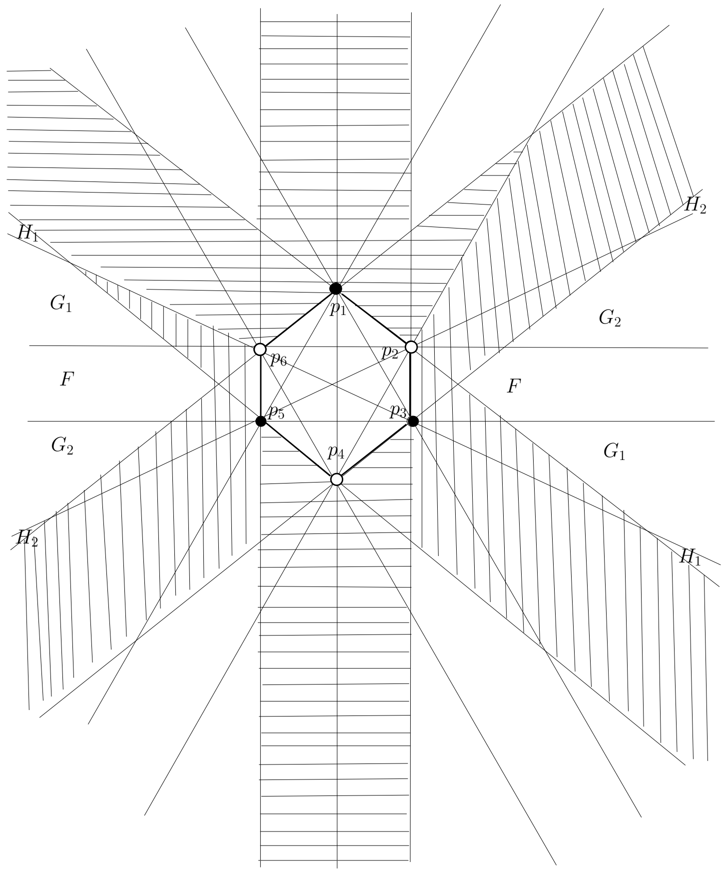

Figure 2.20: The five D_3-orbits on external Q-regions associated to a pentagonal 7-configurations with $R_1 = 1$ where the shaded external L-polygons show that these polygons are not taken into account.

$p_3^i, p_4^i, p_5^i, p_6^i \in \mathcal{P}^i$, $i = 0, 1$, different from p_7^i are cyclic such that p_6^i are dominant points. By Lemma 2.10.2, for each $i = 0, 1$, the external Q-regions G_j^i and H_j^i, $j = 1, 2$, are not crossed by six conics $Q_{k,7}^i$ passing through five points of $\mathcal{P}$ other than p_k^i and p_7^i for every $k = 1, \ldots, 6$. This is the reason why for each $i = 0, 1$, these regions can not collapse during a Q-deformation $\{\mathcal{P}_{\widehat{7}}^t\}$, $t \in [0, 1]$. Therefore, we can extend this deformation to the Q-deformation $\{\mathcal{P}^t\}$, $t \in [0, 1]$. From Figure 2.20 the two Q-regions F_1^i, F_2^i (respectively, the two Q-regions H_1^i, H_2^i) differ by a projective transformation for each $i = 0, 1$. Therefore, in both cases of the positions of p_7^0 and p_7^1, $\mathcal{P}^0$ is Q-deformation equivalent to $\mathcal{P}^1$. □

The following result is immediate consequence of Lemma 2.10.4.

Corollary 2.10.5. *The spaces* $QC^7_{(1,2,4,0)_j}$, $QC^7_{(1,6,0,0)_j}$, $j = 1, 2$ *are connected. Moreover, the space* $QC^7_{(1,2,4,0)_1}$ *(respectively, the space* $QC^7_{(1,6,0,0)_1}$*) is equal to* *the space $QC^7_{(1,2,4,0)_2}$ (respectively, the space $QC^7_{(1,6,0,0)_2}$).* $\square$

From now on, in both cases $j = 1, 2$, the spaces $QC^7_{(1,2,4,0)_j}$ and $QC^7_{(1,6,0,0)_j}$ are denoted by just $QC^7_{(1,2,4,0)}$ and $QC^7_{(1,6,0,0)}$.

By Corollary 2.10.5, we obtain Table 2.9. This table shows the correspondence between D_3-orbits in $\Lambda_Q(\mathcal{P})$ for any pentagonal configuration $\mathcal{P} \in QC^6$ and Q-deformation classes of the augmented configurations in QC^7 (i.e., each of them is obtained from $\mathcal{P}$ by adding just one point of $\mathbb{R}P^2$ to one of the Q-regions in $\Lambda_Q(\mathcal{P})$).

Table 2.9: The five D_3-orbits of Q-regions associated to a hexagonal configuration in QC^6 representing the three Q-deformation classes of pentagonal configurations with $R_1 = 1$ in QC^7.

D_3-orbits	Q-deformation classes in QC^7
$[G]^Q_3$	$QC^7_{(1,4,2,0)}$
$[H_1]^Q_3$, $[H_2]^Q_3$	$QC^7_{(1,2,4,0)}$
$[F_1]^Q_3$, $[F_2]^Q_3$	$QC^7_{(1,6,0,0)}$

Let $\mathcal{P}$ be a pentagonal configuration with $R_1 = 1$ in QC^7, and assume that $\mathcal{P}_{\widehat{p}} \in QC^6_1$ for some $p \in \mathcal{P}$. The triplet $\left(\Gamma(\mathcal{P}), d_{\mathcal{P}}, v_{\mathcal{P}_{\widehat{p}}}\right)$ is called the *dv-decorated adjacency graph* of $\mathcal{P}$, where $d_{\mathcal{P}}$ is d-decoration of $\Gamma(\mathcal{P})$, and $v_{\mathcal{P}_{\widehat{p}}}$ is the v-decoration of $\mathcal{P}_{\widehat{p}}$.

The dv-decorated adjacency graphs representing three Q-deformation classes of pentagonal configurations with $R_1 = 1$ in QC^7 are shown in Figure 2.21.

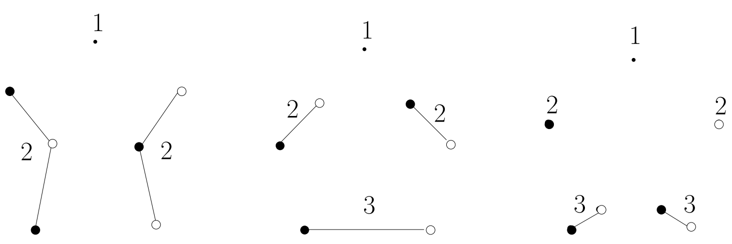

(a) $QC^7_{(1,6,0,0)}$ (b) $QC^7_{(1,4,2,0)}$ (c) $QC^7_{(1,2,4,0)}$

Figure 2.21: The three Q-deformation classes for pentagonal 7-configurations with $R_1 = 1$ in QC^7.

2.11 Proof of Theorem 2.5.1

By Proposition 2.8.2 we see that there is one Q-deformation class for heptagonal configurations in QC^7. By Proposition 2.9.1 we see that there are 7 Q-deformation classes for hexagonal configurations QC^7. By Proposition 2.10.1 we see that there are 6 Q-deformation classes for pentagonal configurations in QC^7. Therefore, there are totally 14 Q-deformation classes in QC^7.

CHAPTER 3

CONFIGURATIONS OF POINTS IN $\mathbb{R}P^1 \times \mathbb{R}P^1$

3.1 Permutation diagrams

Let C_n be a cyclic subgroup of the permutation group S_n generated by the cyclic permutation $(2\ 3\ \ldots\ n\ 1)$, or in other words, C_n consists of the permutations preserving the cyclic order of the set $\{1, \ldots, n\}$. We denote by D_n the dihedral subgroup of S_n formed by the permutations which preserve or reverse this order.

We consider an *RL-cyclic action* of the group $C_n \times C_n$ on the symmetry group S_n defined by $(a, b)\sigma = a\sigma b$, where $\sigma \in S_n$ and $a, b \in C_n$. We call the orbit of a permutation $\sigma \in S_n$ under the *RL*-cyclic action the *permutation class* of σ, and denoted it by $[\sigma]$. In addition, we consider an *RL-dihedral action* of the group $D_n \times D_n$ on the group S_n defined similarly. We call the orbit of a permutation $\sigma \in S_n$ under the *RL*-dihedral action the *coarse permutation class* of σ, and denoted it by $\langle\sigma\rangle$.

For example, in the case of $n = 4$, there are three permutation classes, namely, [1234], [1243], and [4321] and two coarse permutation classes, namely, $\langle 1234\rangle$ and $\langle 1243\rangle$. We may indicate that the coarse class $\langle 1234\rangle$ splits into a pair of permutation classes [1234] and [4321].

These permutation classes, $[\sigma]$, can be represented by certain diagrams $Z_{[\sigma]}$ shown on Figure 3.1(a)-(c). Similarly, these coarse permutation classes $\langle\sigma\rangle$ can be represented by diagrams $Z_{\langle\sigma\rangle}$ on the same Figure 3.1(d)-(e).

The following proposition is straightforward.

Figure 3.1: The permutation class diagrams $Z_{[\sigma]}$ and coarse permutation class diagrams $Z_{\langle\sigma\rangle}$ for $\sigma \in S_4$.

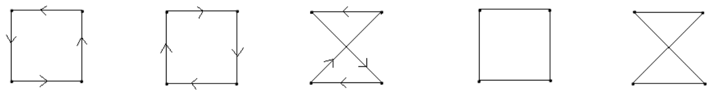

(a) $Z_{[1234]}$ (b) $Z_{[4321]}$ (c) $Z_{[1243]}$ (d) $Z_{\langle 1234\rangle}$ (e) $Z_{\langle 1243\rangle}$

Proposition 3.1.1. *The group S_5 has 8 permutation classes and 4 coarse permutation classes. The coarse permutation classes are $\langle 12345\rangle$, $\langle 12543\rangle$, $\langle 13425\rangle$, and $\langle 13524\rangle$. Each of them splits, respectively, into a pair of permutation classes, namely,* $([12345], [54321])$*,* $([12354], [45321])$*,* $([13254], [45231])$*, and* $([13524], [42531])$. □

Remark 3.1.2. *One coarse permutation class $\langle\sigma\rangle$ for $\sigma \in S_n$ may contain maximum 4 permutation classes $[\sigma]$. But for $n = 5$ or less, there may be maximum two permutation classes $[\sigma]$ in one class $\langle\sigma\rangle$.*

The following diagrams represent the above 8 permutation classes $[\sigma]$, and 4 coarse permutation classes $\langle\sigma\rangle$.

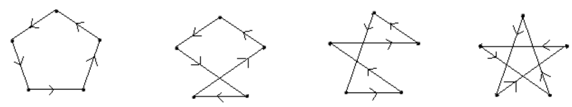

(f) $Z_{[12345]}$ (g) $Z_{[12543]}$ (h) $Z_{[13425]}$ (i) $Z_{[13524]}$

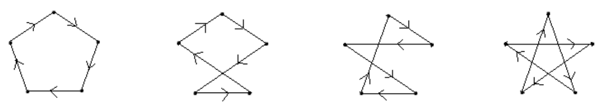

(j) $Z_{[54321]}$ (k) $Z_{[34521]}$ (l) $Z_{[52431]}$ (m) $Z_{[42531]}$

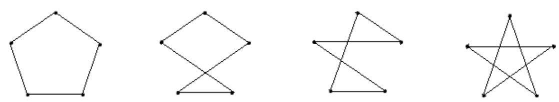

(n) $Z_{\langle 12345\rangle}$ (o) $Z_{\langle 12543\rangle}$ (p) $Z_{\langle 13425\rangle}$ (q) $Z_{\langle 13524\rangle}$

Figure 3.2: The permutation class diagrams $Z_{[\sigma]}$ and the coarse permutation class diagrams $Z_{\langle\sigma\rangle}$ for $\sigma \in S_5$.

For a given permutation $\sigma = \begin{pmatrix} i_1 & i_2 & \cdots & i_n \end{pmatrix} \in S_n$, we will introduce 3 objects: a *permutation diagram* Z_σ, a *permutation class diagram* $Z_{[\sigma]}$, and a *coarse permutation class diagram* $Z_{\langle\sigma\rangle}$. Choose n points in $\mathbb{R}P^2$ such that they form a regular n-gon and numerate them with $1, \ldots, n$ in the counterclockwise direction. We obtain a permutation diagram with arrows by joining the vertices i_1 to i_2, i_2 to i_3, and so on. In the last part of the construction of the permutation diagram, we close the diagram by joining the vertices i_n to i_1. The vertex i_1 in this construction is called the *initial vertex* of this diagram, and we denote the vertex in bold. As σ, we take, for example, the permutation $\sigma = (3\ 1\ 4\ 2) \in S_4$, so its permutation diagram Z_σ is homeomorphic to

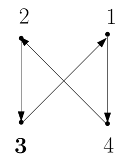

Figure 3.3: The permutation diagram $Z_{(3142)}$ with initial vertex 3 for permutation $(3142) \in S_4$.

If in the same diagram shown on Figure 3.3 you choose 1 as the initial point, then it becomes a permutation diagram for permutation (1423).

The cyclic group C_n, which is generated by $\mu = (2\ 3\ \cdots\ n\ 1) \in S_n$ can be seen as a subset of the dihedral group D_n since D_n has two generators $\mu = (2\ 3\ \cdots\ n\ 1)$ and $d = (n\ n{-}1\ \cdots\ 1)$ with orders n and 2, respectively, such that $\mu \cdot d \cdot \mu^{-1} = d^{-1}$. The following two trivial propositions show the geometric meaning of the *RL*-cyclic action and *RL*-dihedral action on permutation diagrams.

Proposition 3.1.3. *Assume that Z_σ, $Z_{\mu\sigma}$, $Z_{\sigma\mu}$ are permutation diagrams where $\sigma \in S_n$, and $\mu = (2\ 3\ \cdots\ n\ 1)$ is the generator of the cyclic group C_n. Then:*

(a) The permutation diagram $Z_{\mu\sigma}$ is obtained from Z_σ by a rotation.

(b) The permutation diagram $Z_{\sigma\mu}$ is obtained from Z_σ by change of its initial point. □

Proposition 3.1.4. *Assume that Z_σ, $Z_{d\sigma}$, and $Z_{\sigma d}$ are permutation cycles where $\sigma \in S_n$, and d is the generator of D_n with order 2. Then:*

(a) The permutation diagram $Z_{d\sigma}$ is obtained from Z_σ by a reflection.

(b) The permutation diagram $Z_{\sigma d}$ is obtained from Z_σ by reversion of its orientation. □

By a *permutation class diagram* of $\sigma \in S_n$, we mean the set of permutation diagrams differ from the permutation diagram Z_σ by a rotation, and it is denoted by $Z_{[\sigma]}$. By a *coarse permutation class diagram* of $\sigma \in S_n$, we mean the set of permutation diagrams differ the permutation diagram Z_σ by a rotation and a reflection, and it is denoted by $Z_{\langle\sigma\rangle}$ (see Figures 3.1 and 3.2). By Propositions 3.1.3 and 3.1.4 together with the description, we have the following corollary.

Corollary 3.1.5. *The map $[\sigma] \mapsto Z_{[\sigma]}$ establishes a one-to-one correspondence between the set of permutation classes and that of permutation diagrams. Similarly, the map $\langle\sigma\rangle \mapsto Z_{\langle\sigma\rangle}$ establishes a one-to-one correspondence between the set of coarse permutation classes and that of coarse permutation diagrams.* □

3.2 Bi-ordering

For a given finite set X with cardinality n, an *ordering* on X is a one-to-one map from X to $\{1, \dots, n\}$. The set of all orderings on X is denoted by $Ord(X)$. We say that the set X is *ordered* if it has a distinguished ordering. By a *bi-ordering* on X, we mean a pair of orderings on X, $(f, g) \in Ord^2(X)$.

The symmetric group S_n acts freely and transitively from the right on the set $Ord(X)$. We consider the quotient space $Cyc(X) = Ord(X)/C_n$ of $Ord(X)$ by the action of the cyclic group $C_n \subset S_n$, and call the elements $[f] \in Cyc(X)$ *cyclic orderings on X*. Similarly, we consider the quotient space $Dih(X) = Ord(X)/D_n$ of $Ord(X)$ by the action of the dihedral group $D_n \subset S_n$, and call the elements $[f] \in Dih(X)$ *coarse cyclic orderings on X*.

A pair of cyclic orderings on X, $([f], [g]) \in Cyc^2(X)$ is called *cyclic bi-ordering* on X. We denote by $Cyc^2(X) = Ord(X)/C_n \times Ord(X)/C_n$ the set of cyclic bi-orderings on S. Note that

$$Cyc^2(X) = Ord(X)/C_n \times Ord(X)/C_n = Ord^2(X)/{C_n}^2,$$

and the correspondence

$$([f],[g]) \mapsto [g \circ f^{-1}]$$

defines a map from $Cyc^2(X)$ to $S_n/C_n \times C_n$.

A pair of coarse cyclic orderings on X, $([f],[g]) \in Dih^2(X)$ is called *coarse cyclic bi-ordering* on X. We denote by $Dih^2(X) = Ord(X)/D_n \times Ord(X)/D_n$ the set of coarse cyclic bi-orderings on S. Note that

$$Dih^2(X) = Ord(X)/D_n \times Ord(X)/D_n = Ord^2(X)/{D_n}^2,$$

and the correspondence

$$(\langle f \rangle, \langle g \rangle) \mapsto \langle g \circ f^{-1} \rangle$$

defines a map from $Dih^2(X)$ to $S_n/D_n \times D_n$.

Remark 3.2.1. We can associate a permutation diagram $Z_{g\circ f^{-1}}$ to a bi-ordering (f, g), and a permutation class $Z_{[g\circ f^{-1}]}$ (respectively, a coarse permutation class $Z_{\langle g\circ f^{-1}\rangle}$) to a cyclic bi-ordering $([f],[g])$ (respectively, a coarse cyclic bi-ordering $(\langle f \rangle, \langle g \rangle)$).

3.3 Linearly nondegenerate n-configurations on $\mathbb{R}P^1 \times \mathbb{R}P^1$

For any field $\mathbb{K}$, we say that an n-configuration $\mathcal{P} \in S^n(\mathbb{K}P^1 \times \mathbb{K}P^1)$ is *linearly nondegenerate* if there exists no generatrix of $\mathbb{K}P^1 \times \mathbb{K}P^1$ passing through two points of $\mathcal{P}$. We denote by $LC^n(\mathbb{K}P^1 \times \mathbb{K}P^1)$ the space of linearly nondegenerate n-configurations in $\mathbb{K}P^1 \times \mathbb{K}P^1$. This space is a Zariski open subset of the algebraic variety $S^n(\mathbb{K}P^1 \times \mathbb{K}P^1)$.

As in the space of planar configurations (see Section 2.1), we say that two n-configurations in $LC^n(\mathbb{R}P^1 \times \mathbb{R}P^1)$ are *L-deformation equivalent* if there exists an *L-deformation* between them (equivalently, they are in the same connected components of the space $LC^n(\mathbb{R}P^1 \times \mathbb{R}P^1)$). We say that two n-configurations in $LC^n(\mathbb{R}P^1 \times \mathbb{R}P^1)$ are *coarse L-deformation equivalent* if one of these configurations is L-deformation equivalent to the image of the other under a map in $PGL(2,\mathbb{R})\times PGL(2,\mathbb{R})$ (equivalently, they are in the same connected component of the quotient space $LC^n(\mathbb{R}P^1 \times \mathbb{R}P^1)/PGL(2,\mathbb{R}) \times PGL(2,\mathbb{R})$ with respect to the action of the group $PGL(2,\mathbb{R}) \times PGL(2,\mathbb{R})$ on $\mathbb{R}P^1 \times \mathbb{R}P^1$).

Remark 3.3.1. The group $PGL(2,\mathbb{R})$ has two connected components. So, a coarse deformation class may contain maximum 4 deformation classes. However, if n is not greater than 5, it turns out that there may be not more than two deformation classes in one coarse deformation class. (In terms of the permutation class diagrams, there are two "reflection" operations: one can reverse the direction of the arrows, and one can take a mirror reflection of a diagram with respect to some line. For 5 or less vertices the results are equivalent, that is why you may have not more than two deformation classes in one coarse class.

Any n-configuration $\mathcal{P} \in LC^n(\mathbb{R}P^1 \times \mathbb{R}P^1)$ admits a cyclic bi-ordering as follows: first, let π_1 be the first projection from $\mathbb{R}P^1 \times \mathbb{R}P^1$ to the first oriented line $\mathbb{R}P^1_1$ given by $(x,y) \to x$, and π_2 be the second projection from $\mathbb{R}P^1 \times \mathbb{R}P^1$ to the second oriented line $\mathbb{R}P^1_2$ given by $(x,y) \to y$. We consider the images of points of $\mathcal{P}$ under π_1 and π_2, so we get a pair of n-tuples of points on these lines. Let us enumerate the n points on the first line by $1, 2, \dots, n$ and let us assume that the enumeration of the other n points on the second line is $i_1, i_2, \dots, i_n$. Then, the cyclic orders on these lines induce two cyclic orderings $f_1 : \mathcal{P} \to \{1, \dots, n\}$ and $f_2 : \mathcal{P} \to \{1, \dots, n\}$, where $f_1(p_k) = k$ and $f_2(p_k) = i_k$ for any $p_k \in \mathcal{P}$, $k = 1, \dots, n$. Then, $(f_1, f_2) \in Ord^2(\mathcal{P})$. We shall denote by $\sigma_{\mathcal{P}} = f_2 \circ f_1^{-1}$ the permutation associated to $\mathcal{P}$

$$\begin{pmatrix} 1 & 2 & \cdots & n-1 & n \\ i_1 & i_2 & \cdots & i_{n-1} & i_n \end{pmatrix} \in S_n.$$

This permutation depends on the point which we choose to start the enumeration. Notice that the change of orientation of line $\mathbb{R}P^1_j$, $j = 1, 2$, is the same as the change of the ordering f_j to another one $\bar{f}_j$, where $\bar{f}_j(p_k) = n + 1 - f_j(p_k)$ for any $p_k \in \mathcal{P}$, $k = 1, \dots, n$ denotes the mirror of f_j.

It follows immediately from the definition that permutation class $[\sigma_{\mathcal{P}}]$ (respectively, coarse permutation class $\langle\sigma_{\mathcal{P}}\rangle$) is an invariant under L-deformations (respectively, coarse L-deformations) of $\mathcal{P}$.

For a permutation $\sigma \in S_n$, let us denote the space of all n-configurations in $LC^n(\mathbb{R}P^1 \times \mathbb{R}P^1)$ whose permutation classes are equal to $[\sigma]$ by

$$LC^n_{[\sigma]}(\mathbb{R}P^1 \times \mathbb{R}P^1) = \{\mathcal{P} \in \mathbb{R}P^1 \times \mathbb{R}P^1 : [\sigma_{\mathcal{P}}] = [\sigma]\},$$

and the space of all n-configurations in $LC^n(\mathbb{R}P^1 \times \mathbb{R}P^1)$ whose coarse permutation classes are equal to $\langle\sigma\rangle$ by

$$LC^n_{\langle\sigma\rangle}(\mathbb{R}P^1 \times \mathbb{R}P^1) = \{\mathcal{P} \in \mathbb{R}P^1 \times \mathbb{R}P^1 : \langle\sigma_{\mathcal{P}}\rangle = \langle\sigma\rangle\}.$$

Then, right from the definition we have the following proposition.

Proposition 3.3.2. *The spaces $LC^n_{[\sigma]}(\mathbb{R}P^1 \times \mathbb{R}P^1)$ as well as their quotients $LC^n_{[\sigma]}(\mathbb{R}P^1 \times \mathbb{R}P^1)/SL(2;\mathbb{R}) \times SL(2;\mathbb{R})$ are connected for all $[\sigma] \in S_n/C_n \times C_n$, and the quotient spaces $LC^n_{\langle\sigma\rangle}(\mathbb{R}P^1 \times \mathbb{R}P^1)/PGL(2;\mathbb{R}) \times PGL(2;\mathbb{R})$ are connected for all $\langle\sigma\rangle$ in $S_n/D_n \times D_n$. Equivalently, two configurations $\mathcal{P}$ and $\mathcal{P}' \in LC^n(\mathbb{R}P^1 \times \mathbb{R}P^1)$ are coarse L-deformation equivalent if and only if $\langle\sigma_{\mathcal{P}}\rangle = \langle\sigma_{\mathcal{P}'}\rangle$. And there exists a L-deformation between them if and only if $[\sigma_{\mathcal{P}}] = [\sigma_{\mathcal{P}'}]$.* □

The next result is an immediate consequence of Proposition 3.3.2 and the result in Proposition 3.1.1 (that the diagram $Z_{<\sigma>}$ determines class $< \sigma >$).

Corollary 3.3.3. *The spaces $LC^n_{[\sigma_{\mathcal{P}}]}(\mathbb{R}P^1 \times \mathbb{R}P^1)$ for any n-configuration $\mathcal{P}$ in $LC^n(\mathbb{R}P^1 \times \mathbb{R}P^1)$ are in a one-to-one correspondence with the coarse permutation class diagram $Z_{[\sigma_{\mathcal{P}}]}$. The spaces $LC^n_{\langle\sigma_{\mathcal{P}}\rangle}(\mathbb{R}P^1 \times \mathbb{R}P^1)$ for any n-configuration $\mathcal{P} \in LC^n(\mathbb{R}P^1 \times \mathbb{R}P^1)$ are in a one-to-one correspondence with the coarse permutation class diagram $Z_{\langle\sigma_{\mathcal{P}}\rangle}$.* □

Theorem 3.3.4. *The space $LC^5(\mathbb{R}P^1 \times \mathbb{R}P^1)$ has precisely eight L-deformation classes and four coarse L-deformation classes. The coarse L-deformation classes are $LC^5_{\langle 12345\rangle}(\mathbb{R}P^1 \times \mathbb{R}P^1)$, $LC^5_{\langle 12543\rangle}(\mathbb{R}P^1 \times \mathbb{R}P^1))$, $LC^5_{\langle 13425\rangle}(\mathbb{R}P^1 \times \mathbb{R}P^1)$ and $LC^5_{\langle 13524\rangle}(\mathbb{R}P^1 \times \mathbb{R}P^1)$. Each of them splits into a pair of L-deformation classes, namely, $(LC^5_{[12345]}, LC^5_{[54321]})$, $(LC^5_{[12354]}, LC^5_{[45321]})$, $(LC^5_{[13254]}, LC^5_{[45231]})$, and $(LC^5_{[13524]}, LC^5_{[42531]})$, respectively. (See Figure 3.2.)*

Proof. It follows from Propositions 3.3.2 and Proposition 3.1.1. □

3.4 The real bidegree of real algebraic curves in $\mathbb{R}P^1 \times \mathbb{R}P^1$

Recall that an algebraic curve $A \subset \mathbb{K}P^1 \times \mathbb{K}P^1$ (over any field $\mathbb{K}$) of degree (called also bidegree) $\deg(A) = (d_1, d_2)$ is defined by a polynomial $F(x, y)$ which is homogeneous of degree d_1 with respect to $x = (x_0, x_1)$ and of degree d_2 with respect to $y = (y_0, y_1)$, or in other words,

$$F(x_0, x_1; y_0, y_1) = \sum_{i,j=1}^{d_1,d_2} a_{ij} x_0^i x_1^{d_1-i} y_0^j y_1^{d_2-j} \quad \text{where} \quad a_{ij} \in \mathbb{K}$$

If $\mathbb{K} = \mathbb{C}$, then the bidegree $\deg(A) = (d_1, d_2)$ simply represents the homology class $[A] \in H_2(\mathbb{P}^1 \times \mathbb{P}^1) = \mathbb{Z} \times \mathbb{Z}$.

In the case of a real algebraic curve A with the real locus $\mathbb{R}A \subset \mathbb{R}P^1 \times \mathbb{R}P^1$ we can always speak of the (*mod*2) *real (bi)degree*, which is the class

$$\deg_{\mathbb{R}}(A) = [\mathbb{R}A]_2 \in H_1(\mathbb{R}P^1 \times \mathbb{R}P^1; \mathbb{Z}/2) = \mathbb{Z}/2 \times \mathbb{Z}/2.$$

It is trivial (and well-known) that $\deg_{\mathbb{R}}(A) = \deg(A) \mod 2$ (congruence for each component of the bidegrees).

In certain cases, one can always define a refinement of the real bidegree for real algebraic curves. For instance, this is possible for rational curves, which include, for example, curves of bidegree $(1, d)$, or $(d, 1)$ (more generally, one can do it for so called curves of type I).

Namely, any choice of an orientation of $\mathbb{R}P^1$ gives a fundamental class $[\mathbb{R}A] \in H_1(\mathbb{R}P^1 \times \mathbb{R}P^1) = \mathbb{Z} \times \mathbb{Z}$ for a real rational curve A. We suppose that the orientation of the factors of $\mathbb{R}P^1 \times \mathbb{R}P^1$ is fixed, then the possibility to change the orientation of $[\mathbb{R}A]$ defines the *refinement of the real bidegree of* A, $\widetilde{\deg}_{\mathbb{R}}(A) = [\mathbb{R}A]$ as an equivalence class of pairs $(m_1, m_2) \in \mathbb{Z}^2$ up to simultaneous reversion of sign, $(m_1, m_2) \sim (-m_1, -m_2)$.

Proposition 3.4.1. *A curve of complex bidegree* $(2, 1)$ *on* $\mathbb{P}^1 \times \mathbb{P}^1$ *has one of the three real bidegree* $(2, 1)$*,* $(0, 1)$*, and* $(-2, 1)$.

Proof. For a real curve A with $deg_(A) = (d_1, d_2)$ and $\widetilde{\deg}_{\mathbb{R}}(A) = (m_1, m_2)$, the following conditions are satisfied.

(a) $m_i \equiv d_i \ \ mod\ 2$ for each $i \in \{1, 2\}$

(b) $|m_i| \leq d_i$ for each $i \in \{1, 2\}$.

This completes the proof. $\square$

3.5 Curves of bidegree $(1, 1)$

In what follows, we will need the following simple and well-known fact about curves of bidegree $(1, 1)$ on $\mathbb{P}^1 \times \mathbb{P}^1$. Its proof consists in simple counting of parameters and applying Bezout's theorem with respect to the generatrices $\mathbb{P}^1 \times \{p\}$ and $\{q\} \times \mathbb{P}^1$ for some $p, q \in \mathbb{P}^1$.

Proposition 3.5.1. *Let $\mathcal{P}$ be a 3-configuration in $\mathbb{K}P^1 \times \mathbb{K}P^1$ where $\mathbb{K}$ is a field. Then:*

(a) There exists a curve of bidegree $(1, 1)$ on $\mathbb{K}P^1 \times \mathbb{K}P^1$ passing through three points of $\mathcal{P}$.

(b) If no three points of $\mathcal{P}$ are collinear, then such a curve which is mentioned in the item (a) is unique. In particular, if $\mathcal{P} \in LC^3(\mathbb{K}P^1 \times \mathbb{K}P^1)$, then the curve is unique.

(c) A curve of bidegree $(1, 1)$ passing through three points of $\mathcal{P}$ is nonsingular if and only if $\mathcal{P} \in LC^3(\mathbb{K}P^1 \times \mathbb{K}P^1)$. $\square$

By Adjunction Formula, an irreducible curve of complex bidegree $(1, n)$ (or of complex bidegree $(n, 1)$) for any nonnegative integer n is rational.

3.6 Quadratically nondegenerate n-configurations on $\mathbb{R}P^1 \times \mathbb{R}P^1$

Let $\mathbb{K}$ be a field. An n-configuration $\mathcal{P} \in \mathbb{K}P^1 \times \mathbb{K}P^1$ is called *quadratically nondegenerate* if there exists no generatrix of $\mathbb{K}P^1 \times \mathbb{K}P^1$ passing through two points of $\mathcal{P}$ and there exists no curves with bidegree $(1,1)$ on $\mathbb{K}P^1 \times \mathbb{K}P^1$ containing four points of $\mathcal{P}$. If $\mathbb{K} = \mathbb{R}$, the space of quadratically nondegenerate n-configurations $QC^n(\mathbb{R}P^1 \times \mathbb{R}P^1)$ is a Zariski open subset of the algebraic variety $S^n(\mathbb{R}P^1 \times \mathbb{R}P^1)$. Notice that $QC^n(\mathbb{R}P^1 \times \mathbb{R}P^1) \subset LC^n(\mathbb{R}P^1 \times \mathbb{R}P^1)$.

As in the space of planar configurations (see Section 2.3), we say that two n-configurations in $QC^n(\mathbb{R}P^1 \times \mathbb{R}P^1)$ are *Q-deformation equivalent* if there exists an *Q-deformation* between them (equivalently, they are in the same connected components of the space $QC^n(\mathbb{R}P^1 \times \mathbb{R}P^1)$). We say that two n-configurations in $QC^n(\mathbb{R}P^1 \times \mathbb{R}P^1)$ are *coarse Q-deformation equivalent* if one of these configurations is Q-deformation equivalent to the image of the other under a map in $PGL(2,\mathbb{R}) \times PGL(2,\mathbb{R})$ (equivalently, they are in the same connected component of the quotient space $QC^n(\mathbb{R}P^1 \times \mathbb{R}P^1)/PGL(2,\mathbb{R}) \times PGL(2,\mathbb{R})$ with respect to the action of the group $PGL(2,\mathbb{R}) \times PGL(2,\mathbb{R})$ on $\mathbb{R}P^1 \times \mathbb{R}P^1$).

3.7 Curves of bidegree $(1,2)$ and bidegree $(2,1)$

The following simple and well-known fact gives some sufficient conditions for the existence and uniqueness of a nonsingular curve of bidegree $(1,2)$, or $(2,1)$ on $\mathbb{K}P^1 \times \mathbb{K}P^1$ for any field $\mathbb{K}$.

Proposition 3.7.1. *Let $\mathcal{P}$ be a 5-configuration in $\mathbb{K}P^1 \times \mathbb{K}P^1$ where $\mathbb{K}$ is a field. Then:*

(a) There exists a curve of bidegree $(1,2)$ (or, of bidegree $(2,1)$) on $\mathbb{K}P^1 \times \mathbb{K}P^1$ passing through five points of $\mathcal{P}$.

(b) A curve of bidegree $(1,2)$ (or, of bidegree $(2,1)$) passing through five points of $\mathcal{P}$ is unique and it is nonsingular if and only if $\mathcal{P} \in QC^5(\mathbb{K}P^1 \times \mathbb{K}P^1)$. □

Form now on, for a given 5-configuration $\mathcal{P} \in QC^5(\mathbb{R}P^1 \times \mathbb{R}P^1)$, we shall denote by $A^1_{\mathcal{P}}$ and $A^2_{\mathcal{P}}$ the curves of complex bidegree $(1,2)$ and $(2,1)$ passing through five points of $\mathcal{P}$, respectively.

Remark 3.7.2. The blow-up of $\mathbb{P}^1 \times \mathbb{P}^1$ at a 5-configuration $\mathcal{P}$ gives a non-singular del Pezzo surface degree 3 if and only if this configuration is quadratically nondegenerate. The 27 lines on the cubic surface (i.e., the anti-canonical model of the del Pezzo surface) are the exceptional curves over the 5 blown-up points, the proper transformations of the 10 generatrices passing through each of the five points, the proper transformations of the 10 curves of complex bidegree $(1, 1)$ passing through each of $\binom{5}{3}$ triples of points chosen among the given 5 points, and the proper transformations of $A^1_{\mathcal{P}}$ and $A^2_{\mathcal{P}}$.

Proposition 3.7.3. *Two nonsingular real algebraic curves of complex bidegree* $(2, 1)$ *on* $\mathbb{P}^1 \times \mathbb{P}^1$ *are projectively equivalent if they have the same refinement of real bidegree.*

Proof. On a given curve A of complex bidegree $(2, 1)$ choose any point, $p = (x_1, x_2)$, blow up it, and then blow down generatrices $x_1 \times \mathbb{P}^1$ and $\mathbb{P}^1 \times x_2$. $\mathbb{P}^1 \times \mathbb{P}^1$ will be transformed into a plane $\mathbb{P}^2$, and the image of curve A will be a conic A'. The generatrix $x_1 \times \mathbb{P}^1$ will be contracted to a point $p_1 \in \mathbb{P}^2 \setminus A'$, and the generatrix $\mathbb{P}^1 \times x_2$ to a point on A'. Such triples (A', p_1, p_2) are clearly projectively equivalent over $\mathbb{C}$. Over $\mathbb{R}$, however, there are two options: point p_1 may lie in the interior of the ellipse $A'(\mathbb{R})$, or in its exterior. The first case corresponds to A having $\widetilde{\deg}_{\mathbb{R}}(A) = (2, 1)$, and the second case corresponds to A having $\widetilde{\deg}_{\mathbb{R}}(A) = (0, 1)$. $\square$

3.8 A further project on Q-deformation classification of configurations of 5 points in $\mathbb{R}P^1 \times \mathbb{R}P^1$

We sketch below some incomplete project on the Q-deformation classification of 5-configurations of points in $\mathbb{R}P^1 \times \mathbb{R}P^1$.

Remark 3.8.1. The curve $A^1_{\mathcal{P}}$ (respectively, $A^2_{\mathcal{P}}$) for $\mathcal{P} \in QC^5(\mathbb{R}P^1 \times \mathbb{R}P^1)$ is a rational and nonsingular curve, so there is a cyclic order coming from $A^1_{\mathcal{P}}$ (respectively, from $A^2_{\mathcal{P}}$) as follows: Case 1: Assume that $\widetilde{\deg}_{\mathbb{R}}(A^1_{\mathcal{P}}) = (1, 0)$. We recall from Section 3.3 that $\mathcal{P}$ admits a cyclic bi-ordering, and that this bi-ordering associates $\mathcal{P}$ with a permutation $\sigma_{\mathcal{P}} \in S_5$. Let us denote by $p_i^{\sigma_{\mathcal{P}}(i)}$, $i = 1, \dots, 5$, the points of $\mathcal{P}$. Denote by p_i and $p^{\sigma_{\mathcal{P}}(i)}$, the images $\pi_1(p_i^{\sigma_{\mathcal{P}}(i)})$ and $\pi_2(p_i^{\sigma_{\mathcal{P}}(i)})$ standing on the i-th place and the $\sigma_{\mathcal{P}}(i)$-th place, respectively.

The image of the real part $\mathbb{R}A^1_{\mathcal{P}}$ under π_2 is topologically circle, and the circle contains the points $p^{\sigma_{\mathcal{P}}(i)}$, $i = 1, \ldots, 5$. We can continuously move these points along this circle such that two points $p^{\sigma_{\mathcal{P}}(i_1)}$, $p^{\sigma_{\mathcal{P}}(i_5)}$ among the five points $p^{\sigma_{\mathcal{P}}(i)}$ for some distinct numbers $i_1, i_5 \in \{1, \ldots, 5\}$ lie on the circle as shown in Figure 3.4.

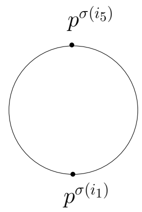

Figure 3.4

For the positions of the remaining points $p^{\sigma_{\mathcal{P}}(i_k)}$, $k = 2, 3, 4$, on this circle, there are 8 possibilities shown in Figure 3.5 up to deformations. This is equivalent to say that there are eight cyclic orders coming from $A^1_{\mathcal{P}}$ with $\widetilde{\deg}_{\mathbb{R}}(A^1_{\mathcal{P}}) = (1, 0)$ for any configurations $\mathcal{P} \in QC^5(\mathbb{R}P^1 \times \mathbb{R}P^1)$.

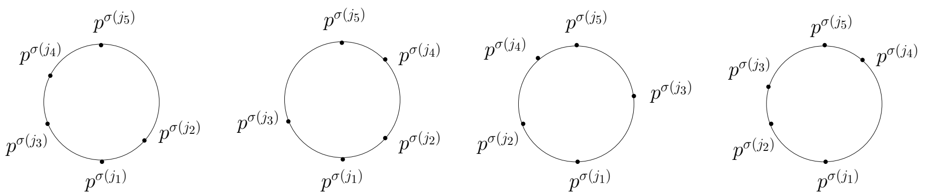

(a) (12543) (b) (12453) (c) (13542) (d) (14532)

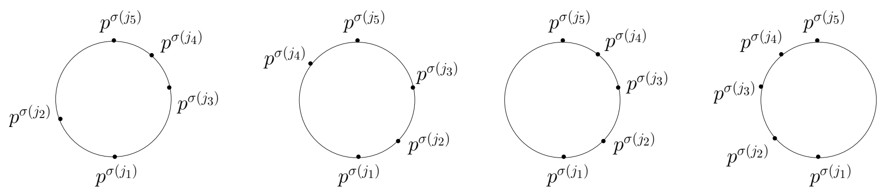

(e) (13452) (f) (12354) (g) (12345) (h) (15432)

Figure 3.5: The eight cyclic orders coming from $A^1_{\mathcal{P}}$ with $deg_{\mathbb{R}}(A^1_{\mathcal{P}}) = (1, 0)$ for any configurations $\mathcal{P} \in QC^5(\mathbb{R}P^1 \times \mathbb{R}P^1)$.

Case 2: Assume that $\widetilde{\deg}_{\mathbb{R}}(A^1_{\mathcal{P}}) = (1, 2)$. In this case the image of the real part $\mathbb{R}A^1_{\mathcal{P}}$ under π_2 is a double covering over the second factor $\mathbb{R}P^1$. In this case, it is not easy to understand at which point we are starting.

All the presented research may lead to the insight that the pair $(\widetilde{\deg}_{\mathbb{R}}(A), [\sigma])$ for any $[\sigma]$ in $S_5/C_5 \times C_5$ are invariants for the Q-deformation classes in $QC^5(\mathbb{R}P^1 \times$

$\mathbb{R}P^1$). Similarly, the pair $(\widetilde{\deg}_{\mathbb{R}}(A), \langle\sigma\rangle)$ for any $\langle\sigma\rangle$ in $S_5/D_{10}{\times}D_{10}$ are invariants for the coarse Q-deformation classes in $QC^5(\mathbb{R}P^1 \times \mathbb{R}P^1)$). Although we don't know which $[\sigma]$ (respectively, $\langle\sigma\rangle$) are possible for which $\widetilde{\deg}_{\mathbb{R}}(A)$, we believe that the space $QC^5(\mathbb{R}P^1 \times \mathbb{R}P^1)$ has four coarse Q-deformation classes. Each of them splits into a pair of Q-deformation classes among the eight. This can be investigated in a further study.

CHAPTER 4

CREMONA TRANSFORMATION OF PLANE CONFIGURATIONS OF POINTS

The aim of this chapter is to understand how an n-configuration $\mathcal{P} \in QC^n$ for $n = 6, 7$ changes under the quadratic Cremona transformations, Cr_{ijk}, based at a triple of points, p_i, p_j, p_k, of the configuration $\mathcal{P} = \{p_1, \ldots, p_n\}$. Recall that such transformation consists in blowing up $\mathbb{P}^2$ at points p_i, p_j, p_k and then blowing down the images of lines L_{ij}, L_{jk}, and L_{ki} passing through the pairs $\{p_i, p_j\}$, $\{p_j, p_k\}$, and $\{p_k, p_i\}$ of points, respectively. We denote by $Cr_{ijk}(\mathcal{P})$ a new n-configuration formed by the $n-3$ points different from p_i, p_j, p_k, and the three images of L_{ij}, L_{jk}, L_{ki}, which are denoted p_{ij}, p_{jk}, p_{ki}, or (abuse of the notation if it does not lead to a confusion) by p_k, p_i, p_j, respectively.

4.1 Cremona transformations of 6-configurations

The modifications of a hexagonal configuration $\mathcal{P} \in QC^6_1$ under quadratic Cremona transformations based at six distinct triples of points (up to the action of the monodromy group of the hexagonal configuration which preserves dominant and subdominant points of $\mathcal{P}$) are as shown in Figure 4.1.

Theorem 4.1.1. *The Q-deformation classes of all 6-configurations in QC^6 are obtained from hexagonal configurations in QC^6_1 by quadratic Cremona transformations based at some triple of points of these configuration as shown in Figure 4.1.*

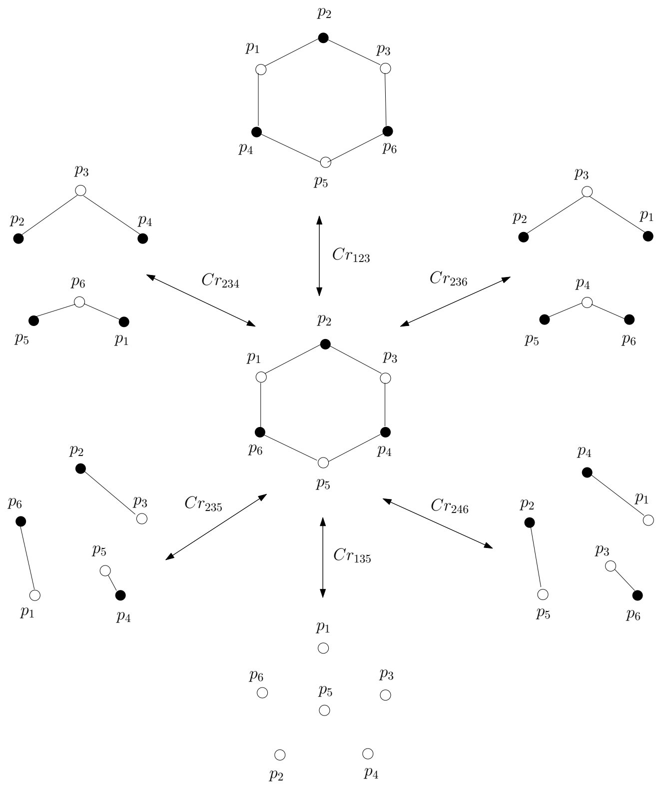

Figure 4.1: The images of a configuration $\mathcal{P} \in QC_1^6$ under quadratic Cremona transformations for any six triples. The black and white circles show the outer and inner point, respectively.

Proof. Figure 4.1 shows the deformation classes of 6-configurations (i.e., QC_1^6, QC_2^6, QC_3^6, and QC_4^6) obtained from a hexagonal configuration $\mathcal{P}$ by Cr_{ijk} after different choices of the base points p_i, p_j, p_k. The proof of it is a straightforward analysis using a model $[x : y : z] \mapsto [yz : xz : xy]$ of a Cremona transformation. □

The reason why we only consider the quadratic Cremona transformations based at six triples of points for a given hexagonal 6-configuration shown in Figure 4.1 comes from the following observation.

Remark 4.1.2. Due to Finashin [F], the monodromy groups of 6-configurations (i.e., the group of symmetries of 6-configurations in QC^6 preserving dominant and subdominant points) which belong to the Q-deformation classes QC_1^6, or QC_2^6, or QC_3^6, or QC_6^6 are D_3, or $\mathbb{Z}_4$, or D_3, or the icosahedral symmetry group, respectively. By using these results, we get the following observations:

(a) Assume that $\mathcal{P} \in QC^6_1$, and that the numeration $p_1, \ldots, p_6$ of the points of $\mathcal{P}$ is cyclic. Then there are six distinct triples up to the action of D_3, namely, $\{p_1p_2p_4\}$, $\{p_1p_2p_5\}$, $\{p_1p_2p_3\}$, $\{p_1p_2p_6\}$, $\{p_1p_3p_5\}$, $\{p_2p_4p_6\}$.

(b) Assume that $\mathcal{P} \in QC^6_2$, and that the numeration $p_1, \ldots, p_5$ of points of $\mathcal{P}$ other than p_6 is cyclic such that p_6 is inside the Q-region B associated to $\mathcal{P}_{\hat{6}}$ (see Figure 2.4). Then there are six distinct triples up to the action of $\mathbb{Z}_4$, namely, $\{p_1p_2p_4\}$, $\{p_1p_2p_5\}$, $\{p_1p_2p_6\}$, $\{p_1p_3p_5\}$, $\{p_1p_3p_6\}$, $\{p_1p_2p_3\}$.

(c) Assume that $\mathcal{P} \in QC^6_3$, and that the numeration $p_1, \ldots, p_5$ of points of $\mathcal{P}$ other than p_6 is cyclic such that p_6 is inside the Q-region C associated to $\mathcal{P}_{\hat{6}}$ (see Figure 2.4). Then there are six distinct triples up to the action of D_3, namely, $\{p_1p_3p_5\}$, $\{p_1p_2p_5\}$, $\{p_1p_3p_4\}$, $\{p_1p_3p_6\}$, $\{p_1p_2p_4\}$, $\{p_3p_5p_6\}$.

(d) Assume that $\mathcal{P} \in QC^6_6$, and that the numeration $p_1, \ldots, p_5$ of points of $\mathcal{P}$ other than p_6 is cyclic such that p_6 is inside the Q-region D associated to $\mathcal{P}_{\hat{6}}$ (see Figure 2.4). Then there are two distinct triples up to icosahedral symmetry group, namely, $\{p_1p_3p_5\}$, $\{p_1p_2p_5\}$. $\square$

Lemma 4.1.3. *Let $\mathcal{P} = \{p_1, \ldots, p_6\}$ be a configuration in QC^6, and for all $i \in \{1, \ldots, 6\}$, Q_i be the conics passing through five points of $\mathcal{P}$ other than p_i. Then:*

(a) For each $i \neq j \in \{1, \ldots, 6\}$, the image of the line L_{ij} under $Cr_{i\,j\,k}$ for some $k \in \{1, \ldots, 6\} \setminus \{i, j\}$ is a point p_{ij}. However, the image of a line L_{ij} under $Cr_{k\,l\,m}$ for some $k, l, m \in \{1, \ldots, 6\} \setminus \{i, j\}$ is the conic passing through the five points p_i, p_j, p_k, p_l, p_m of $Cr_{k\,l\,m}(\mathcal{P})$.

(b) For each $i \in \{1, \ldots, 6\}$, the image of the conic Q_i under $Cr_{j\,k\,l}$ for some $j, k, l \in \{1, \ldots, 6\} \setminus \{i\}$ is the line L_{nm} joining remaining two points $p_n, p_m \in \mathcal{P}$, where $n, m \in \{1, \ldots, 6\} \setminus \{i, j, k, l\}$.

(c) For each $i \neq j \in \{1, \ldots, 6\}$, the image of the conic Q_i under $Cr_{i\,j\,k}$ for some $j, k \in \{1, \ldots, 6\} \setminus \{i\}$ is the conic passing through five points of $Cr_{i\,j\,k}(\mathcal{P}_{\hat{i}})$.

Proof. By the definition of quadratic Cremona transformations, the proof of the first part of item (a) is trivial. The proof of the second part of (a) immediately follows from item (b) since $Cr^2 = Cr \circ Cr = id$, i.e. $Cr^{-1} = Cr$, if $XYZ \neq 0$.

Hence, we start to prove the part (b). Since $\mathcal{P} \in QC^6$, the conic Q_i is irreducible for each $i \in \{1, \ldots, 6\}$. The well known fact is that any irreducible projective conic is projectively equivalent to the conic

$$XY + YZ + XZ = 0 \tag{4.1}$$

for some homogenous coordinates X, Y, Z. More precisely, for the irreducible conic Q_i and three points p_j, p_k, p_l on Q_i, there is a unique projective transformation mapping Q_i to (4.1) and the three points to $q_j = [1 : 0 : 0]$, $q_k = [0 : 1 : 0]$ and $q_l = [0 : 0 : 1]$, respectively. The image of the conic (4.1) under $Cr_{j\,k\,l}$ is a line since

$$\begin{aligned} YZXZ + XZXY + YZXY &= 0 \\ XYZ(Z + X + Y) &= 0 \\ Z + X + Y &= 0. \end{aligned}$$

To prove item (c), it is enough to observe that we can find a unique projective transformation sending p_1, p_2, p_3 and $p_4 \in \mathcal{P}$ to $[0 : 0 : 1]$, $[0 : 1 : 0]$, $[1 : 0 : 0]$ and $[1 : 1 : 1]$, respectively. Thus, the conic Q_1 is projectively equivalent to a conic

$$Z^2 + aXY + bYZ + cXZ = 0 \tag{4.2}$$

for some $a, b, c \in \mathbb{R}$. The image of the conic (4.2) under Cr_{1kl} is a conic since

$$\begin{aligned} (XY)^2 + aYZXZ + bXZXY + cYZXY &= 0 \\ XY(XY + aZ^2 + bXZ + cYZ) &= 0 \\ XY + aZ^2 + bXZ + cYZ &= 0 \end{aligned}$$

Therefore, the proof is completed. □

The following statement shows the modification (i.e., the images) of quadratically nondegenerate 6-configurations other than hexagonal under quadratic transformations.

Proposition 4.1.4. *Let $\mathcal{P}$ be a 6-configuration in QC^6_2, or QC^6_3, or QC^6_6, and assume that the numeration $p_1, \ldots, p_5$ of points of $\mathcal{P}_{\hat{6}}$ are cyclic such that the* *point $p_6 \in \mathcal{P}$ is inside the Q-region B, or C, or D, respectively (see Figure 2.4). Then the images of $\mathcal{P}$ under the quadratic Cremona transformations based in triples of points of $\mathcal{P}$ are as shown in Figure A.1(a)-(d) in Appendix A, respectively.* □

Proof. The proof is a straightforward analysis using a model $[x : y : z] \to [yz : xz : xy]$ of a quadratic Cremona transformation. □

Let $M_{i,j}$, $i, j = 1, 2, 3, 6$, denote the number of quadratic Cremona transformations which take a 6-configuration in the Q-deformation class QC^6_i to a 6-configuration in the Q-deformation class QC^6_j. The next statement is an immediate consequence of Lemma 4.1.2, the observation of modifications of a hexagonal 6-configuration under Cremona transformations given in Figure 4.1, and Propositions 4.1.4.

Corollary 4.1.5. *Assume that $M = \{M_{i,j}\}$ is a matrix whose entries $M_{i,j}$, $i, j =$ 1, 2, 3, 6, are as introduced above. Then, the matrix is equal to*

$$M = \begin{pmatrix} 3 & 9 & 7 & 1 \\ 6 & 8 & 6 & 0 \\ 8 & 9 & 3 & 1 \\ 10 & 0 & 10 & 0 \end{pmatrix}$$

□

4.2 Cremona transformations of 7-configurations

The modification of a heptagonal configuration $\mathcal{P} \in QC^7$ under quadratic Cremona deformations based at fourteen distinct triples of points (up to the action of permutations in D_7, the group of symmetries of the principle heptagon, preserving dominant and subdominant points of $\mathcal{P}$ on the set of all triples of points of $\mathcal{P}$) is as shown in Figure 4.2.

Theorem 4.2.1. *The Q-deformation class of any 7-configuration in QC^7 is obtained from a heptagonal configuration in $QC^7_{(7,0,0,0)}$ by a quadratic Cremona* *transformation based at a triple of points of the* 7*-configuration (see Figure 4.2).*

Proof. Let $\mathcal{P} \in QC^7_{(7,0,0,0)}$ be a heptagonal configuration. Removing points of $\mathcal{P}$ not involved into Cremona transformation one-by-one and applying Theorem 4.1.1 to analyze possible position of the points in the image. $\square$

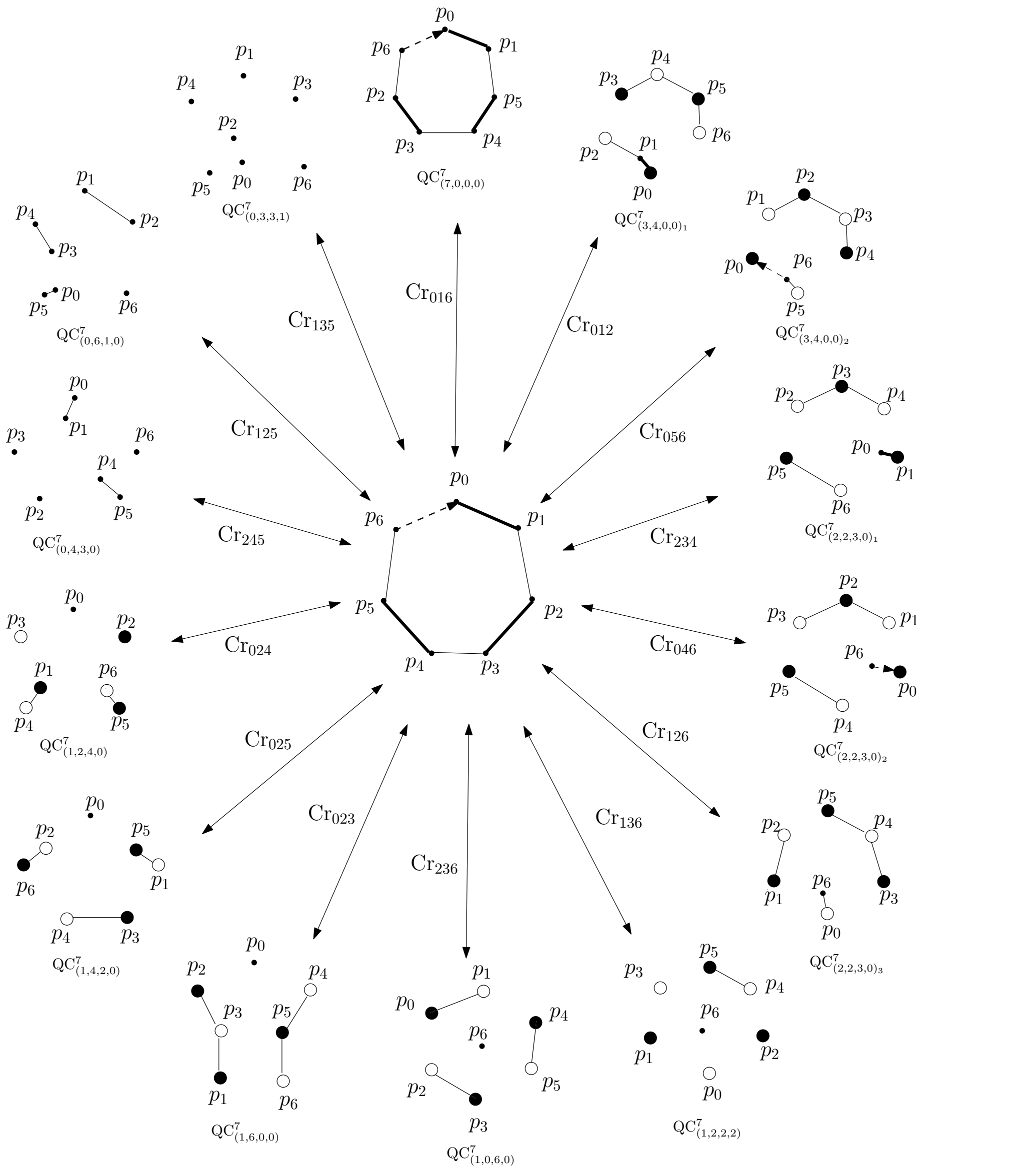

Figure 4.2: The images of a configuration $\mathcal{P} \in QC^7_{(7,0,0,0)}$ under Cremona transformations based at fourteen distinct triples. In this figure, the labeled points and edges with 1 show the d-decoration of these configurations (see Section 2.1).

CHAPTER 5

CONFIGURATIONS OF LINES IN $\mathbb{R}P^3$

5.1 Triple linking numbers

The linking number of a pair of oriented skew lines $\overrightarrow{L_1}, \overrightarrow{L_2}$ in the oriented 3-dimensional real projective space $\mathbb{R}P^3$ is $\pm\frac{1}{2}$. We denote by $lk(\overrightarrow{L_1}, \overrightarrow{L_2})$ the *doubled linking number* of these lines in order to make it an integer, $+1$, or -1. If we change the orientation of one of these lines, then we obtain

$$lk(-\overrightarrow{L_1}, \overrightarrow{L_2}) = lk(\overrightarrow{L_1}, -\overrightarrow{L_2}) = -lk(\overrightarrow{L_1}, \overrightarrow{L_2})$$

where the sign "-" of $\overrightarrow{L_i}$ means that the orientation of the line is reversed.

Following Viro [VV], we introduce the *triple linking number* of (non-oriented) lines L_1, L_2, and L_3 by formula

$$lk(L_1, L_2, L_3) = lk(\overrightarrow{L_1}, \overrightarrow{L_2}).\ lk(\overrightarrow{L_1}, \overrightarrow{L_3}).\ lk(\overrightarrow{L_2}, \overrightarrow{L_3}),$$

where $\overrightarrow{L_i}$ is the line L_i with arbitrary orientation for each $i \in \{1, 2, 3\}$. The triple linking number $lk(L_1, L_2, L_3)$ is well-defined, i.e, it is independent of the orientations of the lines L_i and independent of the order of these lines (cf. [VV]).

By an n-configuration $\mathcal{L} = \{L_1, \ldots, L_n\}$ of skew lines in $\mathbb{R}P^3$ we mean a set of pairwise disjoint lines, L_i. For an n-configuration $\mathcal{L}$ of skew lines, let us denote by $lk_+(\mathcal{L})$ (respectively, $lk_-(\mathcal{L})$) the number of positive triple linking numbers of any triples of lines of $\mathcal{L}$ (respectively, the number of negative triple linking numbers of any triples of lines of $\mathcal{L}$). By the *total linking code associated to* $\mathcal{L}$, we mean the pair of $(lk_+(\mathcal{L}), lk_-(\mathcal{L}))$.

Two lines L_0, L_1 of an n-configuration of skew lines $\mathcal{L}$ in $\mathbb{R}P^3$ are said to be *internal adjacent* in $\mathcal{L}$ if they can be connected by a continuous family of lines, L_t, so that L_t do not intersect any remaining lines of $\mathcal{L}$, for all $t \in [0, 1]$. It is obvious from the definition that internal adjacency in $\mathcal{L} = \{L_1, \ldots, L_n\}$ is an equivalence relation; we will write $L_i \sim L_j$ if lines L_i and L_j, of $\mathcal{L}$ are internal adjacent. As it was observed in [VV], L_0 is internal adjacent to L_1 if there is a one-sheeted hyperboloid in $\mathbb{R}P^3$ which separates the pair of lines from the remaining lines of $\mathcal{L}$.

Proposition 5.1.1. [VD]. *Let $\mathcal{L}$ be an n-configuration of skew lines in $\mathbb{R}P^3$ for $n > 3$, and assume that $L, L' \in \mathcal{L}$ are internal adjacent lines. Then, all of the triple linking numbers $lk(L, L', M)$ for any $M \in \mathcal{L}$ have the same value* $+1$ *or* -1. □

Corollary 5.1.2. [VD]. *Let $\mathcal{L}$ be an n-configuration of skew lines in $\mathbb{R}P^3$ for $n > 3$, and assume that $L, L' \in \mathcal{L}$ are internal adjacent lines. Then, $lk(L, K, M) = lk(L', K, M)$ for any $K, M \in \mathcal{L}$ other than L, L'.* □

Given an n-configuration $\mathcal{L}$ of skew lines in $\mathbb{R}P^3$, we associate a sign + or − to each adjacency class in $\mathcal{L}$. By the *sign of an adjacency class* on $\mathcal{L}$, we mean the sign of the triple linking numbers $lk(L, L', M)$ where L, L' are two lines in the adjacency class, and $M \in \mathcal{L}$.

5.2 Derived configuration of lines and derivative trees

Let $\mathcal{L}$ be an n-configuration of skew lines in $\mathbb{R}P^3$. A *derived configuration $\mathcal{L}^{(1)}$ of $\mathcal{L}$ in level* 1 is a configuration obtained by taking one line from each internal adjacency class in $\mathcal{L}$. If $\mathcal{L}^{(1)} \neq \mathcal{L}$, then a derived configuration of $\mathcal{L}^{(1)}$ in level 1 is called a *derived configuration of $\mathcal{L}$ in level* 2. It is denoted by $\mathcal{L}^{(2)}$. Similarly, if $\mathcal{L}^{(1)} \neq \mathcal{L}^{(2)}$, then the derived configuration of $\mathcal{L}^{(2)}$ in level 1 is called a *derived configuration of $\mathcal{L}$ in level* 3, and it is denoted by $\mathcal{L}^{(3)}$. Proceeding in this way, the derived configuration of $\mathcal{L}$ in level n is the derive configuration of $\mathcal{L}^{(n-1)}$ in level 1, and denoted by $\mathcal{L}^{(n)}$.

Note that the deformation classes of the derived configurations of $\mathcal{L}$ in all levels do not depend on the choice of representatives.

An n-configuration $\mathcal{L}$ of skew lines in $\mathbb{R}P^3$ is called *completely decomposable* if there exists $i \in \mathbb{Z}^+$ such that $\mathcal{L}^{(i)}$ is a configuration of one line. The positive number i is called the *height* of the n-configuration.

To a completely decomposable n-configuration $\mathcal{L}$ of skew lines of height i, we associates a tree of degree i as follows: vertices of the tree in level k are distinct internal adjacency classes in the derived configuration $\mathcal{L}^{(k)}$ for all $k \in \{1, 2, \ldots, i\}$. An edge between a vertex v^k in level k and a vertex v^{k+1} in level $k+1$ where $k \in \{2, \ldots, i-1\}$ represents a line in the internal adjacency class v^{k+1} taken from the internal adjacency class v^k in $\mathcal{L}^{(k)}$. The branches at each vertex in level 1 stand for lines in this class. We call this tree the *derivative tree* of $\mathcal{L}$. The vertex in the level i is called the *root vertex* of the derivative tree of of $\mathcal{L}$.

To draw the derivative tree of a completely decomposable n-configuration $\mathcal{L}$ of skew lines of degree i, we follow two steps:

1. Determine the signs of all internal adjacency classes in $\mathcal{L}^{(k)}$ for each $1 \leq k \leq i$ unless the internal adjacency classes in $\mathcal{L}^{(k)}$ contains one line, and unless there is a unique internal adjacency class in $\mathcal{L}^{(k)}$ which contains two lines.
2. Start to align the vertices horizontally in each level in which we use the symbols, big circles, to represent these vertices, and we put signs of the vertices in the middle of these circles.

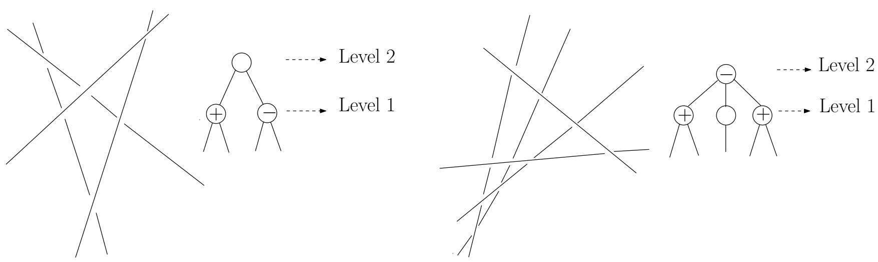

(a) $J\langle 1243\rangle$ (b) $J\langle 12534\rangle$

Figure 5.1: The configurations of 4 and 5 skew lines in $\mathbb{R}P^3$, together with their derivative trees of degree 2.

Example 5.2.1. Consider the above 4-configuration and 5-configuration of lines given in Figure 5.1(a) and (b), respectively. Their derivative trees are shown in these figures together with these configurations.

5.3 Deformations and coarse deformations of configurations of skew lines

We say that two n-configurations $\mathcal{L}_0$,$\mathcal{L}_1$ of skew lines in $\mathbb{R}P^3$ are *L-deformation equivalent* if they can be joined by a continuous family of n-configurations of skew lines, $\mathcal{L}_t$, for any $t \in [0, 1]$, and *coarse L-deformation equivalent* if one of them is L-deformation equivalent to the image of the other under a projective transformation of $\mathbb{R}P^3$.

For an n-configuration $\mathcal{L}$ of skew lines in $\mathbb{R}P^3$ we denote by $\overline{\mathcal{L}}$ its mirror image which is defined to be the image of $\mathcal{L}$ under a reflection about a hyperplane in $\mathbb{R}P^3$, that is, double linking number of each pair of lines of $\overline{\mathcal{L}}$ has an opposing sign of that of each pair of lines of $\mathcal{L}$. An n-configuration of skew lines in $\mathbb{R}P^3$ is *achiral* if it is deformation equivalent to its mirror image. Otherwise, it is *chiral*.

5.4 Join configurations of $n \leq 6$ of skew lines

Following [M1], to a given permutation $\sigma : \{1, \dots, n\} \to \{1, \dots, n\}$, we associate an n-configuration of skew lines in $\mathbb{R}P^3$ as follows: let us fix two disjoint lines L and L' such that their linking number is -1 and let us fix an n-tuples of points on the first line L and on the second line L'. Let us cyclically enumerate such pair of n-tuples of points on the first line L by $1, 2, \dots, n$ and on the second line L' by $\sigma(1), \dots, \sigma(n)$ in the direction of the orientations of these lines. Hence, we get an n-configuration of skew lines L_k obtaining by joining k to $\sigma(k)$, $k = 1, \dots, n$. This configuration is called a *join n-configuration*, and it is denoted by $J(\sigma(1)\sigma(2)\dots\sigma(n))$, or for short $J(\sigma)$.

Proposition 5.4.1. [VV]. *Any n-configuration of skew lines in $\mathbb{R}P^3$ for $n \leq 5$ is L-deformation equivalent to a join n-configuration.* □

5.5 Classification of 6-configurations of lines

For a permutation $\sigma \in S_n$, we call the set of all n-configurations of skew lines which are L-deformation equivalent to $J(\sigma)$ in $\mathbb{R}P^3$ the *L-deformation join class*, and it is denoted by $J[\sigma]$. Similarly, the set of all join n-configurations of skew lines which are coarse L-deformation equivalent to $J(\sigma)$ the *coarse L-deformation join class*, and it is denoted by $J\langle\sigma\rangle$.

Recall (see Section 3.1) that we denote by $[\sigma]$ the orbit (i.e., the permutation class) of σ under RL-cyclic action on S_n, and by $\langle\sigma\rangle$ the orbit (i.e., the coarse permutation class) of σ under RL-dihedral action on S_n. By the construction of $J(\sigma)$ and these definitions, the following statement is trivial.

Lemma 5.5.1. *The sets $J[\sigma]$ for any permutation $\sigma \in S_n$ are in a one to one correspondence with the permutation class $[\sigma]$. The sets $J\langle\sigma\rangle$ for any permutation $\sigma \in S_n$ are in a one to one correspondence with the coarse permutation class $\langle\sigma\rangle$.* □

Theorem 5.5.2. [M1]. *A 6-configurations of skew lines in $\mathbb{R}P^3$ belongs to one of the 15 L-deformation join classes, namely, $J[123456]$, $J[123465]$, $J[123564]$, $J[124365]$, $J[124635]$, $J[125634]$, $J[123654]$, $J[135264]$, $J[12453]$, $J[654321]$, $J[564321]$, $J[465321]$, $J[563421]$, $J[536421]$, $J[436521]$, or it is L-deformation equivalent to one of the four 6-configurations of skew lines L, M, $\overline{L}$, $\overline{M}$ where $\overline{L}$ and $\overline{M}$ represented the mirror image of L and M, respectively. (See Figure 5.2.)*

5.6 Derivative trees of join configurations

In this section, for a given permutation σ in S_n, we construct the derivative tree of a join configuration $J(\sigma)$.

Let $\sigma \in S_n$ be a permutation, and assume that $\{\sigma(i + j) : j \in \{1, \ldots, k_i)\}$ is the set consisting of the maximal number of consecutive integers for each subset $\{i+1, \ldots, i+k_i\}$ of consecutive integers in $\{1, \ldots, n\}$ where $k_i \in \{2, \ldots, n\}$. Then, the set of lines $\{L_{i+1}, \ldots, L_{i+k_i}\}$ is an internal adjacency class with k_i element in a

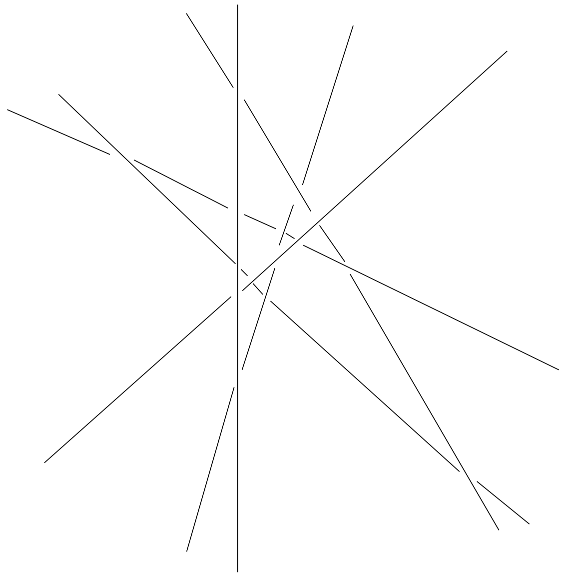

(a) M

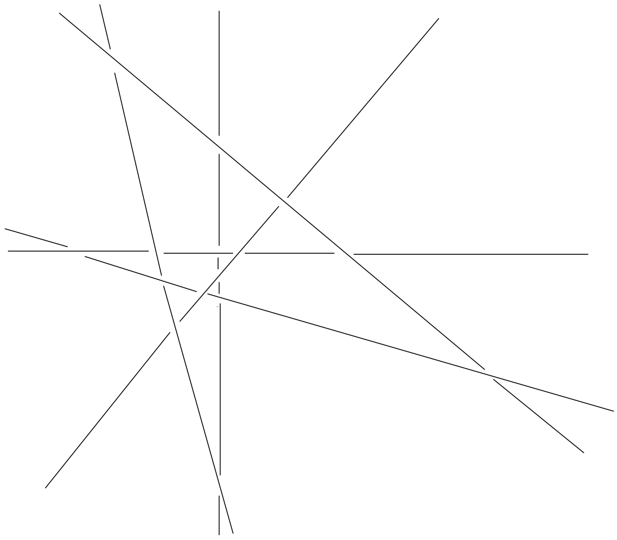

(b) L

Figure 5.2: Two 6-configurations of skew lines in $\mathbb{R}P^3$, M and L.

join n-configuration $J(\sigma)$. The sign of this internal adjacency class in $J(\sigma)$ is positive if the permutation

$$\begin{pmatrix} i+1 & i+2 & \cdots & i+k_i-1 & i+k_i \\ \sigma(i+1) & \sigma(i+2) & \cdots & \sigma(i+k_i-1) & \sigma(i+k_i) \end{pmatrix} \in S_{k_i}$$

is even. Otherwise, the sign of these equivalence class is negative. Thus, we can sketch the derivative tree of $J(\sigma)$ as introduced in Section 5.2.

Example 5.6.1. As σ, let us take the identity permutation

$$\sigma = \begin{pmatrix} 1 & 2 & 3 & 4 \\ 1 & 2 & 3 & 4 \end{pmatrix} \in S_4.$$

Note that the image of the set $\{1, 2, 3, 4\}$ consisting of consecutive integers under σ is the set of the maximal number of consecutive integers. Therefore, there are only one internal adjacency equivalence class in $J(\sigma)$, namely, $\{L_1, L_2, L_3, L_4\}$. The sign of this internal adjacency class is "+" since the identity permutation is even. This implies that all triple linking numbers are $+1$. The derivative tree of $J(\sigma)$ together with the total linking code is as shown in Figure 5.4.

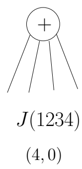

Figure 5.3: The derivative tree of (1234)

Example 5.6.2. As σ, let us take

$$\begin{pmatrix} 1 & 2 & 3 & 4 & 5 & 6 \\ 1 & 2 & 3 & 6 & 5 & 4 \end{pmatrix} \in S_6.$$

Note that two subsets $\{1, 2, 3\}$ and $\{4, 5, 6\}$ consist of consecutive integers in $\{1, 2, 3, 4, 5, 6\}$ such that the images of these subsets under σ are also the sets of the maximal number of consecutive integers. Therefore, there are two internal adjacency equivalence classes in $J(\sigma)$, namely, $\{L_1, L_2, L_3\}$ and $\{L_4, L_5, L_6\}$. The sign of the former internal adjacency class is "+" since the identity permutation

$$\sigma_1 = \begin{pmatrix} 1 & 2 & 3 \\ 1 & 2 & 3 \end{pmatrix}$$

is even. However, the sign of the latter one is "$-$" since the permutation of S_3

$$\sigma_2 = \begin{pmatrix} 4 & 5 & 6 \\ 6 & 5 & 4 \end{pmatrix}$$

is odd. Therefore, the derivative tree of $J(\sigma)$ is as shown in Figure 5.4.

The following statement is an immediate consequence of Lemma 5.5.1.

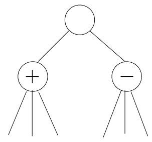

Figure 5.4: The derivative tree of (123654)

Lemma 5.6.3. *Any two permutations from the same permutation class* $[\sigma]$ *for* $\sigma \in S_n$ *have topologically same derivative tree. That is, derivative trees are topological invariants for deformation join classes* $J[\sigma]$. □

For $3 \leq n \leq 6$, the distinct L-deformation classes of n-configurations of skew lines in $\mathbb{R}P^3$ are summarized in Figures 5.5 and 5.6 in terms of permutations classes and derivative trees if they exists. From Figure 5.6, it can be seen that not every 6-configuration of lines has a derivative tree. Of the 19 L-deformation classes of 6-configuration of skew lines, 15 are L-deformation join classes. Of those 12 L-deformation classes have derivative trees. The remaining 4 have no derivative trees and are not join configurations.

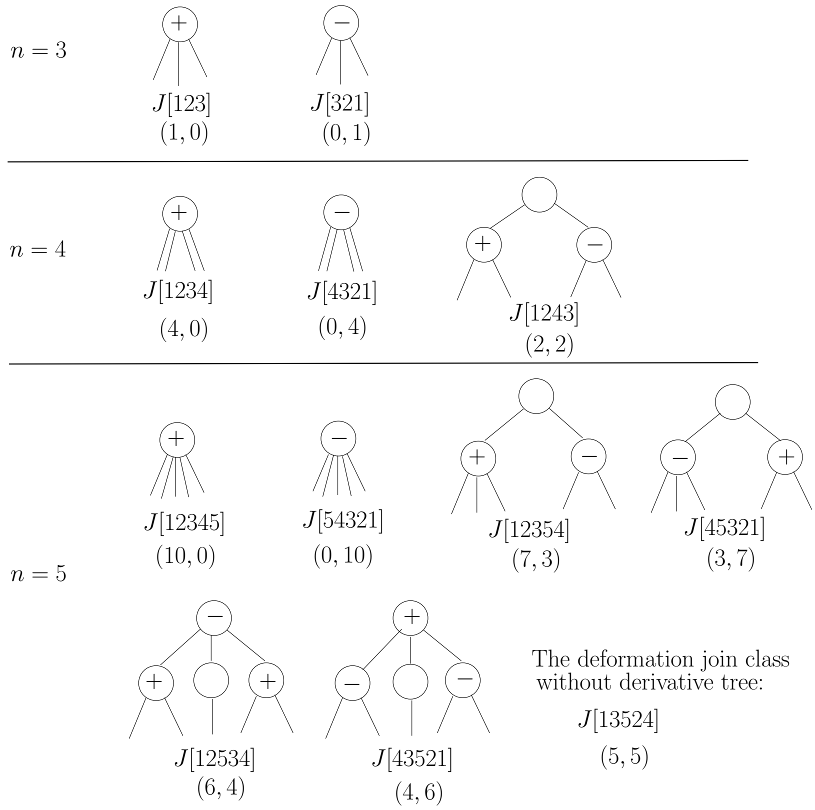

Figure 5.5: The L-deformation classes of n-configurations of skew lines, $n \leq 5$.

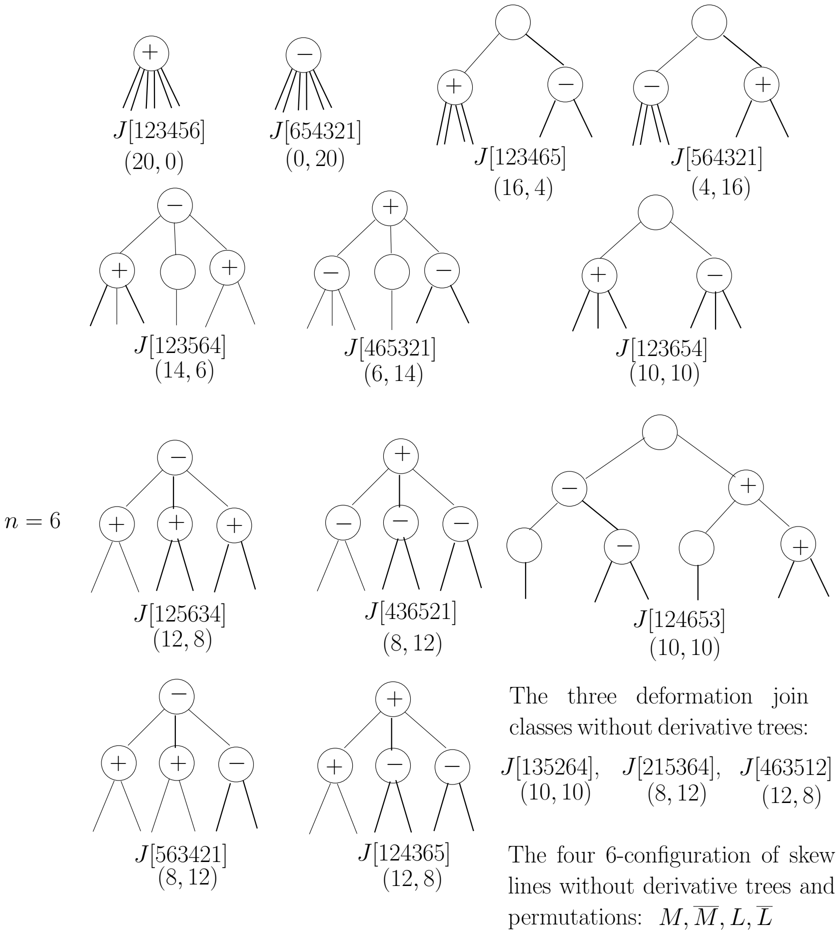

Figure 5.6: The 19 L-deformation classes of 6-configurations of skew lines in $\mathbb{R}P^3$.

CHAPTER 6

CONFIGURATIONS OF LINES ON REAL CUBIC SURFACES

6.1 Real lines on real cubic surfaces

In this section, we shall give an answer to the question on the existence of a nonsingular real cubic surface containing a given 6-configuration of skew lines in the oriented projective space $\mathbb{R}P^3$.

A *double six* $(\mathcal{L}, \mathcal{L}')$ is a pair of ordered sets $\mathcal{L}$ and $\mathcal{L}'$, each consisting of 6 skew lines in $\mathbb{P}^3$ where $\mathcal{L} = \{a_1, \ldots, a_6\}$, $\mathcal{L}' = \{b_1, \ldots, b_6\}$ such that a_i and b_j, $1 \leq i, j \leq 6$ intersect at a point if $i \neq j$ and are disjoint if $i = j$.

Proposition 6.1.1. *The following statements hold:*

(a) *If there exists a line L on a cubic surface X, which intersects five skew lines in $\mathbb{R}P^3$, then the five lines lie on the cubic surface X.*

(b) *If five skew lines in $\mathbb{R}P^3$ lie on a real nonsingular cubic surface X, then there exists a line L on this surface, which intersects all these lines.*

(c) *Six skew lines $L_1, \ldots, L_6$ lie on some cubic surface X if and only if there exist another set of six skew lines $L'_1, \ldots, L'_6$, such that L_i, and L'_j, $1 \leq i, j \leq 6$, intersect at a point if $i \neq j$ and are disjoint if $i = j$ (in other words, the two sets of lines form a double six).*

Proof. For the proof of item (a), let L_1, L_2, L_3, L_4, L_5 be skew lines in $\mathbb{R}P^3$, and assume that there exists a line $L \subset \mathbb{R}P^3$ which intersects the line L_i, $i = 1, \ldots, 5$, at a point p_i. We shall choose some 19 points from the lines L_i, $i = 1, 2, 3, 4, 5$. The 19 points are p_i, $i = 1, 2, 3, 4$, additional 12 distinct points being 3 points other than p_i per each line L_i where $i \in \{1, \ldots, 4\}$, and three additional points different from p_5 taken from the line L_5. Counting parameters, it can be easily observed that there is a cubic surface $X \subset \mathbb{R}P^3$ containing these 19 points. Since the line L_i contains four points of X it lies on this surface for each $i \in \{1, \ldots, 4\}$. Similarly, L also lies on this surface, so the cubic surface X contains the point $p_5 \in L \cap L_5$. Therefore, L_5 is also lying on the cubic surface X.

To prove item (b), let us assume that five skew lines lie on a nonsingular cubic surface X. By blowing down these lines, we get a del Pezzo surface of degree 8, i.e. it is either $\mathbb{P}^1 \times \mathbb{P}^1$ or $\mathbb{P}^2 \# \overline{\mathbb{P}^2}$ with 5 points. Firstly, assume that we obtain $\mathbb{P}^1 \times \mathbb{P}^1$ with five points. Notice that these points form a quadratically nondegenerate 5-configuration on $\mathbb{P}^1 \times \mathbb{P}^1$. Otherwise, after blowing up these points, we get singular cubic surface. Recall (see Proposition 3.7.1) that there exist a curve of bidegree $(2, 1)$ (or, of bidegree $(1, 2)$ curve) passing through these five points. The proper transformation of this curve is the required line on this cubic surface. Now, we assume that we obtain $\mathbb{P}^2 \# \overline{\mathbb{P}^2}$ with five points. Note that none of the five points lie on $\overline{\mathbb{P}^2}$. Otherwise, after blowing up the five points we get a singular cubic surface. By blowing down the exceptional curve on $\mathbb{P}^2 \# \overline{\mathbb{P}^2}$ over the blown up point, say $p \in \mathbb{P}^2$, we obtain a projective plane with five points and p. The proper transformation of the plane conic passing through the five points other than p is the curve whose self intersection is 4 passing through the five points on $\mathbb{P}^2 \# \overline{\mathbb{P}^2}$. The proper transformation of this curve is the required line on X.

For the proof of item (c), firstly, we assume that the ordered sets $\{L_1, \ldots, L_6\}$ and $\{L'_1, \ldots, L'_6\}$ of skew lines in $\mathbb{R}P^3$ form a double six, that is, L_i, and L'_j, $1 \leq i, j \leq 6$, intersect at a point if $i \neq j$, and are disjoint if $i = j$ (see Figure 6.1). We shall choose some 19 points among the 30 intersection points of these lines. The chosen 19 points are denoted by black points in this figure. There is a cubic surface $X \subset \mathbb{R}P^3$ containing these 19 points. Since each of the lines L_1 and L'_1 contains some four points of X they lie on this surface. Thus, X contains the intersection point of $L_1 \cap L'_6$ and the intersection point, denoted by cross in this

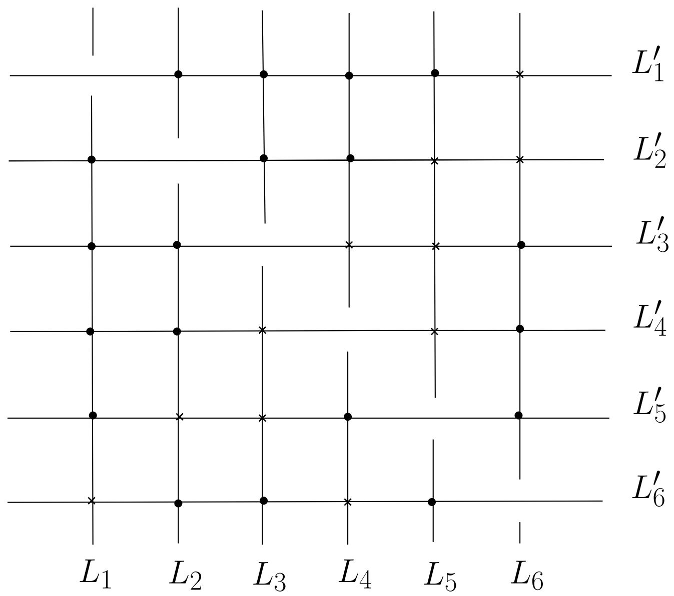

Figure 6.1: A double six $(\mathcal{L}, \mathcal{L}')$, where $\mathcal{L} = \{L_1, \ldots, L_6\}$, $\mathcal{L}' = \{L'_1, \ldots, L'_6\}$ in $\mathbb{R}P^3$. By the black points on these lines, we show the chosen 19 points to construct a cubic surface.

figure, of $L'_1 \cap L_6$. Consequently, each of the lines L_6 and L'_6 contains some four points of X, so they lie on this surface. Proceeding in this way, we can show that L_i, L'_i lie on this cubic surface for all $i \in \{1, \ldots, 6\}$. The converse of this statement is a well known fact. This complete the proof. □

Although the formal definition of double six does not say directly that it should be realizable on some cubic surface, we know from Proposition 6.1.1(b) that this is correct.

Corollary 6.1.2. *Any double six configuration in $\mathbb{R}P^3$ can be embedded in a nonsingular cubic surface.* □

6.2 The four types of real double sixes

Given a nonsingular real cubic M-surface X, by blowing down a suitable configuration of six skew lines on X we can obtain a planar 6-configuration lying inside one of the four Q-deformation classes QC^6_σ, $\sigma = 1, 2, 3, 6$, in QC^6.

We say that a double six $(\mathcal{L}, \mathcal{L}')$ on a nonsingular real cubic M-surface is corresponding to a Q-deformation class QC_i^6, $i = 1, 2, 3, 6$, if the 6-configuration of points, $\mathcal{P}_{\mathcal{L}}$, obtained by blowing down lines of $\mathcal{L}$ lies in QC_i^6. Let us denote by n_i the number of double sixes corresponding to the Q-deformation class QC_i^6, where $i \in \{1, 2, 3, 6\}$. Due to Ludwing Schläfli, on a nonsingular cubic surface there are 36 double sixes (see [D1]). Then, we have $n_1 + n_2 + n_3 + n_6 = 36$.

Theorem 6.2.1. *Among* 36 *double sixes on a nonsingular real cubic M-surface,* 10 *double sixes are corresponding to QC_1^6,* 15 *double sixes are corresponding to QC_2^6,* 10 *double sixes are corresponding to QC_3^6, and* 1 *double six is corresponding to QC_6^6.*

Proof. Let n_i be the number of double sixes on a nonsingular real cubic M-surface which are corresponding to QC_i^6, $i = 1, 2, 3, 6$. Due to Lemma 4.1.5, we get the following Figure 6.2.

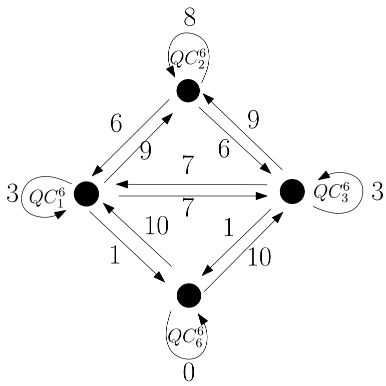

Figure 6.2: The labeled vertices represent double sixes $(\mathcal{L}_i, \mathcal{L}_i')$ corresponding to QC_i^6, $i = 1, 2, 3, 6$, and the labeled arrows represent the number of elementary Cremona transformations sending the 6-configuration $\mathcal{P}_{\mathcal{L}_i} \in QC_i^6$ to the 6-configuration $\mathcal{P}_{\mathcal{L}_j} \in QC_j^6$ for any $i, j \in \{1, 2, 3, 6\}$.

By this figure, we notice that $9n_1 = 6n_2$, $7n_1 = 7n_3$, $n_1 = 10n_6$, and $6n_2 = 9n_3$. Since $n_1 + n_2 + n_3 + n_6 = 36$ we get

$$\begin{aligned} n_1 + \frac{3}{2}n_1 + n_1 + \frac{1}{10}n_1 &= 36 \\ \frac{36}{10}n_1 &= 36 \\ n_1 &= 10 \end{aligned}$$

Therefore, $n_2 = 15$, $n_3 = 10$ and $n_6 = 1$. □

6.3 Elliptic and hyperbolic lines on a blow-up model

The concept of hyperbolic and elliptic lines were introduced by Segre [Se]. We shall determine ellipticity and hyperbolicity of lines in the blowup model of a real del Pezzo surface of degree 3 whose anti-canonical model is a real cubic M-surface depending on the 6-configuration of blown up points.

Take a real line L on a nonsingular real cubic surface X and consider the one parameter family of planes $\pi_t \subset \mathbb{P}^3$ containing this line for all $t \in \mathbb{P}^1$. Then, we get $X \cap \pi_t = L \cup \Omega_t$ where Ω_t are residual conics. The set $\{\Omega_t : t \in \mathbb{P}^1\}$ of residual conics is called the *residual pencil associated to L*. For each $t \in \mathbb{P}^1$, $\Omega_t \cap L = \{q_t, q_t^{'}\}$. Then, we have a double covering $\varphi : L \to \mathbb{P}^1$ such that $\varphi : \{q_t, q_t^{'}\} \to t$. Two branch points of φ are called the *Segre points*.

Following Segre [Se], a real line L on a nonsingular real cubic surface is called *hyperbolic* if the Segre points are real, and called *elliptic* if they are complex conjugate to each other (see Figure 6.3).

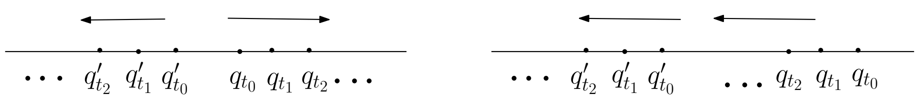

(a) the case of hyperbolic line (b) the case of elliptic line

Figure 6.3: The points $q_t, q_t^{'}$ of the intersection $\Omega_t \cap L$, $t \in [0, 1]$, where L, Ω_t are as introduced above.

For a given configuration $\mathcal{P} \in QC^6$, let us denote by $X_{\mathcal{P}}$ the nonsingular real del Pezzo M-surface of degree 3 obtained from $\mathbb{P}^2$ blown-up the six real points of $\mathcal{P}$, and by $Y_{\mathcal{P}}$ the image of $X_{\mathcal{P}}$ under the anti-canonical map $f_{\mathcal{P}} : X_{\mathcal{P}} \to \mathbb{P}^3$. Note that $Y_{\mathcal{P}}$ is a nonsingular cubic surface. Among the 27 real exceptional curves on $X_{\mathcal{P}}$, the six ones are E_i corresponding to points p_i, the fifteen ones are A_{ij}, which are the proper transformations of the lines L_{ij} joining two points $p_i, p_j \in \mathcal{P}$, and the remaining six ones are $\widetilde{Q}_i$, which are the proper transformations of the conics Q_i through all the points except the point p_i, where $1 \leq i < j \leq 6$.

The residual pencil $\{\Omega_t : t \in \mathbb{P}^1\}$ in a blow-up model $X_{\mathcal{P}}$ of del Pezzo surfaces of degree 3 in terms of a given 6-configuration $\mathcal{P} \in QC^6$ is as follows:

(a) The residual pencil $\{\Omega_t\}$ associated to $E_i \subset X_{\mathcal{P}}$, $i = 1, \ldots, 6$, consists of the rational cubic curves passing through all six points of $\mathcal{P}$ and having a node at $p_i \in \mathcal{P}$.

(b) The residual pencil $\{\Omega_t\}$ associated to $A_{ij} \subset X_{\mathcal{P}}$, $i, j = 1, \ldots, 6$, consists of conics passing through four points of $\mathcal{P}$ other than p_i and p_j.

(c) The residual pencil $\{\Omega_t\}$ associated to $\widetilde{Q}_i \subset X_{\mathcal{P}}$, $i = 1, \ldots, 6$, consists of lines passing through the point $p_i \in \mathcal{P}$.

Let A be a nodal cubic curve in $\mathbb{R}P^2$ with a node a point $p \in A$. Notice that $A \setminus \{p\} = \mathcal{O} \cup \mathcal{J}$, where the homology class $[\mathcal{J} \cup p]$ is nontrivial in $H_1(\mathbb{R}P^2)$ while the homology class $[\mathcal{O} \cup p]$ is trivial. We say that $\mathcal{O}$ is the *finite loop* and $\mathcal{J}$ is the *infinite loop* of A. Equivalently, one can define that the finite loop is the contractible piece of A in $\mathbb{R}P^2$, and that the infinite loop is the uncontractible piece of A in $\mathbb{R}P^2$ (for an example, see Figure 6.4).

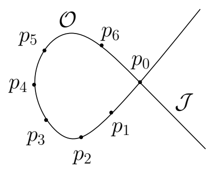

Figure 6.4: The finite loop $\mathcal{O}$ and infinite loop $\mathcal{J}$ of a nodal cubic A.

We reproduce the following results from Finashin and Kharlamov (see [FK3]), in our own versions, after some modifications.

Theorem 6.3.1. *For a 6-configuration $\mathcal{P} = \{p_1, \ldots, p_6\} \in QC^6$, the following statements hold:*

(a) In the cases $\mathcal{P} \in QC^6_k$, $k = 1, 3$, if $p_i \in \mathcal{P}$ is subdominant, then the real line $f_{\mathcal{P}}(E_i) \subset Y_{\mathcal{P}}$ is hyperbolic while the real line $f_{\mathcal{P}}(\widetilde{Q}_i) \subset Y_{\mathcal{P}}$ is elliptic. Otherwise, $f_{\mathcal{P}}(E_i)$ is elliptic while $f_{\mathcal{P}}(\widetilde{Q}_i)$ is hyperbolic. Furthermore, if both of the points $p_i, p_j \in \mathcal{P}$ are of the same kind (i.e., dominant or subdominant), then the real line $f_{\mathcal{P}}(A_{ij}) \subset Y_{\mathcal{P}}$ is elliptic. Otherwise, $f_{\mathcal{P}}(A_{ij})$ is hyperbolic.

(b) In the case $\mathcal{P} \in QC^6_2$, if $p_i \in \mathcal{P}$ is subdominant, then the real lines $f_{\mathcal{P}}(E_i)$, $f_{\mathcal{P}}(\widetilde{Q}_i) \subset Y_{\mathcal{P}}$ are both elliptic. Otherwise, the lines $f_{\mathcal{P}}(E_i)$, $f_{\mathcal{P}}(\widetilde{Q}_i)$ are both

hyperbolic. Furthermore, if both of the points $p_i, p_j \in \mathcal{P}$ are of the same kind (i.e., dominant or subdominant), then the real line $f_{\mathcal{P}}(A_{ij}) \subset Y_{\mathcal{P}}$ is hyperbolic. Otherwise, $f_{\mathcal{P}}(A_{ij})$ is elliptic.

(c) In the case $\mathcal{P} \in QC^6_6$, the real lines $f_{\mathcal{P}}(E_i)$, $f_{\mathcal{P}}(\widetilde{Q}_i) \subset Y_{\mathcal{P}}$ are both elliptic while the real line $f_{\mathcal{P}}(A_{ij}) \subset Y_{\mathcal{P}}$ is hyperbolic for any $1 \le i < j \le 6$.

Proof. Firstly, we shall show the ellipticity and hyperbolicity of the exceptional curve $E_i \subset X_{\mathcal{P}}$, $i = 1, \dots, 6$ for all the cases of $\mathcal{P} \in QC^6_k$, $k = 1, 2, 3, 6$.

Note that the residual pencil $C^i_{\mathcal{P}}$ associated to the exceptional curve $E_i \subset X_{\mathcal{P}}$, $i = 1, \dots, 6$, consists of the rational cubic curves passing through all six points of $\mathcal{P}$ and having a node at $p_i \in \mathcal{P}$. We see from Figure 11.4 that a nodal cubic $A \in C^i_{\mathcal{P}}$ with empty finite loop (i.e., the finite loop not containing any points of $\mathcal{P}$) occurs in the cases $\mathcal{P} \in QC^6_1$, or $\mathcal{P} \in QC^6_3$ if the point p_i is subdominant, and in the case $\mathcal{P} \in QC^6_2$ if the point p_i is dominant. Since the cubic A in the pencil $C^i_{\mathcal{P}}$ becomes a cubic with a solitary node in this pencil as shown on Figure 6.5 the line $f_{\mathcal{P}}(E_i)$ is hyperbolic. For the remaining cases on $\mathcal{P}$ and p_i, $f_{\mathcal{P}}(E_i)$ is elliptic since we can not get a cubic with a solitary node at p_j in the pencils $C_{\mathcal{P}}$ since these pencils do not contain a nodal cubic with empty finite loop (see Figure 11.4).

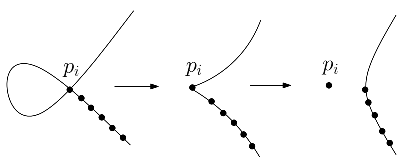

Figure 6.5: The degeneration of a nodal cubic with empty loop to a cubic with a solitary node

Secondly, we shall show the ellipticity and hyperbolicity of the exceptional curve $A_{ij} \subset X_{\mathcal{P}}$, $i \neq j \in \{1, \dots, 6\}$ for all the cases $\mathcal{P} \in QC^6_k$, $k = 1, 2, 3, 6$.

Note that the residual pencil $\{\Omega^{ij}_t\}$ associated to the exceptional curve $A_{ij} \subset X_{\mathcal{P}}$, $i \neq j \in \{1, \dots, 6\}$, consists of the conics Q^{ij}_t passing through four points of $\mathcal{P}$ other than p_i and p_j. We denote by q_t, q'_t the intersection points $Q^{ij}_t \cap A_{ij}$ for each t. If $p_i, p_j \in \mathcal{P}$ are both the same type, i.e. dominant or subdominant, then $f_{\mathcal{P}}(A_{ij})$ is hyperbolic in the cases $\mathcal{P} \in QC^6_i$, $i = 2, 6$, and is elliptic in the cases

$\mathcal{P} \in QC_i^6$, $i = 1, 3$ since the intersection points $\{q_t, q_t'\} = Q_t \cap A_{ij}$ for any t lie in $\mathbb{R}P^1$ as shown in Figure 6.3(a) for the cases $\mathcal{P} \in QC_i^6$, $i = 2, 6$, and lie in $\mathbb{R}P^1$ as shown in Figure 6.3(b) for the cases $\mathcal{P} \in QC_i^6$, $i = 1, 3$. Similarly, if one of the points p_i, p_j is dominant and the other is subdominant, then $f_{\mathcal{P}}(A_{ij})$ is hyperbolic in the cases $\mathcal{P} \in QC_i^6$, $i = 1, 3$, and is elliptic in the case $\mathcal{P} \in QC_2^6$. For example, see Figure 6.6 in which $\mathcal{P}$ is a hexagonal configuration in QC^6.

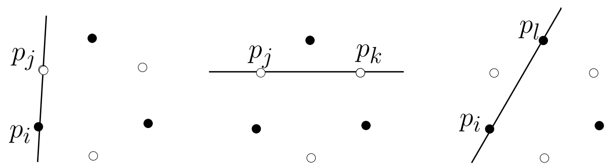

(a) hyperbolic line A_{ij} (b) elliptic line A_{jk} (c) elliptic line A_{il}

Figure 6.6: The examples of hyperbolic and elliptic lines on $X_{\mathcal{P}}$ for $\mathcal{P} \in QC_1^6$, which are the proper images of lines L_{ij}, L_{jk}, and L_{il}.

Finally, we shall show the ellipticity and hyperbolicity of the exceptional curve $\widetilde{Q}_i \subset X_{\mathcal{P}}$, $i = 1, \ldots, 6$, for all the cases $\mathcal{P} \in QC_k^6$, $k = 1, 2, 3, 6$.

Note that the residual pencil $\{\Omega_t^i\}$ associated to the exceptional curve $\widetilde{Q}_i \subset X_{\mathcal{P}}$, $i = 1, \ldots, 6$, consists of the conics consists of lines L_t^i passing through the point $p_i \in \mathcal{P}$. We denote by q_t, q_t' the intersection points $L_t^i \cap Q_i$ for any t. In the cases $\mathcal{P} \in QC_i^6$, $i = 1, 2, 3$, if $p_i \in \mathcal{P}$ is dominant then $f_{\mathcal{P}}(Q_j)$ is hyperbolic since the intersection points $\{q_t, q_t'\} = L_t \cap Q_j$ for any t lie in $\mathbb{R}P^1$ as shown in Figure 6.3(a), and in the cases $\mathcal{P} \in QC_i^6$, $i = 1, 2, 3, 6$ if $p_j \in \mathcal{P}$ is subdominant then $f_{\mathcal{P}}(Q_j)$ is elliptic since the intersection points $\{q_t, q_t'\} = L_t \cap Q_j$ for any t lie in $\mathbb{R}P^1$ as shown in Figure 6.3(b). For example, see Figure 6.7 in which $\mathcal{P}$ is a hexagonal configuration in QC^6. This completes the proof. □

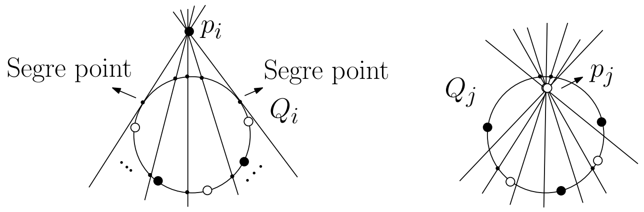

(a) hyperbolic line $\widetilde{Q}_i$ (b) elliptic line $\widetilde{Q}_j$

Figure 6.7: The examples of hyperbolic and elliptic lines on $X_{\mathcal{P}}$ for $\mathcal{P} \in QC_1^6$, which are the proper images of conics Q_i, Q_j.

CHAPTER 7

REAL DEL PEZZO SURFACES

7.1 The marked real del Pezzo M-surfaces of degree 2 and 3

A *marked real del Pezzo M-surface* of degree d is a pair $(X, \mathcal{L})$ consisting of a real del Pezzo surface X of degree d with a maximal set $\mathcal{L}$ (i.e., that of containing $9-d$ real skew lines on X) of real skew lines under inclusion. We call $\mathcal{L}$ a *marking* on X. As an example, consider the pair $(X_{\mathcal{P}}, E_{\mathcal{P}})$, where $X_{\mathcal{P}}$ is the del Pezzo surface of degree $9-n$ obtained by blowing up $\mathbb{P}^2$ at points of $\mathcal{P} \in QC^n$, $1 \le n \le 7$, and $E_{\mathcal{P}}$ is the set of exceptional curves over the blown up points.

Any marked real del Pezzo M-surface arises from a blow-up model described in the previous paragraph (see [Man]), and a deformation of such surfaces are obtained from deformations of configurations of points by blowing up at these points (see [DIK], p.76-77). Thus, the next statement follows immediately from Theorems 2.3.5 and 2.5.1.

Theorem 7.1.1. *There are four deformation classes of marked real del Pezzo M-surfaces of degree* 3*, and there are fourteen deformation classes of marked real del Pezzo M-surfaces of degree* 2*.* □

7.2 Combinatorial anti-canonical correspondence

Given $\mathcal{P} \in QC^n$, $n \le 7$, let us denote by $\mathbb{P}_{\mathcal{P}}$ the real projective space of all real cubic curves in $\mathbb{P}^2$ passing through n points of $\mathcal{P}$. There is a rational map from $\mathbb{P}^2$ to $\widehat{\mathbb{P}}_{\mathcal{P}}$ given by $x \to \widehat{L_x}$, where $\widehat{\mathbb{P}}_{\mathcal{P}}$ and $\widehat{L_x}$ are the polar duals of $\mathbb{P}_{\mathcal{P}}$ and the set of all cubics passing trough n points of $\mathcal{P}$ in addition a point $x \in \mathbb{P}^2$. This map is not well-defined at the points of $\mathcal{P}$, by blowing up these points, the map is extended to $f_{\mathcal{P}} : X_{\mathcal{P}} \to \widehat{\mathbb{P}}_{\mathcal{P}}$, which is called the anti-canonical map, where $X_{\mathcal{P}}$ is the del Pezzo surface $X_{\mathcal{P}}$ of degree $d = 9 - n$ (see Figure 7.1). We shall denote by $\mathcal{L}_{\mathcal{P}}$ the image $f_{\mathcal{P}}(E_{\mathcal{P}})$ where $E_{\mathcal{P}}$ is the set of exceptional curves $E_i \subset X_{\mathcal{P}}$, $i = 1, \ldots, n$ over the blown up points $p_i \in \mathcal{P}$.

$$\begin{tikzcd}
(\mathbb{P}^2, \mathcal{P}) \arrow[r, "f_{\mathcal{P}} \circ \pi^{-1}"] & (\widehat{\mathbb{P}}_{\mathcal{P}}, \mathcal{L}_{\mathcal{P}}) \\
(X_{\mathcal{P}}, E_{\mathcal{P}}) \arrow[u, "\pi"] \arrow[ur, "f_{\mathcal{P}}"'] &
\end{tikzcd}$$

Figure 7.1: The commutative diagram.

Let P be a real projective space which is projectively equivalent to $\mathbb{R}P^{9-n}$. We denote by $LL^n(\mathrm{P})$, or for short LL^n if some projective surface P is fixed, the space of linearly nondegenerate configurations of n real lines in P. Concerning "linearly nondegenerate", we describe what does it mean only in the cases $n = 6, 7$ (see the end of Section 2.2 and Section 5.1). For $n < 6$, the definition is not clarified because this case is not considered. For the quotient space $LL^n(\mathrm{P})/PGL(10 - n, \mathbb{R})$, we use the well-defined notation $LL^n/PGL(10 - n, \mathbb{R})$ since it is independent of the choice of $\mathrm{P} \cong \mathbb{P}^{9-n}$.

We shall denote by $[LL^n]$ and $\langle LL^n \rangle$ for $n = 6, 7$ the set of all L-deformation classes and all coarse L-deformation classes in $LL^n(\mathbb{RP}^{9-n})$, respectively. In fact, in the case of $n = 7$, since $PGL(3, \mathbb{R})$ is connected there is no difference between L-deformation classes and coarse deformation classes in $LL^7(\mathbb{RP}^2)$. That is, $[LL^7] = \langle LL^7 \rangle$. However, some of the L-deformation classes in $LL^6(\mathbb{RP}^3)$ may consist of two connected components of the quotient space $LL^6/PGL(4, \mathbb{R})$ since the group $PGL(4, \mathbb{R})$ is not connected (in fact, it has two connected components). Thus, $\langle LL^6 \rangle$ can be identified with the set of connected components of the quotient space $LL^6/PGL(4, \mathbb{R})$. Note that these quotients do not depend on a particular choice of a projective space $P \cong \mathbb{P}^{9-n}$.

For an n-configuration $\mathcal{P} \in QC^n$, it is well-known fact that the space $\widehat{\mathbb{P}}_{\mathcal{P}}$ is projectively equivalent to $\mathbb{P}^{9-n}$. The map $f_{\mathcal{P}} \circ \pi^{-1} : \mathbb{P}^2 \to \widehat{\mathbb{P}}_{\mathcal{P}}$ induces a map $\phi^n : QC^n/PGL(3,\mathbb{R}) \to LL^n/PGL(10-n,\mathbb{R})$ sending the orbit of $\mathcal{P}$ in $QC^n/PGL(3,\mathbb{R})$ to the orbit of $\mathcal{L}_{\mathcal{P}}$ in $LL^n/PGL(10-n,\mathbb{R})$. This map is called the *anti-canonical correspondence*. Our research concerns the cases $n = 6$ and $n = 7$. If $n = 6$, then the corresponding configurations of lines $\mathcal{L}_{\mathcal{P}}$ in $LL^n(\widehat{\mathbb{P}}_{\mathcal{P}})$ are 6-configuration of skew lines. If $n = 7$, then the corresponding configurations of lines are known in literature as Aronhold sets (for details see Section 9.3).

The map ϕ^n induces another map $[\phi^n]$ between Q-deformation classes in QC^n and coarse L-deformation classes in $LL^n(\widehat{\mathbb{P}}_{\mathcal{P}})$, and this map is called the *combinatorial anti-canonical correspondence*. (See Figure 7.2.) It will be convenient to use the abbreviation CAC-correspondence for the combinatorial anti-canonical correspondence $[\phi^n] : [QC^n] \to \langle LL^n \rangle$.

$$\begin{tikzcd}
\mathcal{P} \in QC^n \arrow[r, "f_{\mathcal{P}}\circ\pi^{-1}"] \arrow[d] & \mathcal{L}_{\mathcal{P}} \in LL^n(\widehat{\mathbb{P}}_{\mathcal{P}}) \arrow[d] \\
QC^n/PGL(3,\mathbb{R}) \arrow[r, "\phi^n"] \arrow[d] & LL^n/PGL(10-n,\mathbb{R}) \arrow[d] \\
{[QC^n]} \arrow[r, "{[\phi^n]}"] & \langle LL^n \rangle
\end{tikzcd}$$

Figure 7.2: The anti-canonical and the combinatorial anti-canonical correspondences, where the vertical arrows on above stand for the natural quotient maps.

7.3 Marking on anti-canonical models

Let X be a real del Pezzo M-surface of degree 3, and assume that $(E, \widetilde{E})$ is a double six on its anti-canonical model (i.e., a cubic M-surface in $\mathbb{P}^3$). Then, we may say that E and $\widetilde{E}$ are two markings on X, and we call them *complementary*. The planes $\mathbb{P}^2$ and $\widetilde{\mathbb{P}}^2$ obtained by blowing down E and $\widetilde{E}$, respectively are called the *complementary planes*, and the 6-configurations $\mathcal{P} \subset \mathbb{P}^2$ and $\widetilde{\mathcal{P}} \subset \widetilde{\mathbb{P}}^2$ obtained as the result of blowing down E and $\widetilde{E}$, respectively are called the *complementary* 6-*configurations*. So, starting from $\mathcal{P} \in QC^6$, we can blow up $\mathcal{P}$ to obtain marking $E_{\mathcal{P}} \subset X_{\mathcal{P}}$, and then blow down the complementary marking

$\widetilde{E_{\mathcal{P}}}$ to obtain the complementary 6-configuration $\widetilde{\mathcal{P}}$ on the complementary plane $\widetilde{\mathbb{P}}^2$.

$$\begin{tikzcd} & (X_{\mathcal{P}}, E_{\mathcal{P}} \cup E_{\widetilde{\mathcal{P}}}) \arrow[dl, "\pi"'] \arrow[dr, "\widetilde{\pi}"] & \\ (\mathbb{P}^2, \mathcal{P}) \arrow[rr, "\xi"] & & (\widetilde{\mathbb{P}}^2, \widetilde{\mathcal{P}}) \end{tikzcd}$$

Figure 7.3: The correspondence between 6-configurations $E_{\mathcal{P}}$ and their complementary 6-configurations $\widetilde{E_{\mathcal{P}}}$ in QC^6 where π and $\widetilde{\pi}$ stand for the blowing up of points of $\mathcal{P}$ and $\widetilde{\mathcal{P}}$ in the planes $\mathbb{P}^2$ and $\widetilde{\mathbb{P}}^2$, respectively.

Theorem 7.3.1. *Assume that $\mathcal{P}$, $\widetilde{\mathcal{P}} \in QC^6$ are complementary 6-configurations to each other. Then they belong to the same Q-deformation class (i.e., QC^6_1, or QC^6_2, or QC^6_3, or QC^6_6).*

Remark 7.3.2. The configurations $\mathcal{P}$ and $\widetilde{\mathcal{P}}$ belong to the different planes. However, $\mathbb{P}^2/PGL(3,\mathbb{R}) = \widetilde{\mathbb{P}}^2/PGL(3,\mathbb{R})$ is a canonical identification, and the corresponding deformation classes in $\mathbb{P}^2$ and $\widetilde{\mathbb{P}}^2$ are identified with the connected components of the corresponding quotient.

Proof of Theorem 7.3.1. The proof is based on the following observation.

Lemma 7.3.3. *If $\mathcal{P} \subset \mathbb{P}^2$ and $\widetilde{\mathcal{P}} \subset \widetilde{\mathbb{P}}^2$ are complementary 6-configurations to each other, then the composition $Cr_{123} \circ Cr_{456} \circ Cr_{123}$ of elementary Cremona transformations transforms the plane $\mathbb{P}^2$ into the plane $\widetilde{\mathbb{P}}^2$, and sends $\mathcal{P}$ to $\widetilde{\mathcal{P}}$.*

Proof of Lemma 7.3.3. Let $\mathcal{P} = \{p_1, \dots, p_6\} \in QC^6$, and $E_{\mathcal{P}} = \{E_1, \dots, E_6\}$, $\widetilde{E_{\mathcal{P}}} = \{\widetilde{Q}_1, \dots, \widetilde{Q}_6\}$ be the complementary markings on $X_{\mathcal{P}}$, where E_i and $\widetilde{Q}_i$, $i = 1, \dots, 6$, are, respectively, the exceptional divisor over the blown up point p_i and the proper transformation of the conic Q_i passing through five points of $\mathcal{P}$ other than p_i. Let $\widetilde{\mathcal{P}} \subset \widetilde{\mathbb{P}}^2$ be the complementary 6-configuration obtained blowing down the exceptional curves $\widetilde{Q}_i$, $i = 1, \dots, 6$. Using Lemma 4.1.3, we obtain Figure 7.4 which shows the transformations of the exceptional curves $E_1, \dots, E_6 \subset X_{\mathcal{P}}$ in each step of $Cr_{123} \circ Cr_{456} \circ Cr_{123}$. In particular, it shows that the marking $\{E_1, \dots, E_6\}$ are interchanged with the complementary marking $\{\widetilde{Q}_1, \dots, \widetilde{Q}_6\}$. ◻

$$
\begin{array}{ccccccc}
E_1 & \xleftrightarrow{Cr_{123}} & A_{23} & \xleftrightarrow{Cr_{456}} & \widetilde{Q}_1 & \xleftrightarrow{Cr_{123}} & \widetilde{Q}_1 \\
E_2 & \longleftrightarrow & A_{13} & \longleftrightarrow & \widetilde{Q}_2 & \longleftrightarrow & \widetilde{Q}_2 \\
E_3 & \longleftrightarrow & A_{12} & \longleftrightarrow & \widetilde{Q}_3 & \longleftrightarrow & \widetilde{Q}_3 \\
E_4 & \longleftrightarrow & E_4 & \longleftrightarrow & A_{56} & \longleftrightarrow & \widetilde{Q}_4 \\
E_5 & \longleftrightarrow & E_5 & \longleftrightarrow & A_{46} & \longleftrightarrow & \widetilde{Q}_5 \\
E_6 & \longleftrightarrow & E_6 & \longleftrightarrow & A_{45} & \longleftrightarrow & \widetilde{Q}_6
\end{array}
$$

Figure 7.4: The modifications of the exceptional curves E_i, $\widetilde{Q}_i \subset X_{\mathcal{P}}$, $i \in \{1, \ldots, 6\}$, under $Cr_{123} \circ Cr_{456} \circ Cr_{123}$, in which $A_{ij} \subset X_{\mathcal{P}}$ are the proper transformation of lines L_{ij} joining two points p_i and p_j of a given configuration $\mathcal{P} \in QC^6$.

To complete the proof of this theorem, note that the image of any configuration $\mathcal{P} \in QC^6$ under $Cr_{123} \circ Cr_{456} \circ Cr_{123}$ is Q-deformation equivalent to $\mathcal{P}$, that is, they belong to the same Q-deformation class in QC^6 as illustrated in Figure 7.5.

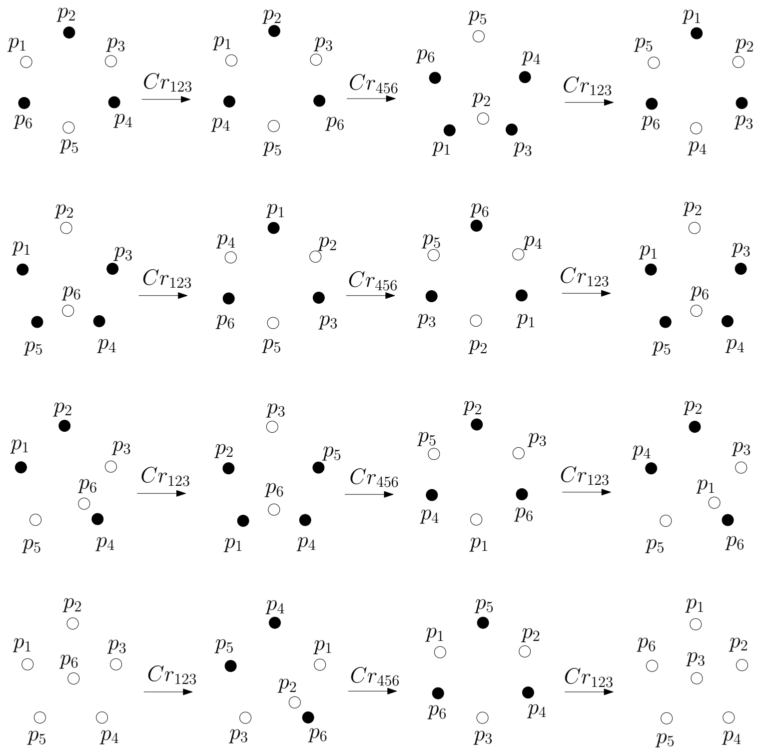

Figure 7.5: The modification of a 6-configuration from each of the classes QC^6_i, $i = 1, 2, 3, 6$, under $Cr_{123} \circ Cr_{456} \circ Cr_{123}$.

□

CHAPTER 8

ANTI-CANONICAL CORRESPONDENCE FOR REAL CUBIC SURFACES

8.1 *CAC*-correspondence for cubic surfaces

In the Theorem 2.3.5, we show that there are exactly four Q-deformation classes in QC^6, namely, QC^6_1,QC^6_2,QC^6_3 and QC^6_6. The following theorem answers to the question about the corresponding four L-deformation classes of configurations of six skew lines in $\mathbb{R}P^3$ (among the 19 classes mentioned in Theorem 5.5.2).

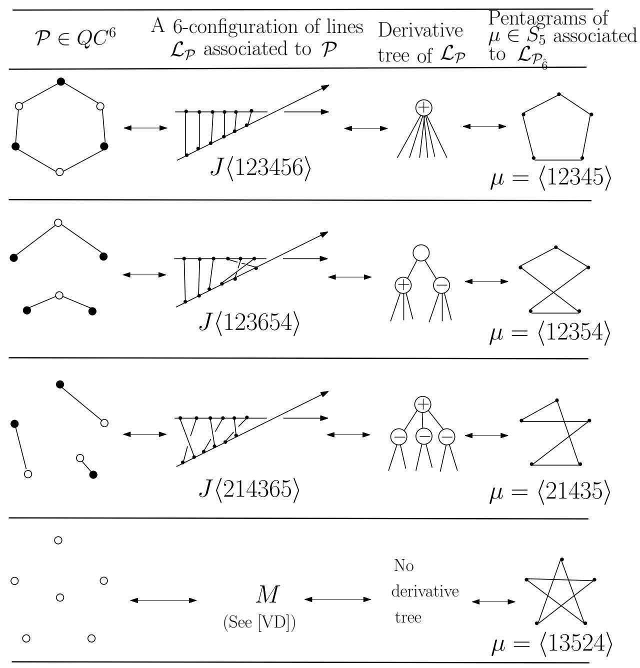

Figure 8.1: The *CAC*-correspondence between Q-deformation classes in QC^6 and L-deformation classes of 6-configuration of skew lines in $\mathbb{R}P^3$.

Theorem 8.1.1. *The CAC-correspondence* $[\phi^6]$ *sends the Q-deformation classes* QC^6_1*,* QC^6_2*,* QC^6_3*, and* QC^6_6*, respectively to the coarse L-deformation classes* $J\langle 123456\rangle$*,* $J\langle 123654\rangle$*,* $J\langle 214365\rangle$*, and* M *(see Figure 8.1).*

Proof. Let us take a 6-configuration $\mathcal{P} = \{p_1, \dots, p_6\} \in QC^6$ with the corresponding marked cubic surface $(Y_{\mathcal{P}}, \mathcal{L}_{\mathcal{P}})$ where $L_i \in \mathcal{L}_{\mathcal{P}}$, $i = 1, \dots, 6$, is the line $f_{\mathcal{P}}(E_i)$ represented by the exceptional curve E_i over p_i. We denote by $\widetilde{\mathcal{L}}_{\mathcal{P}} = \{\widetilde{L}_1, \dots, \widetilde{L}_6\}$ and $\widetilde{\mathcal{P}} = \{\widetilde{p}_1, \dots, \widetilde{p}_6\}$ the complementary marking on $Y_{\mathcal{P}}$ and the complementary configuration in $\widetilde{\mathbb{P}}^2$, respectively. Consider any quadruple of distinct exceptional curves from $\mathcal{L}_{\mathcal{P}}$, without loss of generality we can choose L_1, L_2, L_3, L_4. The four exceptional curves L_1, L_2, L_3, L_4 together with two curves $\widetilde{L}_5$, $\widetilde{L}_6$ from the complementary marking $\widetilde{\mathcal{L}}_{\mathcal{P}}$ induce a join configuration $J(\sigma)$ for some $\sigma \in S_4$ (see Figure 8.2).

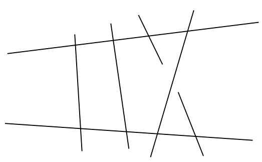

Figure 8.2: The join configuration $J(\sigma)$ for some $\sigma \in S_4$.

To find this permutation, we shall analyze in which order the points $\widetilde{p}_1, \widetilde{p}_2, \widetilde{p}_3, \widetilde{p}_4$ of $\widetilde{\mathcal{P}}$ lie on the curves $\widetilde{\pi}(f_{\mathcal{P}}^{-1}(\widetilde{L}_5)), \widetilde{\pi}(f_{\mathcal{P}}^{-1}(\widetilde{L}_6))$, where $\widetilde{\pi} : X_{\mathcal{P}} \to \widetilde{\mathbb{P}}^2$ is the blow-up of $\widetilde{\mathbb{P}}^2$. This will allow us to compare the sign of $lk(L_i, L_j, L_k)$, $1 \le i, j, k \le 4$.

The proof is based on the following observations.

Lemma 8.1.2. *All triple linking numbers* $lk(L_i, L_j, L_k)$ *of lines* $L_i, L_j, L_k \in \mathcal{L}_{\mathcal{P}}$ *for any hexagonal configuration* $\mathcal{P} \in QC^6_1$ *and for any* $1 \le i < j < k \le 6$ *have the same value* $+1$ *or* -1*.*

Proof of Lemma 8.1.2. Assume that $\mathcal{P} = \{p_1, \dots, p_6\}$ is a hexagonal configuration, and that the numeration of the points of $\mathcal{P}$ is cyclic. Let $(Y_{\mathcal{P}}, \mathcal{L}_{\mathcal{P}})$ be the corresponding marked cubic surface where $L_i \in \mathcal{L}_{\mathcal{P}}$, $i = 1, \dots, 6$, is the line $f_{\mathcal{P}}(E_i)$ represented by the exceptional curve E_i over p_i. Let $\widetilde{\mathcal{L}}_{\mathcal{P}} = \{\widetilde{L}_1, \dots, \widetilde{L}_6\}$ and $\widetilde{\mathcal{P}} = \{\widetilde{p}_1, \dots, \widetilde{p}_6\}$ be the complementary marking on $Y_{\mathcal{P}}$ and the complementary configuration in $\widetilde{\mathbb{P}}^2$, respectively. Consider the quadruple of distinct exceptional curves L_1, L_2, L_3, L_4 from $\mathcal{L}_{\mathcal{P}}$, and take two curves $\widetilde{L}_5, \widetilde{L}_6$ from $\widetilde{\mathcal{L}}_{\mathcal{P}}$. The images $\pi(f_{\mathcal{P}}^{-1}(\widetilde{L}_k))$, $k = 5, 6$, is the conic $\widetilde{Q}_k$ passing through five points of $\widetilde{\mathcal{P}}$ other than $\widetilde{p}_k$. The points $\widetilde{p}_1, \widetilde{p}_2, \widetilde{p}_3, \widetilde{p}_4$ appear on the conics $\widetilde{Q}_5$ and $\widetilde{Q}_6$ in consecutive orders. For a certain orientation of $\mathbb{R}P^3$ we get $lk(L_i, L_j, L_k) = +1$ for any $1 \leq i < j < k \leq 4$ since these two orders induce an identity permutation $\left(\begin{smallmatrix} 1 & 2 & 3 & 4 \\ 1 & 2 & 3 & 4 \end{smallmatrix}\right) \in S_4$ (see Example 5.3). We can pass from any quadruple of lines on $Y_{\mathcal{P}}$ to any other quadruple of lines on $Y_{\mathcal{P}}$ in several steps, by changing just one line in each step. So, the signs of all triple linking numbers should be the same. Therefore, the total linking codes, i.e. the pair (lk_+, lk_-) is $(20, 0)$ (or, $(0, 20)$ for another choice of orientation of $\mathbb{R}P^3$). □

The next statement follows from Lemma 8.1.2 and Figure 5.6.

Corollary 8.1.3. *For each $\mathcal{P} \in QC^6_1$, $\mathcal{L}_{\mathcal{P}} \in J\langle 123456\rangle$.* □

Lemma 8.1.4. *Let $\mathcal{P} \in QC^6_6$, and assume that the numeration $p_1, \ldots, p_5$ of points of $\mathcal{P}$ other than p_6 is cyclic such that the point p_6 is inside the Q-region D as shown in Figure 2.4. Then, for some orientation of $\mathbb{R}P^3$ the triple linking numbers $lk(L_i, L_j, L_k)$ of lines $L_i, L_j, L_k \in \mathcal{L}_{\mathcal{P}}$ on $Y_{\mathcal{P}}$ (namely, for the orientation $lk(L_1, L_2, L_3) = +1$) are like indicated in the table shown in Figure 8.3.*

$lk(L_1, L_2, L_3) = +1$	$lk(L_1, L_2, L_4) = -1$
$lk(L_1, L_2, L_5) = +1$	$lk(L_1, L_2, L_6) = -1$
$lk(L_1, L_3, L_6) = +1$	$lk(L_1, L_3, L_4) = -1$
$lk(L_1, L_4, L_5) = +1$	$lk(L_1, L_3, L_5) = -1$
$lk(L_1, L_4, L_6) = +1$	$lk(L_1, L_5, L_6) = -1$
$lk(L_2, L_3, L_4) = +1$	$lk(L_2, L_3, L_5) = -1$
$lk(L_2, L_4, L_6) = +1$	$lk(L_2, L_3, L_6) = -1$
$lk(L_2, L_5, L_6) = +1$	$lk(L_2, L_4, L_5) = -1$
$lk(L_3, L_4, L_5) = +1$	$lk(L_3, L_4, L_6) = -1$
$lk(L_3, L_5, L_6) = +1$	$lk(L_4, L_5, L_6) = -1$

Figure 8.3: Triple linking numbers of lines of $\mathcal{L}_{\mathcal{P}}$ for $\mathcal{P} \in QC^6_6$ satisfying the conditions in Lemma 8.1.4.

Proof of Lemma 8.1.4. Assume that $(Y_{\mathcal{P}}, \mathcal{L}_{\mathcal{P}})$ is the corresponding marked cubic surface where $L_i \in \mathcal{L}_{\mathcal{P}}$, $i = 1, \ldots, 6$, is the line $f_{\mathcal{P}}(E_i)$ represented by the exceptional curve E_i over p_i. Let $\widetilde{\mathcal{L}}_{\mathcal{P}} = \{\widetilde{L}_1, \ldots, \widetilde{L}_6\}$ and $\widetilde{\mathbb{P}}^2 = \{\widetilde{p}_1, \ldots, \widetilde{p}_6\}$

be the complementary marking on $Y_{\mathcal{P}}$ and the complementary configuration in $\widetilde{\mathbb{P}}^2$, respectively. Consider the quadruple of distinct lines L_1, L_2, L_3, L_4 in $Y_{\mathcal{P}}$ from $\mathcal{L}_{\mathcal{P}}$, and take two curves $\widetilde{L}_5$, $\widetilde{L}_6$ from $\widetilde{\mathcal{L}}_{\mathcal{P}}$. The images $\pi(f_{\mathcal{P}}^{-1}(\widetilde{L}_k))$, $k = 5, 6$, are the conics $\widetilde{Q}_k$ passing through five points of the complementary configuration $\widetilde{\mathcal{P}}$ other than $\widetilde{p}_k$. The points $\widetilde{p}_1, \widetilde{p}_2, \widetilde{p}_3, \widetilde{p}_4$ appear on the conics $\widetilde{Q}_5$ and $\widetilde{Q}_6$ in these orders $\widetilde{p}_2$, $\widetilde{p}_3$, $\widetilde{p}_1$, $\widetilde{p}_4$ and $\widetilde{p}_1$, $\widetilde{p}_2$, $\widetilde{p}_3$, $\widetilde{p}_4$, respectively. For a certain orientation of $\mathbb{R}P^3$ we get $lk(L_1, L_2, L_3) = lk(L_2, L_3, L_4) = +1$ and $lk(L_1, L_2, L_4) = lk(L_1, L_3, L_4) = -1$ since these two orders induce the permutation $\left(\begin{smallmatrix} 2 & 3 & 1 & 4 \\ 1 & 2 & 3 & 4 \end{smallmatrix}\right) \in S_4$. Let us consider the quadruple of distinct skew lines L_1, L_2, L_3, L_5 in $Y_{\mathcal{P}}$ and two lines $\widetilde{L}_4$, $\widetilde{L}_6$ from $\widetilde{\mathcal{L}}_{\mathcal{P}}$. The points $\widetilde{p}_1, \widetilde{p}_2, \widetilde{p}_3, \widetilde{p}_5$ appear on the conics $\widetilde{Q}_4$ and $\widetilde{Q}_6$ in these orders $\widetilde{p}_1$, $\widetilde{p}_2$, $\widetilde{p}_5$, $\widetilde{p}_3$ and $\widetilde{p}_1$, $\widetilde{p}_2$, $\widetilde{p}_5$, $\widetilde{p}_3$, respectively. If we respect to the previous chosen orientation of $\mathbb{R}P^3$ and the triple linking number of the lines L_1, L_2, L_3 as found in the previous line, then we get $lk(L_1, L_2, L_5) = lk(L_2, L_3, L_5) = lk(L_1, L_3, L_5) = +1$ since the induced permutation is $\left(\begin{smallmatrix} 1 & 2 & 5 & 3 \\ 1 & 2 & 5 & 3 \end{smallmatrix}\right)$. Note that after relabeling the points $\widetilde{p}_1, \widetilde{p}_2, \widetilde{p}_3, \widetilde{p}_5$ we see that the permutation is an identity permutation in S_4. We can pass from any quadruple of lines on $Y_{\mathcal{P}}$ to any other quadruple of lines on $Y_{\mathcal{P}}$ in several steps, by changing just one line in each step. By proceeding the same way, we shall get the table shown in Figure 8.3. □

The proofs of the next two results are analogous to the one Lemma 8.1.4, and so we omit them.

Lemma 8.1.5. *Let $\mathcal{P} \in QC^6_2$, and assume that the numeration $p_1, \ldots, p_5$ of points of $\mathcal{P}$ other than p_6 is cyclic such that the point p_6 is inside the Q-region B as shown in Figure 2.4. Then, for some orientation of $\mathbb{R}P^3$ the linking numbers of lines $L_i, L_j, L_k \in \mathcal{L}_{\mathcal{P}}$ on $Y_{\mathcal{P}}$ (namely, for the orientation $lk(L_1, L_2, L_3) = +1$) are like indicated in the table shown in Figure 8.4.* □

Lemma 8.1.6. *Let $\mathcal{P} \in QC^6_3$, and assume that the numeration $p_1, \ldots, p_5$ of points of $\mathcal{P}$ other than p_6 is cyclic such that the point p_6 is inside the Q-region C as shown in Figure 2.4. Then, for some orientation of $\mathbb{R}P^3$ the linking numbers of lines $L_i, L_j, L_k \in \mathcal{L}_{\mathcal{P}}$ on $Y_{\mathcal{P}}$ (namely, for the orientation $lk(L_1, L_2, L_3) = +1$) are like indicated in the table shown in Figure 8.5.* □

$lk(L_1, L_2, L_3) = +1$	$lk(L_1, L_4, L_5) = -1$
$lk(L_1, L_2, L_5) = +1$	$lk(L_1, L_4, L_6) = -1$
$lk(L_1, L_3, L_6) = +1$	$lk(L_2, L_4, L_6) = -1$
$lk(L_1, L_2, L_4) = +1$	$lk(L_2, L_5, L_6) = -1$
$lk(L_1, L_2, L_6) = +1$	$lk(L_1, L_5, L_6) = -1$
$lk(L_2, L_3, L_4) = +1$	$lk(L_3, L_4, L_5) = -1$
$lk(L_1, L_3, L_4) = +1$	$lk(L_3, L_5, L_6) = -1$
$lk(L_1, L_3, L_5) = +1$	$lk(L_2, L_4, L_5) = -1$
$lk(L_2, L_3, L_5) = +1$	$lk(L_3, L_4, L_6) = -1$
$lk(L_2, L_3, L_6) = +1$	$lk(L_4, L_5, L_6) = -1$

Figure 8.4: Triple linking numbers of lines of $\mathcal{L}_{\mathcal{P}}$ for $\mathcal{P} \in QC_2^6$ satisfying the conditions in Lemma 8.1.5.

$lk(L_1, L_2, L_3) = +1$	$lk(L_1, L_2, L_4) = -1$
$lk(L_1, L_2, L_5) = +1$	$lk(L_1, L_2, L_6) = -1$
$lk(L_1, L_4, L_5) = +1$	$lk(L_1, L_3, L_6) = -1$
$lk(L_1, L_3, L_5) = +1$	$lk(L_1, L_3, L_4) = -1$
$lk(L_1, L_5, L_6) = +1$	$lk(L_2, L_4, L_5) = -1$
$lk(L_2, L_3, L_5) = +1$	$lk(L_2, L_5, L_6) = -1$
$lk(L_2, L_3, L_6) = +1$	$lk(L_3, L_4, L_5) = -1$
$lk(L_1, L_4, L_6) = +1$	$lk(L_3, L_5, L_6) = -1$
$lk(L_3, L_4, L_6) = +1$	
$lk(L_4, L_5, L_6) = +1$	
$lk(L_2, L_3, L_4) = +1$	
$lk(L_2, L_4, L_6) = +1$	

Figure 8.5: Triple linking numbers of lines of $\mathcal{L}_{\mathcal{P}}$ for $\mathcal{P} \in QC_3^6$ satisfying the conditions in Lemma 8.1.6.

By Lemmas 8.1.4, 8.1.5 and 8.1.6, we see that if $\mathcal{P} \in QC_6^6$, or $\mathcal{P} \in QC_2^6$, or $\mathcal{P} \in QC_3^6$ then the total linking codes are $(10, 10)$, $(12, 8)$ (or, $(8, 12)$ for another choice of orientation of $\mathbb{R}P^3$), (10,10), respectively. However, we see from Figure 5.6 that, among 19 L-deformation classes, the five L-deformation classes that consist of 6-configurations of skew lines with the total linking codes $(10, 10)$, namely, $J(123654)$, $J(124653)$, $J(135264)$, M, and $\overline{M}$, the four L-deformation classes that consist of 6-configurations of lines with the total linking codes $(12, 8)$, namely, $J(125634)$, $J(124365)$, $J(124635)$, L, and the four L-deformation classes that consist of 6-configurations of skew lines with the total linking codes $(8, 12)$, namely, $J(436521)$, $J(564321)$, $J(536421)$, $\overline{L}$.

Fix an orientation of $\mathbb{R}P^3$ and consider a 6-configuration of skew lines in $\mathbb{R}P^3$, $\mathcal{L} = \{L_1, \ldots, L_6\}$. We denote by $\mathcal{L}_{\hat{i}}$, $i = 1, \ldots, 6$, the 5-configuration of skew lines in $\mathbb{R}P^3$ obtained from $\mathcal{L}$ by removing the line L_i. The set

$$d(\mathcal{L}) = \{(lk_+(\mathcal{L}_{\hat{1}}), lk_-(\mathcal{L}_{\hat{1}})), \ldots, (lk_+(\mathcal{L}_{\hat{6}}), lk_-(\mathcal{L}_{\hat{6}}))\}$$

is called the *derivative linking code of* $\mathcal{L}$. Note that if we change the orientation of $\mathbb{R}P^3$, then the first and second entries of all pair $\big(lk_+(\mathcal{L}_{\hat{i}}), lk_-(\mathcal{L}_{\hat{i}})\big)$ are changed simultaneously.

Remark 8.1.7. We say that an n-configuration of skew lines $\mathcal{L} = \{L_1, \ldots, L_n\}$ in $\mathbb{R}P^3$ is *symmetric* if all $\mathcal{L}_{\hat{i}}$ are L-deformation equivalent to each other. It can be easily shown that any 6-configuration of skew lines in each of the L-deformation classes $J[123456]$, $J[125634]$, M, $\overline{M}$, L, $\overline{L}$ among the 19 deformation classes (see Theorem 5.5.2) is symmetric.

Straightforward analysis gives the following derivative linking codes, which allows to figure out which ones correspond to the 6-configuration $\mathcal{L}_{\mathcal{P}}$ for $\mathcal{P} \in QC^6_i$, $i = 2, 3, 6$.

Table 8.1: The derivative codes of 6-configurations of skew lines in $\mathbb{R}P^3$ with total linking code $(10, 10)$.

$d(J(123654)) = \{(3,7),(3,7),(3,7),(7,3),(7,3),(7,3)\}$
$d(J(124653)) = \{(4,6),(4,6),(6,4),(3,7),(6,4),(6,4)\}$
$d(J(135264)) = \{(4,6),(6,4),(5,5),(6,4),(4,6),(5,5)\}$
$d(M) = d(\overline{M}) = \{(5,5),(5,5),(5,5),(5,5),(5,5),(5,5)\}$

Table 8.2: The derivative codes of 6-configurations of skew lines in $\mathbb{R}P^3$ with total linking code $(12, 8)$.

$d(J(125634)) = \{(6,4),(6,4),(6,4),(6,4),(6,4),(6,4)\}$
$d(J(124365)) = \{(4,6),(4,6),(7,3),(7,3),(7,3),(7,3)\}$
$d(J(124635)) = \{(5,5),(5,5),(7,3),(6,4),(6,4),(7,3)\}$
$d(L) = \{(4,6),(4,6),(4,6),(4,6),(4,6),(4,6)\}$

Table 8.3: The derivative codes of 6-configurations of skew lines in $\mathbb{R}P^3$ with the total linking code $(8, 12)$.

$d(J(436521)) = \{(4,6),(4,6),(4,6),(4,6),(4,6)\}$
$d(J(563421)) = \{(6,4),(6,4),(3,7),(3,7),(3,7),(3,7)\}$
$d(J(536421)) = \{(5,5),(5,5),(3,7),(4,6),(4,6),(3,7)\}$
$d(\overline{L}) = \{(6,4),(6,4),(6,4),(6,4),(6,4),(6,4)\}$

Using the tables given Figures 8.3, 8.4 and 8.5, we easily calculate all pairs $(lk_+(\mathcal{L}_{\mathcal{P}\hat{i}}), lk_-(\mathcal{L}_{\mathcal{P}\hat{i}}))$ for $\mathcal{P} \in QC^6_j$, $j = 2, 3, 6$ as shown in Table 8.4.

Table 8.4: Total triple number and the derivative linking code of $\mathcal{L}_{\mathcal{P}}$ for any $\mathcal{P} \in QC^6$.

$\mathcal{P} \in QC^6$	Total triple numbers	The derivative linking codes of $\mathcal{L}_{\mathcal{P}}$
$\mathcal{P} \in QC^6_2$	(10,10)	$d(\mathcal{L}_{\mathcal{P}}) = \{(6,4),(6,4),(6,4),(6,4),(6,4),(6,4)\}$
$\mathcal{P} \in QC^6_3$	(12,8) or (8,12)	$d(\mathcal{L}_{\mathcal{P}}) = \{(4,6),(4,6),(7,3),(7,3),(7,3),(7,3)\}$
$\mathcal{P} \in QC^6_6$	(10,10)	$d(\mathcal{L}_{\mathcal{P}}) = \{(5,5),(5,5),(7,3),(6,4),(6,4),(7,3)\}$

By comparing the results in Tables 8.1, 8.2, 8.3 with the ones in Table 8.4, we observe that $\mathcal{L}_{\mathcal{P}}$ is coarse L-deformation equivalent to $J(125634)$, $J(124365)$ and M if $\mathcal{P} \in QC^6_2$, $\mathcal{P} \in QC^6_3$, and $\mathcal{P} \in QC^6_6$, respectively. Together with the result in Corollary 8.1.3, this completes the proof of Theorem 8.1.1. □

The next statement is an immediate consequence of this theorem.

Corollary 8.1.8. *A* 6*-configuration* $\mathcal{L}$ *of skew lines in* $\mathbb{R}P^3$ *is L-deformation equivalent (or, coarse L-deformation equivalent) to a* 6*-configuration of skew lines on some cubic surface if and only if* $\mathcal{L}$ *belongs to one of the L-deformation classes* $J[123456]$*,* $J[654321]$*,* $J[123654]$*,* $J[214365]$*,* $J[125634]$*,* M*,* $\overline{M}$ *(or, to one of the coarse L-deformation classes* $J\langle 123456\rangle$*,* $J\langle 123654\rangle$*,* $J\langle 214365\rangle$*,* M*).* □

CHAPTER 9

ANTI-CANONICAL MODELS OF REAL DEL PEZZO SURFACES OF DEGREE 2

9.1 CAC-correspondence for del Pezzo surfaces of degree 2

Throughout the rest of this chapter, by a cubic curve *based at* $\mathcal{P}$, we mean a plane cubic curve passing trough n points of a given planar n-configuration $\mathcal{P}$.

We recall (see Section 7.2) that for a given 7-configuration $\mathcal{P} \in QC^7$, we denote by $\widehat{\mathbb{P}}_{\mathcal{P}}$ the polar dual of the space formed by cubic curves based at $\mathcal{P}$, and by $f_{\mathcal{P}} : X_{\mathcal{P}} \to \widehat{\mathbb{P}}_{\mathcal{P}}$ the anticanonical map defined by the anticanonical divisor of the del Pezzo surface $X_{\mathcal{P}}$.

Remark 9.1.1. The following properties (see, e.g. [H]) can be easily verified:

(a) The space $\mathbb{P}_{\mathcal{P}}$ of cubic curves based at any planar 7-configuration $\mathcal{P}$ is a plane provided that no five points of $\mathcal{P}$ are collinear.

(b) The rational map $f_{\mathcal{P}} : X_{\mathcal{P}} \to \widehat{\mathbb{P}}_{\mathcal{P}}$ is (generically) two-to-one if no 4 points of $\mathcal{P}$ are collinear and all 7 points of $\mathcal{P}$ do not lie on a conic. More precisely, under the two assumptions the map $f_{\mathcal{P}} : X_{\mathcal{P}} \to \widehat{\mathbb{P}}_{\mathcal{P}}$ is a double covering branched along a quartic curve C.

(c) $\mathcal{P} \in QC^7$ if and only if the quartic curve C mentioned in part (b) is non-singular.

Recall that we denote by $[\phi^7]$ the combinatorial anti-canonical correspondence (i.e., for short CAC-correspondence) between Q-deformation classes in QC^7 and coarse L-deformation classes in $LL^7(\widehat{\mathbb{P}}_{\mathcal{P}})$, see Section 7.2. The next statement which claims about the independence of the CAC-correspondence under the choice of configuration $\mathcal{P}$ (that is, if you choose a Q-deformation equivalent configuration then this map will give the same value) follows from Lemmas 9.1.3 and 9.1.5.

Proposition 9.1.2. *The CAC-correspondence $[\phi^7] : [QC^7] \to [LL^7]$ is well-defined.* □

Let $\mathcal{P} = \{p_1, \ldots, p_7\} \in QC^7$ be a 7-configuration. We denote by A_i, $i = 1, \ldots, 7$, the cubic curve based at $\mathcal{P}$ with a node at the point p_i. The set $\mathcal{A}_{\mathcal{P}}$ formed by these cubics A_i is a 7-configuration in $\mathbb{P}_{\mathcal{P}}$. The well-know fact is that the anti-canonical map $f_{\mathcal{P}} : X_{\mathcal{P}} \to \widehat{\mathbb{P}}_{\mathcal{P}}$ maps both the exceptional curve $E_i \subset X_{\mathcal{P}}$ (i.e., over blown up point p_i) and the proper image $\widetilde{A}_i \subset X_{\mathcal{P}}$ of the nodal cubic A_i to the same bitangent line L_i to a nonsingular quartic C in $\widehat{\mathbb{P}}_{\mathcal{P}}$ for each $i \in \{1, \ldots, 7\}$. We denote by $\mathcal{L}_{\mathcal{P}} = \{L_1, \ldots, L_7\}$ the 7-configuration of bitangent lines.

Proposition 9.1.3. *The set $\mathcal{L}_{\mathcal{P}}$ for any configuration $\mathcal{P} \in QC^7$ is a polar dual to $\mathcal{A}_{\mathcal{P}}$ in $\mathbb{P}_{\mathcal{P}}$. That is, $\mathcal{L}_{\mathcal{P}} = \widehat{\mathcal{A}}_{\mathcal{P}}$ for any $\mathcal{P} \in QC^7$.*

Proof. Let y be a point in $\widehat{\mathbb{P}}_{\mathcal{P}}$, and $\{x, g(x)\}$ be the inverse image of this point under the anti-canonical map $f_{\mathcal{P}} : X_{\mathcal{P}} \to \widehat{\mathbb{P}}_{\mathcal{P}}$, where g is a Geiser involution. The pencil of plane cubics passing through $p_1, \ldots, p_7, x, g(x)$ is a line in $\mathbb{P}_{\mathcal{P}}$. We denote this line by L_x. Let $L_y \subset \mathbb{P}_{\mathcal{P}}$ be the dual line of the point y.

The proof of this proposition is based on the following simple observation.

Lemma 9.1.4. *For any $i = 1, \ldots, 7$, the following three conditions are equivalent:*

(a) $A_i \in L_y$.

(b) The pencil $L_x \subset \mathbb{P}_{\mathcal{P}}$ contains A_i.

(c) $y \in L_i = f_{\mathcal{P}} \circ \pi^{-1}(A_i)$. □

For each $i \in \{1, \ldots, 7\}$, the set of cubics passing through the eight points $\widehat{L_1}, \ldots, \widehat{L_7}$, and A_i is a pencil in $\mathbb{P}_{\mathcal{P}}$. Let B_i be the ninth base point of the pencil.

Note that the two plane cubics A_i and B_i passing through $p_1, \ldots, p_7 \in \mathcal{P}$ induce a pencil in $\mathbb{P}^2$, and assume that two additional based points of the pencil are x and $g(x)$. Let us denote by L_x this pencil, and by $y \in \widehat{\mathbb{P}}_{\mathcal{P}}$ the image of x and $g(x)$ under $f_{\mathcal{P}} \circ \pi^{-1}$. Since L_x contains A_i, by Lemma 9.1.4 we have $A_i \in L_y$ and $y \in L_i = f_{\mathcal{P}} \circ \pi^{-1}(A_i)$, where $L_y \subset \mathbb{P}_{\mathcal{P}}$ is the polar dual of the point y.

This completes the proof of this proposition. □

Lemma 9.1.5. *If $\mathcal{P} \in QC^7$, then $\mathcal{A}_{\mathcal{P}} \in LC^7(\mathbb{P}_{\mathcal{P}})$.*

Proof. Let $\mathcal{P} = \{p_1, \ldots, p_7\}$, and assume that $\mathcal{A}_{\mathcal{P}} \notin LC^7(\mathbb{P}_{\mathcal{P}})$. Then, there is a line $L \subset \mathbb{P}_{\mathcal{P}}$ containing three points A_i, A_j, A_k of $\mathcal{A}_{\mathcal{P}}$ for some $1 \le i < j < k \le 7$. Let us denote by $\hat{A}_i$, $\hat{A}_j$, $\hat{A}_k$ the lines in $\widehat{\mathbb{P}}_{\mathcal{P}}$ which are the polar duals of A_i, A_j, A_k, respectively, and by $\widetilde{A}_i$, $\widetilde{A}_j$, $\widetilde{A}_k$ the proper images of the nodal cubics A_i, A_j, $A_k \in \mathbb{P}^2$, respectively. Then, we have

$$f_{\mathcal{P}}(E_i) = \hat{A}_i = f_{\mathcal{P}}(\widetilde{A}_i), \quad f_{\mathcal{P}}(E_j) = \hat{A}_j = f_{\mathcal{P}}(\check{A}_i), \quad f_{\mathcal{P}}(E_k) = \hat{A}_k = f_{\mathcal{P}}(\widetilde{A}_i)$$

where E_i, $i = 1, \ldots, 7$, are the exceptional lines over the blown up points $p_i \in \mathcal{P}$. Since $A_i, A_j, A_k \in \mathcal{A}_{\mathcal{P}}$ are collinear their polar duals $\hat{A}_i$, $\hat{A}_j$, $\hat{A}_k$ are concurrent. However, E_i, E_j, E_k are skew, and the map $f_{\mathcal{P}}$ is two-to-one, so $\hat{A}_i$, $\hat{A}_j$, $\hat{A}_k$ are not concurrent (otherwise, E_i, E_j, E_k are not skew). However, this yields the contradiction that the surface $X_{\mathcal{P}}$ is singular. □

9.2 Lifting the bitangents to del Pezzo surfaces

Recall that given a del Pezzo surface of degree 2, X, the anti-canonical map $f : X \to \mathbb{P}^2$ is a double covering branched over a nonsingular quartic $C \subset \mathbb{P}^2$. Conversely, the double covering of $\mathbb{P}^2$ branched over a nonsingular quartic C is a del Pezzo surface of degree 2. We denote this surface by X_C, and the anti-canonical map defined by the anti-canonical divisor of X_C by $f_C : X_C \to \mathbb{P}^2$.

In this section, our aim is to construct a one-to-one correspondence between the set of decorated bitangent lines to the real locus $\mathbb{R}C$ of C and the set of the decorated lines on the real locus $\mathbb{R}X_C$ of the del Pezzo surface X_C.

Proposition 9.2.1. *Assume that X is a real del Pezzo surface of degree 2, and $f : X \to \mathbb{P}^2$ is its anti-canonical map, that is, a double covering branched over some real quartic $C \subset \mathbb{P}^2$. Assume also that X is M-surface, i.e., its real locus $\mathbb{R}X$ is homeomorphic to $\mathbb{R}P^2 \# 7\mathbb{R}P^2$. Then:*

(a) The quartic C is M-curve, i.e., its real locus $\mathbb{R}C$ has four connected components (ovals).

(b) The image $W = f(\mathbb{R}X)$ is the complement in $\mathbb{R}P^2$ of the four topological discs bounded by the four ovals of $\mathbb{R}C$.

(c) The restriction $f|_{\mathbb{R}X}$ of the projection f is a trivial double covering over the interior of W. In particular, $\mathbb{R}X$ is homeomorphic to the double $W_A \cup W_B$ of W. Here W_A and W_B are two copies of W, identified with it by the projection f, and having common boundary $\partial W_A = \partial W_B$.

Proof. The first and second statements follow from evaluation of the Euler class

$$-6 = \chi(\mathbb{R}P^2 \# 7\mathbb{R}P^2) = \chi(X(\mathbb{R})) = 2\chi(W),$$

since $\chi(W) = -3$ is only possible in the case described there. The final statement follows from a more general fact, which concerns real double coverings $X \to \mathbb{P}^2$ branched along curves of degree $2m$: the corresponding "real double covering" $\mathbb{R}X \to W = f(\mathbb{R}X)$ is trivial provided m is even (which follows for instance from evaluation of the corresponding Stiefel-Whitney class w_1). □

There are 28 bitangents to a nonsingular quartic $C \subset \mathbb{P}^2$, and in the case of quartic M-curves all these bitangents are real. Each bitangent line, L, to C in $\mathbb{P}^2$ is covered by two lines $L^1, L^2 \subset X_C$ which are conjugate under Geiser involution of the double covering $f_C : X_C \to \mathbb{P}^2$ (see [DO]), so, in particular, we have 56 real lines in a real del Pezzo M-surface.

The lines L^1, L^2 intersect in X_C at q_1 and q_2, which are projected by f_C into the tangency points $\{p_1, p_2\} = L \cap C$. To distinguish L^1 from L^2, we use the presentation $\mathbb{R}X_C = W_A \cup W_B$ given in Proposition 9.2.1 (here indices A and B are assigned to the two copies of W in an arbitrary way). Each segment of L^1 and L^2 between q_1 and q_2 goes either inside region W_A, or inside W_B. At points

q_1 and q_2 these lines change the region in which they are passing. For example, see Figure 9.1.

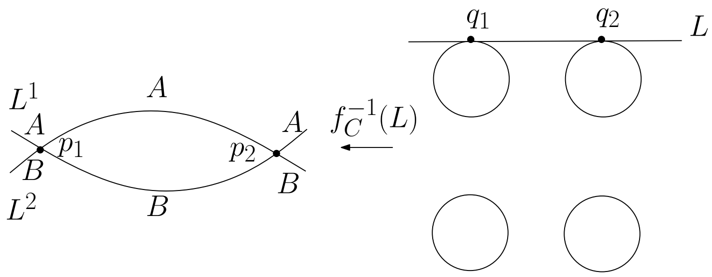

Figure 9.1: A decoration of the preimage of a bitangent line.

We decorate one of the segments of L between p_1 and p_2 with letter A and the other segment by B. This indicates the region (respectively, W_A or W_B) containing the corresponding segment of the lifted line. So, each bitangent L can be decorated in two ways corresponding to its lifting to L^1 and L^2. A bitangent to a quartic C with one fixed decoration is called a *decorated bitangent*.

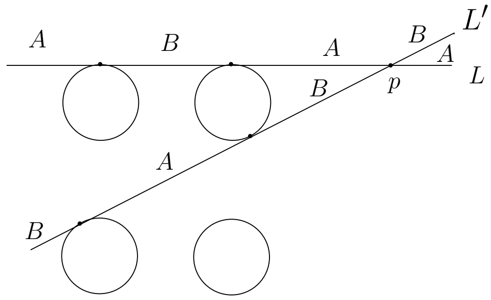

Figure 9.2: Two decorated bitangents to a quartic C whose corresponding liftings in X_C are skew lines.

Given two decorated bitangents, L and L', the corresponding two lines in X_C are skew (i.e., do not intersect) if and only if the segments of L and L' containing the intersection point $p = L \cap L'$ are marked by different letters (one segment by letter A and another by letter B), see Figure 9.2.

9.3 Azygetic triples and Aronhold sets

There are two kind of triples of bitangent lines, L_1, L_2, L_3, to a nonsingular quartic C, which differ by the way they can be lifted to the double covering $X_C \to \mathbb{P}^2$ branched along the quartic C. For the first kind of triples, called the *syzygetic triples* there exist liftings $\widetilde{L}_i$ of L_i, $i = 1, 2, 3$, such that each pair of them intersect at a point. For the second kind of triples, called the *azygetic triples*, there exist liftings forming a skew triple of lines $\widetilde{L}_i$ in X_C (i.e., no pair of them intersects). In fact, for arbitrary choice of liftings, the number of intersecting pairs of lines $\widetilde{L}_i$ is odd for azygetic triples and even for syzygetic triples.

Remark 9.3.1. According to a more classical definition, a triple of bitangent lines to a nonsingular quartic is syzygetic if the six bitangency points on them lie on one conic, see [PSV]. It is not difficult to show that the both definitions are equivalent.

A set of seven bitangents, $\mathcal{L} = \{L_1, \ldots, L_7\}$, to a nonsingular quartic C is called an *Aronhold set* if these bitangents can be lifted to a disjoint set of lines in X_C. It is well known (and not difficult to see) that $\mathcal{L}$ is an Aronhold set if and only if each triple of its bitangents is azygetic.

In the real setting, there exists another characterization of syzygetic and azygetic triples. Namely, a triple of real bitangents to a real nonsingular quartic C divides $\mathbb{R}P^2$ into 4 triangles, and it is trivial to observe that the number of tangency points on the sides of the triangles must have the same parity: either even for every triangle, or odd for every triangle. In the first case, the triple of bitangents turns out to be syzygetic, and in the second case, azygetic (see Figure 9.3).

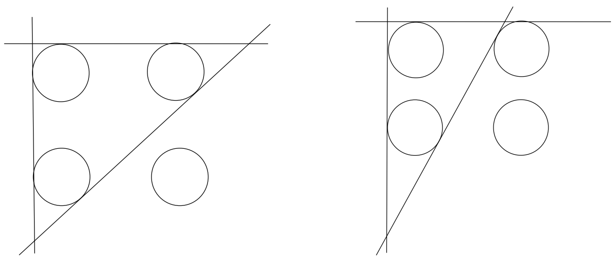

(a) syzygetic triples (b) azygetic triples

Figure 9.3: An example of the syzygetic and azygetic triples

We prove such characterization of real azygetic triples of bitangents in a somewhat more general setting, in the case of an arbitrary number of real bitangents.

Proposition 9.3.2. *Assume that $\mathcal{L} = \{L_1, \ldots, L_n\}$ is an Aronhold set. Consider* *any of the polygons, into which the plane $\mathbb{R}P^2$ is divided by these n lines. Then the number of tangency points on the boundary of this polygon have the same parity as the number of its sides.*

Proof. Let $C \subset \mathbb{P}^2$ be a nonsingular quartic to which the lines $L_1, \ldots, L_n$ are bitangent, and assume that X_C is the double covering branched over C, and $f_C : X_C \to \mathbb{P}^2$ is the anti-canonical map. Let P be a k-gon one of these polygons where $3 \leq k \leq n$. Let us cyclically relabel the bitangent lines $L^1, \ldots, L^k$ of $\mathcal{L}$ which form the edges of this k-gon, and numerate cyclically the vertices $v_1, \ldots, v_k$ of the k-gon as shown in Figure 9.4.

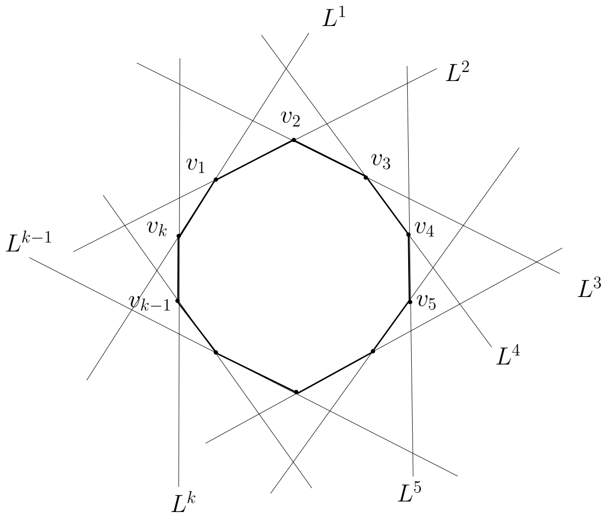

Figure 9.4: The k-gon whose edges are formed by the bitangent lines L^1,...,L^k.

We denote by $[\widetilde{v_1 v_2}]$,...,$[\widetilde{v_k v_1}] \subset X_C$ the liftings of edges $[v_1 v_2]$,...,$[v_k v_1]$ of this k-gon, respectively and by $\widetilde{v_i}$, $i = 1, \ldots, k$, the lifting of the vertex v_i, which is lying on the line segment $[\widetilde{v_i v_{i+1}}]$. The point $\widetilde{v}_{i+1}$ is on the same half (W_A or W_B, where $\mathbb{R}X_C = W_A \cup W_B$ and $W_A = W_B = f_C(\mathbb{R}X_C)$) as $\widetilde{v_i}$ if there exist even number of tangency points on the edges $[v_i v_{i+1}]$. On the other hand the points $\widetilde{v_i}$, $\widetilde{v}_{i+1}$ are on the opposite half if there exist odd number of tangency points on the edges $[v_i v_{i+1}]$. $\square$

CHAPTER 10

ANTI-CANONICAL CORRESPONDENCE FOR REAL DEL PEZZO SURFACES OF DEGREE 2

10.1 Complementary 7-configurations

For a 7-configuration $\mathcal{P} = \{p_1, \dots, p_7\} \in QC^7$ we can define the complementary one (like it was done in Section 7.3 for 6-configurations). Namely, the del Pezzo surface $X_{\mathcal{P}}$, obtained by blowing up $\mathbb{P}^2$ at the points of $\mathcal{P}$, contains the marking $\{E_1, \dots, E_7\}$ formed by the exceptional divisors, as well as its complementary marking, $\{\widetilde{E}_1, \dots, \widetilde{E}_7\}$, in which the exceptional curve $\widetilde{E}_i$, $i = 1, \dots, 7$, is represented in the $\mathbb{P}^2$ by a nodal cubic based at the points of $\mathcal{P}$, with a node at $p_i \in \mathcal{P}$. Since the lines $\widetilde{E}_i$ are disjoint, we can blow down them to obtain the complementary plane $\widetilde{\mathbb{P}}^2$ with the complementary configuration $\widetilde{\mathcal{P}} = \{\widetilde{p}_1, \dots, \widetilde{p}_7\}$, where the point $\widetilde{p}_i$ is the result of blowing down $\widetilde{E}_i$.

$$\begin{array}{ccc}
(X_{\mathcal{P}}, E_{\mathcal{P}} \cup \widetilde{E}_{\mathcal{P}}) & \xrightarrow{g} & (X_{\mathcal{P}}, E_{\mathcal{P}} \cup \widetilde{E}_{\mathcal{P}}) \\
\Big\downarrow{\scriptstyle \pi} & & \Big\downarrow{\scriptstyle \widetilde{\pi}} \\
(\mathbb{P}^2, \mathcal{P}) & \xrightarrow{\quad \xi \quad} & (\widetilde{\mathbb{P}}^2, \widetilde{\mathcal{P}})
\end{array}$$

Figure 10.1: The correspondence between $E_{\mathcal{P}}$ and $\widetilde{E}_{\mathcal{P}}$ for a given 7-configuration $\mathcal{P} \in QC^7$. In this diagram, g is the Geiser involution (i.e., the deck transformation of the double covering $f_{\mathcal{P}} : X_{\mathcal{P}} \to \mathbb{P}^2$), sending $E_{\mathcal{P}}$ to $\widetilde{E}_{\mathcal{P}}$, and $\pi, \widetilde{\pi}$ stand for the blow-ups.

Proposition 10.1.1. *If $\mathcal{P}, \widetilde{\mathcal{P}} \in QC^7$ are complementary to each other, then they are projectively equivalent.*

Proof. The regular map $\xi : \mathbb{P}^2 \to \widetilde{\mathbb{P}}^2$ defined by $\xi(x) = (\widetilde{\pi} \circ g \circ \pi^{-1})(x)$ for any $x \in \mathbb{P}^2$ is the required projective transformation sending $\mathcal{P}$ to $\widetilde{\mathcal{P}}$ (see the table shown in Figure 10.1). □

The following result is an immediate consequence of Proposition 10.1.1 and the fact that the group $PGL(3, \mathbb{R})$ is connected.

Corollary 10.1.2. *If $\widetilde{\mathcal{P}}$, $\mathcal{P} \in QC^7$ are complementary to each other, then they belong to the same Q-deformation class in QC^7.* □

10.2 The 14 real Aronhold sets representing the 14 Q-deformation classes of planar 7-configurations

For a given 7-configuration $\mathcal{P} \in QC^7$, the image $\mathcal{L}_{\mathcal{P}} = f_{\mathcal{P}}(E_{\mathcal{P}})$ is an Aronhold set (i.e., seven bitangent lines whose liftings are pairwise disjoint on $X_{\mathcal{P}}$) in $\widehat{\mathbb{P}}_{\mathcal{P}}$. Conversely, for a given Aronhold set, in which the seven lines are bitangent to a nonsingular M-quartic $C \subset \mathbb{R}P^2$, by the definition the inverse image of the Aronhold set under $f_C : X_C \to \mathbb{P}^2$ is a 7-configuration of pairwise disjoint exceptional curves on $\mathbb{R}X_C$. By blowing down the exceptional curves, we obtain a 7-configurations in QC^7.

In the Theorem 2.5.1, we show that there are exactly fourteen Q-deformation classes in QC^7. The following theorem answers the question about the anti-canonical corresponding fourteen deformation classes of Aronhold sets in $\mathbb{R}P^2$, cf. the definition of the anti-canonical correspondence on page 87.

Theorem 10.2.1. (see Section 10.3.) *The relative positions of Aronhold sets of bitangent lines and the ovals of a real M-quartic that are associated under the anti-canonical correspondence ϕ^7 to the* 14 *Q-deformation classes QC^7_σ are as shown in Figure B.1(a)-(n) in Appendix B.*

The first step in the proof will be to find the corresponding Aronhold set for a heptagonal configuration, and it is done in Proposition 10.2.2.

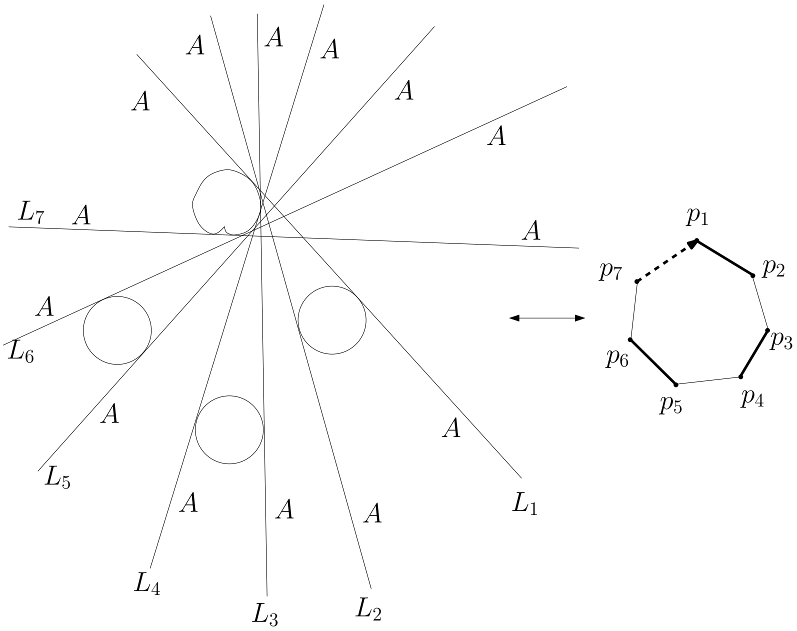

Figure 10.2: The CAC-correspondence between the Aronhold set and the heptagonal configuration in QC^7.

Proposition 10.2.2. *The* 7 *decorated bitangent lines shown in Figure 10.2 form an Aronhold set that is under anti-canonical correspondence with the heptagonal configuration in* QC^7*. The numeration of these bitangent lines gives the canonical numeration of the points of the heptagonal* 7*-configuration (that is, the lines* L_1 *and* L_7 *on this figure represent, respectively, the outer point* p_1 *and the inner point* p_7 *of the heptagonal* 7*-configuration.)*

Proof Proposition 10.2.2. Let C be the real nonsingular quartic M-curve shown in Figure 10.2, and assume that X_C is the double covering of $\mathbb{P}^2$ branched over C and $f_C : X_C \to \mathbb{P}^2$ is its anti-canonical map. It can be easily seen that the seven decorated bitangents lines shown in this figure is an Aronhold set since their lifting under this map are pairwise disjoint lines on $\mathbb{R}X_C$.

For the continuation of the proof of this proposition we need the following lemmas.

Lemma 10.2.3. *Let* $L \subset \mathbb{P}^2$ *be a real line which does not intersect any of the four ovals of the real quartic* M*-curve* C*, but intersects the segments of the seven bitangents, which are decorated by the letter* A *as shown in Figure 10.3. We denote by* $L^1, L^2 \subset X_C$ *the inverse images of the line* L *under* $f_C : X_C \to \mathbb{P}^2$*,*

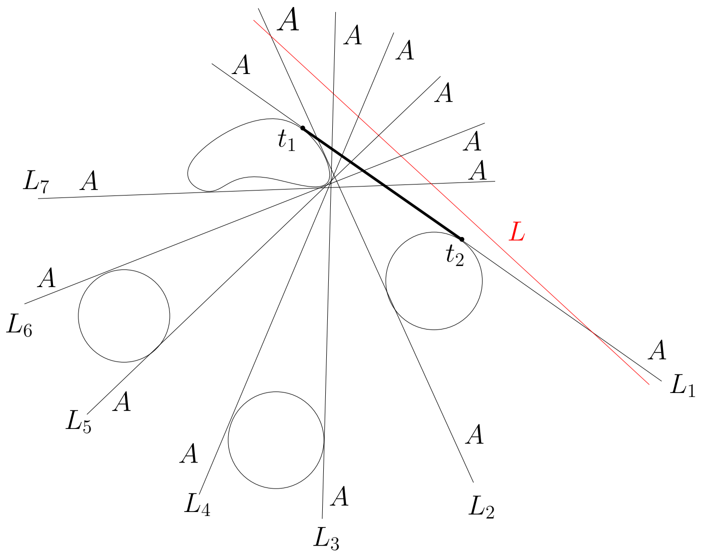

Figure 10.3

and by $\{L_1^A, \ldots, L_7^A\}$ *the set of skew lines in* X_C*, where* $L_i^A \in f_{\mathcal{P}}^{-1}(L_i)$ *for any* $i \in \{1, \ldots, 7\}$*. For each* $i = 1, 2$*, if* L^i *is intersected by even (or, respectively, odd) number of* $L_1^A, \ldots, L_7^A$*, then the image* $\pi(L^i) \subset \mathbb{R}P^2$ *is one-sided (or, respectively, two-sided). In other words, for each* $i = 1, 2$*, if* L^i *is intersected by even (or, respectively, odd) number of* $L_1^A, \ldots, L_7^A$*, then* $\pi(L^i)$ *is the* J*-component (or, respectively, the oval) of the cubic* $\pi(f_C^{-1}(L))$*.*

Proof of Lemma 10.2.3. Each of the liftings L^1, L^2, which are real components of an elliptic curve is one-sided curve on $\mathbb{R}X_C$, and is intersected by even or odd number of $L_1^A, \ldots, L_7^A$ since L^1, L^2 intersect together $L_1, \ldots, L_7$ at seven points. Without loss of generality we can assume that L^1 intersects with even number of lines $L_i^A \subset X_C$. Then the other lifting L^2 must be intersect with odd number of these lines. Each blow-down increases the self intersection of a curve on X_C by 1, and so after blowing down $L_1^A, \ldots, L_7^A$, the image of the real line $L^1 \subset X_{\mathcal{P}}$ under blow-up $\pi : X_C \to \mathbb{P}^2$ is a one-sided curve in $\mathbb{P}^2$ while the image of the real line L^2 is a two-sided curve. Since the image $\pi(f_C^{-1}(L))$ is a plane cubic curve passing through the points $p_1, \ldots, p_7$ which are the blowing down $L_1^A, \ldots, L_7^A$, respectively, the two-sided curve $\pi(L^2)$ must be the oval of the cubic $\pi(f_C^{-1}(L))$, and the one-sided curve $\pi(L^1)$ must be the J-component of this cubic. $\square$

The following result is an immediate consequence of Lemma 10.2.3.

Corollary 10.2.4. *Let C, L, L_i and L_i^A, $i = 1, \ldots, 7$ as in Lemma 10.2.3, and assume that $L \subset \mathbb{P}^2$ is a real line which does not intersect any of the four ovals of the quartic M-curve C, but intersects the segments of the seven bitangents L_i, which are decorated by the letter A as shown in Figure 10.3. Then, $\pi(f_C^{-1}(L))$ is homeomorphic to the plane cubic curve as shown in Figure 10.4.* $\square$

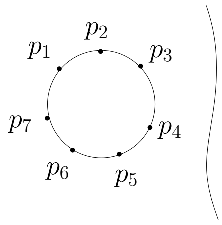

Figure 10.4: The image $\pi(f_C^{-1}(L))$, where L is the line as shown in Figure 10.3. We denote by p_i, $i = 1, \ldots, 7$ the point which is obtained by blowing down the exceptional curve L_i^A in X_C.

Lemma 10.2.5. *Let C, L, L_i and L_i^A, $i = 1, \ldots, 7$ as in Lemma 10.2.3, and assume that $p_1, \ldots, p_7$ are points obtained by blowing down the exceptional curves $L_1^A, \ldots, L_7^A$ in X_C, respectively, and $[t_1 t_2] \subset L_1$ is the line segment illustrated by bold in Figure 10.3. Then, the image $\pi(f_C^{-1}([t_1 t_2]))$ is a finite loop of the nodal cubic $\pi(f_C^{-1}(L_1))$ based at $p_1, \ldots, p_7$ with a node at p_1.*

Proof of Lemma 10.2.5. The finite loop of a nodal cubic in $\mathbb{R}P^2$ intersects with J-component of any plane cubic curve at even number of points while the infinite loop of the nodal cubic intersects with J-component of any plane cubic curve at odd number of points. By Corollary 10.2.4 none of the points $p_1, \ldots, p_7$ lie on the J-component of $\pi(f_C^{-1}(L))$. The line segment $[t_1 t_2]$, which intersects these six bitangent lines L_i, $2 \leq i \leq 7$ does not intersect L, so the loop (i.e., finite or infinite) of the nodal cubic A_1 with a node at p_1 that represents the segment $[t_1 t_2]$ does not intersect this J-component. Thus, it represents the finite loop of the cubic A_1 containing all the seven points. $\square$

By Lemma 10.2.5, we observe that all the points $p_1, \ldots, p_7$ lie in the finite loop of the nodal cubic $A_1 = \pi(L_1^A)$. That is to say that, these points are in convex position. This implies that the 7-configuration $\mathcal{P} = \{p_1, \ldots, p_7\}$ is heptagonal.

By the similar analysis, we observe that the points $p_1, \ldots, p_7$ lie on the nodal cubics A_i, which are obtained by blowing down the exceptional curves L_i^A in X_C, $i = 1, \ldots, 7$, shown in Figure 10.5.

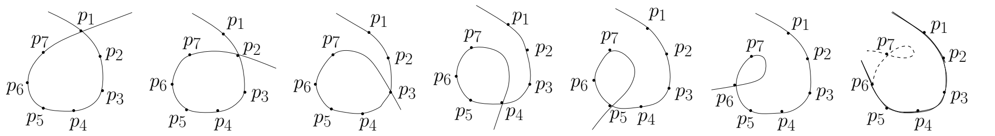

(a) A_1 (b) A_2 (c) A_3 (d) A_4 (e) A_5 (f) A_6 (g) A_7

Figure 10.5: The orders of the points $p_1, \ldots, p_7$ on the nodal cubics A_i, $i = 1, \ldots, 7$, where $p_i = \pi(L_i^A)$, $i = 1, \ldots, 7$ (see Figure 10.3).

Note that the point p_1 can not lie inside the conic $Q_{1,j}$ for each $i = 1, \ldots, 7$. Otherwise, looking at the mutual positions of the conic $Q_{1,j}$ and the nodal cubic A_1, we get a contradiction to Bezout's theorem. In fact it is enough to sketch a piece of $Q_{1,j}$, and so wee see that $Q_{1,j}$ and A_1 intersect at least two additional point different than the five common points, namely, $p_2, \ldots, p_{\hat{j}}, \ldots, p_7$. (See Figure 10.6.) Therefore, p_1 is the outer point.

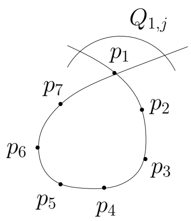

Figure 10.6: The arc of an ellipse $Q_{1,j}$ sketched on the figure contains two extra intersection points.

In order to prove that p_7 is the inner point, it is enough to show that $ind_{p_2}(Q_{1,2}) = 1$ since the dominancy indices of points of any heptagonal configurations in $QC^7_{(7,0,0,0)}$ go in the following cyclic order: $6, 1, 4, 3, 2, 5, 0$, see Proposition 2.6.5. Assume that $ind_{p_2}(Q_{1,2}) = 0$. Since p_1 is the outer point, we have $ind_{p_1}(Q_{1,2}) = 1$. Looking at the mutual positions of the conic $Q_{1,2}$ and the nodal cubic A_2, we also get a contradiction to Bezout's theorem (see Figure 10.7).

The converse of the proof of Proposition 10.2.2 immediately follows from the fact that there is one and only one heptagonal configuration in QC^7 up to Q-deformation. $\square$

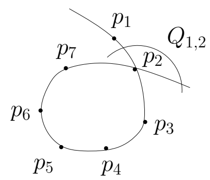

Figure 10.7: The arc of an ellipse $Q_{1,2}$ sketched on the figure contains two extra intersection points.

10.3 Proof of Theorem 10.2.1

The quadratic Cremona transformations base at some triples of points of a given heptagonal 7-configuration in QC^7 produce 7-configurations which belong to the all Q-deformation classes (see Figure 4.2), and that in the configurations of bitangent lines such as these transformations change the three corresponding bitangents on Figure B.1(a) by other three bitangents.

The L-deformation classes of Aronhold sets in LL^7 are obtained from the Aronhold set corresponding to the heptagonal configurations by the quadratic Cremona transformations as shown in Figure B.1.

Corollary 10.3.1. *The CAC-correspondence* $[\phi^7]$ *associates the fourteen Q-deformation classes in* QC^7 *to the eleven L-deformation classes on* LL^7 *(see Theorem 2.5.1 and Figure 2.6).*

Proof. The result is obtained by forgetting the quartic curves in the Aronholds sets of bitangents shown on Figure B.1. □

Remark 10.3.2. A point l of the polar dual $\widehat{\mathbb{P}_{\mathcal{P}}}$ of the space $\mathbb{P}_{\mathcal{P}}$ is a line in $\mathbb{P}_{\mathcal{P}}$, where $\mathcal{P} \in QC^7$ is a 7-configuration. A line in $\mathbb{P}_{\mathcal{P}}$ is a pencil of cubics which in addition of the seven points of $\mathcal{P}$ has 2 other points $x, y \in \mathbb{P}^2$. We have a map f from $\widehat{\mathbb{P}_{\mathcal{P}}}$ to the polar dual $\widehat{\mathbb{P}^2}$ of the initial plane, in which the points of $\mathcal{P}$ lie, given by $f(l) = L_{xy}$, where L_{xy} is a line joining the points x and y. The map $l \mapsto L_{xy}$ establishes a one-to-one correspondence between $\mathbb{P}_{\mathcal{P}}$ and $\mathbb{P}^2$. For more information about this correspondence, see [D2].

CHAPTER 11

APPLICATIONS: COMBINATORIAL PENCILS OF REAL RATIONAL CUBIC CURVES PASSING THROUGH SIX POINTS

For a given quadratically nondegenerate configuration of six real points S. Fiedler-Le Touzé determined topological types of cubics in the pencil of rational cubic curves passing through the six points, one of these points being the node of the cubics and she classified combinatorial pencils, that is, the cyclic sequence of five topological types of such cubics (see [T3]). In this case, we obtained the same result independently (see Theorem 11.2.3). By using the combinatorial anti-canonical correspondence mentioned in Theorem 10.2.1, we find an alternative, perhaps a somewhat different, way to prove the results of S. Fiedler-Le Touzé about the list of such cubics through quadratically nondegenerate configurations of seven real points (see [T3]).

11.1 Partitioned orders

Let $\mathcal{P}$ be a planar n-configuration, and $p \in \mathcal{P}$. By a $(\mathcal{P}, p)$*-based nodal cubic* we mean a nodal cubic passing through points of $\mathcal{P}$, with a node at the point p.

Let $\mathcal{P} = \{p_1, \dots, p_n\} \in QC^n$, and assume that A is a $(\mathcal{P}, p)$-based nodal cubic such that p is equal to p_i for some $i \in \{1, \dots, n\}$. The finite and infinite loop of A (see Section 6.3) describe linear orders on $\mathcal{P}_{fin}$ and $\mathcal{P}_{inf}$, in which the points of $\mathcal{P}$ lie on the nodal cubic A with respect to some orientation of A. By a *partitioned* *order* on $\mathcal{P}_{\hat{i}}$ we mean the pair of the linear ordered subsets $\mathcal{P}_{fin}$ and $\mathcal{P}_{inf}$. More precisely, this partitioned order can be presented by an array with 2 rows and 1 column: in the upper row, we list all points of $\mathcal{P}_{fin}$ and in the lower row we list all points of $\mathcal{P}_{inf}$ with respect to the order of these points. If we change orientation of the nodal cubic A, then we get another partitioned order on $\mathcal{P}_{\hat{i}}$ which is called the *oppositely partitioned order*.

As a matter of convenience, in the presentation of a partition order on $\mathcal{P}_{\hat{i}}$, we list only the indices of the points. For example, as $\mathcal{P}$, we take the configuration $\{p_1, \ldots, p_7\} \in QC^7$. If the $(\mathcal{P}, p_7)$-based nodal cubic A_7 is as shown in Figure 6.4 in which $p = p_7$, then the partitioned order on $\{1, \ldots, 6\}$ defined by the nodal cubic A is either $\binom{1435}{26}$ or $\binom{5341}{62}$.

11.2 Combinatorial pencils of rational cubics passing through 6 points

Let $\mathcal{P} = \{p_1 \ldots, p_6\}$ be a 6-configuration in QC^6. For any $i \in \{1, \ldots, 6\}$, the pencil of $(\mathcal{P}, p_i)$-based nodal cubics contains 5 reducible cubics: $C_i^j = L_{ij} \cup Q_j$, where Q_j are the conics passing through five points of $\mathcal{P}$ other than p_j, and L_{ij} are the lines joining the points p_i and p_j of $\mathcal{P}$, $i \neq j \in \{1, \ldots, 6\}$. Note that partitioned orders on $\mathcal{P} = \{p_1, \ldots, p_6\} \setminus \{p_i\}$ for any $i \in \{1, \ldots, 6\}$ which are defined by the reducible rational cubics C_i^j are deformation invariants for the deformation classes of these reducible rational cubics in $\mathbb{P}^2$.

Remark 11.2.1. Recall that equisingular deformation of a curve is homotopic deformation of the curve, preserving the types of its singularities. A deformation of a rational cubic with "empty" finite loop (that is, with a finite loop containing no base points of the pencil of rational cubics passing through six points, having a node at one of the points) is not equisingular only if the rational cubic degenerates a cuspidal cubic under this deformation. Equivalently, if the first row of a partitioned order on $\mathcal{P}$ for some $i \in \{1, \ldots, 6\}$ is not "empty", then any deformation of $\mathcal{P}$ is equisingular.

Let $\mathcal{P} \in QC_j^6$, $j = 1, 2, 3, 6$, and choose a point $p \in \mathcal{P}$ such that $p = p_i$ for some $i \in \{1, \ldots, 6\}$. The five reduced $(\mathcal{P}, p)$-based nodal cubics, C_j^i, are cyclically ordered if we orient the pencil of $(\mathcal{P}, p)$-based nodal cubics (changing of the orientation reverses the cyclic order). The pair of opposite cyclic orders on the set consisting of the five reduced $(\mathcal{P}, p)$-based nodal cubics is called a *cyclic semiorder*. The semiordered set of the five $(\mathcal{P}, p)$-based nodal cubics is called a *combinatorial pencil* associated to the pair $(QC^6_j, t(p))$, where $\mathcal{P} \in QC^6_j$, and $t(p)$ stands for the type of the point p, i.e. dominant or subdominant. In other words, if p is dominant (or respectively, subdominant) $t(p) = \bullet$ (or, respectively $t(p) = \circ$). We denote this combinatorial pencil by $CP^\bullet_j$ if p is dominant, and by CP°_j if p is subdominant.

Example 11.2.2. Let $\mathcal{P}$ be a hexagonal 6-configuration in QC^6_1, and assume that the numeration $p_1, \ldots, p_6$ of points of $\mathcal{P}$ is cyclic such that p_1 is subdominant with respect to the conic Q_1. Then, the combinatorial pencil CP°_1 is $\{(\genfrac{}{}{0pt}{}{-}{23456}), (\genfrac{}{}{0pt}{}{3456}{2}), (\genfrac{}{}{0pt}{}{23}{456}), (\genfrac{}{}{0pt}{}{56}{234}), (\genfrac{}{}{0pt}{}{2345}{6})\}$ (see Figure 11.1). Similarly, in the case that p_1 is dominant with respect to the conic Q_1, the combinatorial pencil $CP^\bullet_1$ is $\{(\genfrac{}{}{0pt}{}{23456}{-}), (\genfrac{}{}{0pt}{}{2}{3456}), (\genfrac{}{}{0pt}{}{456}{23}), (\genfrac{}{}{0pt}{}{234}{56}), (\genfrac{}{}{0pt}{}{6}{2345})\}$. The remaining five combinatorial pencils $CP^\circ_2, CP^\bullet_2, CP^\circ_3, CP^\bullet_3$ and CP°_6 are shown in Figure 11.2.

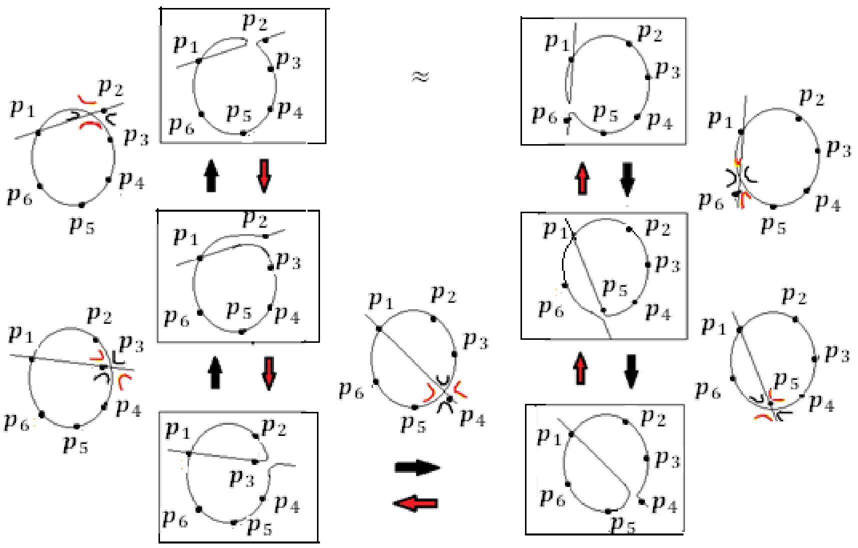

Figure 11.1: The combinatorial pencil CP°_1. This figure shows the case, where $\mathcal{P} \in QC^6_1$, and $p_1 \in \mathcal{P}$ is subdominant.

Let $\mathcal{P} \in QC^6_j$, $j = 1, 2, 3, 6$, and choose a point $p \in \mathcal{P}$ such that $p = p_i$ for some $i \in \{1, \ldots, 6\}$. There are two cyclic orders on the five points of $\mathcal{P}_{\hat{i}}$. One of the cyclic orders comes from the conic Q_i passing through five points of $\mathcal{P}$ other

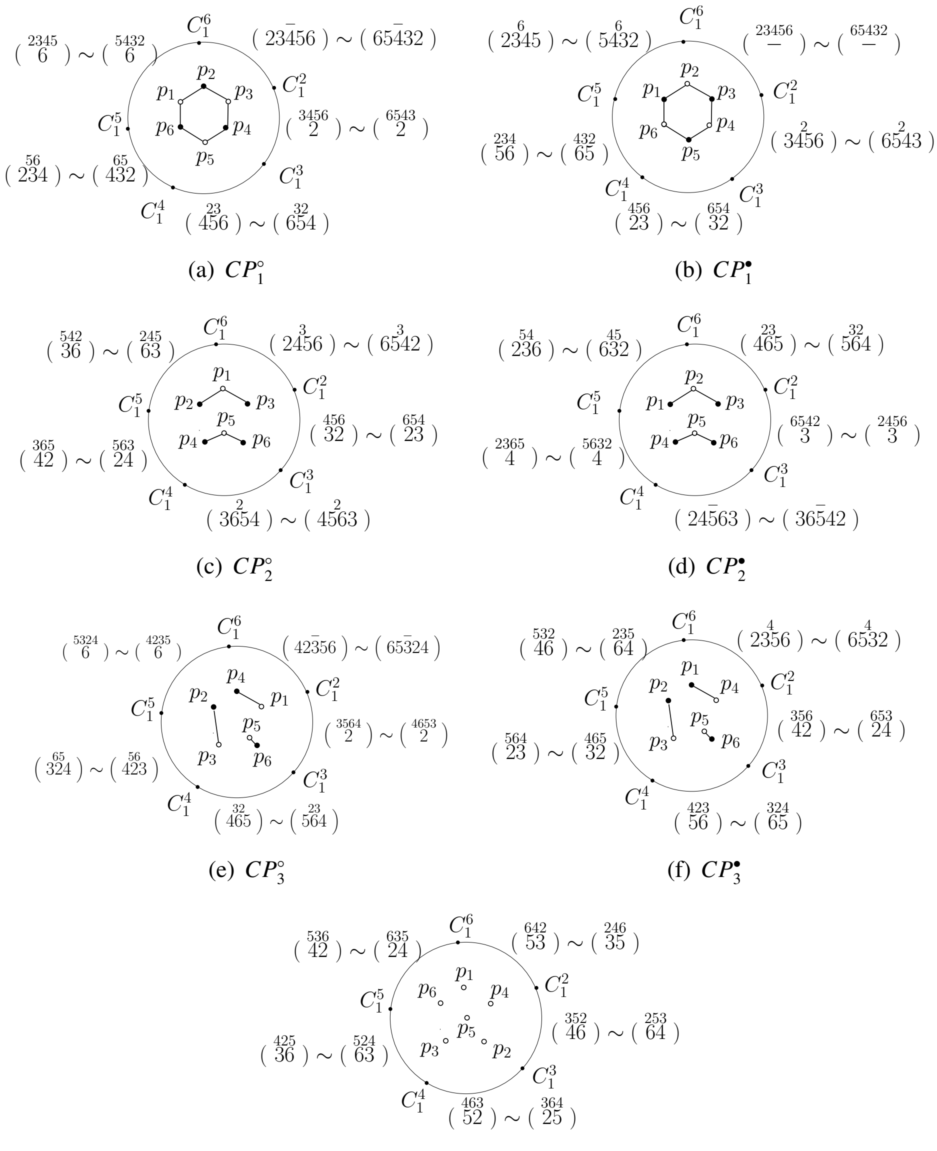

(a) CP_1° (b) $CP_1^{\bullet}$ (c) CP_2° (d) $CP_2^{\bullet}$ (e) CP_3° (f) $CP_3^{\bullet}$ (g) CP_6°

Figure 11.2: Let $\mathcal{P} \in QC_i^6$, $i = 1, 2, 3, 6$, as shown inside each circle, and $p \in \mathcal{P}$, we denote by $CP_i^{\bullet}$ (respectively, CP_i°) the combinatorial pencils associated to QC_i^6 and the type of p, i.e. dominant or subdominant. In this figure, if $p = p_1$, we denote by C_1^j, $j = 2, 3, 4, 5, 6$ the five reduced cubics $L_{1j} \cup Q_j$ with a node at p_1 in each combinatorial pencil. In addition, a labeled ray between two reduced cubics stands for a partitioned order on $\mathcal{P}_{\hat{1}}$.

than p_i, and we denote this order by $[f]$. The other order comes from the pencil of lines base at the point p, and we denote the order by $[g]$. The pair $([f], [g])$ is a cyclic bi-ordering on $\mathcal{P}_{\hat{i}}$. Due to Section 3.2, we associate a permutation class diagram $Z_{[g\circ f^{-1}]}$ to this bi-ordering. Notice that these classes are topological invariants for combinatorial pencils associated to the pair $(QC^6_j, t(p))$ where $t(p)$ stands for the type of the point p. (See Figure 11.3.) In dependently, Fiedler-Le Touzé find the same diagrams (see [T3]) to classify combinatorial pencils.

Theorem 11.2.3. *There are exactly* 4 *distinct combinatorial pencils associated to* $(QC^6_i, t(p))$ *for any* 6*-configuration* $\mathcal{P} \in QC^6_i$ *and any point* $p \in \mathcal{P}$ *(see Figure 11.3).*

Proof. The configuration $\mathcal{P}$ can be in the one of the four deformation classes QC^6_1, QC^6_2, QC^6_3, and QC^6_6. A configuration in the first three deformation classes contain two types of points, subdominant and dominant. However, a configuration in QC^6_6 contains only subdominant points. There are 7 possible combinatorial pencils as shown in Figure 11.2. The bi-cyclic orderings associated to these combinatorial pencils are $\left(\begin{smallmatrix}23456\\23456\end{smallmatrix}\right)$, $\left(\begin{smallmatrix}23456\\23456\end{smallmatrix}\right)$, $\left(\begin{smallmatrix}23456\\36542\end{smallmatrix}\right)$, $\left(\begin{smallmatrix}23456\\23654\end{smallmatrix}\right)$, $\left(\begin{smallmatrix}23456\\65324\end{smallmatrix}\right)$, $\left(\begin{smallmatrix}23456\\46532\end{smallmatrix}\right)$, and $\left(\begin{smallmatrix}23456\\42536\end{smallmatrix}\right)$, respectively. By looking at their permutation class diagram, we see that there are four different combinatorial pencils (see Figure 11.3). □

$CP^\bullet_1$,CP°_1	$CP^\bullet_2$, CP°_2	CP°_3, $CP^\bullet_3$	CP°_6
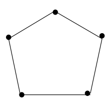	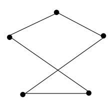	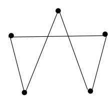	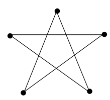

Figure 11.3: The associated graphs for the seven combinatorial pencils for all 6-configurations $\mathcal{P} \in QC^6$. In this table, the notation $CP^\bullet_i$ (respectively, CP°_i) denotes a combinatorial pencil associated to QC^6_i such that $\mathcal{P} \in QC^6_i$ and the type of a point $p \in \mathcal{P}$ (i.e., dominant or subdominant), where $i \in \{1, 2, 3, 6\}$.

Each column of the following table shown in Figure 11.4 shows the number of points of a given 6-configuration $\mathcal{P} \in QC^6_i$, $i = 1, 2, 3, 6$, on the finite loops of the five combinatorial $(\mathcal{P}, p)$-based nodal cubics depending on dominant or subdominant point $p \in \mathcal{P}$, separately.

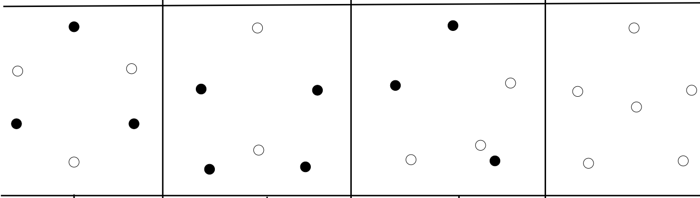

QC_1^6		QC_2^6		QC_3^6		QC_6^6
○	●	○	●	○	●	○
0	5	1	2	0	1	3
4	1	3	4	4	3	3
2	3	1	0	2	3	3
2	3	3	4	2	3	3
4	1	3	2	4	3	3

Figure 11.4: The number of points of $\mathcal{P} \in QC_i^6$, $i = 1, 2, 3, 6$, on the finite loops of five combinatorial $(\mathcal{P}, p)$-based nodal cubics depending on dominant or subdominant point $p \in \mathcal{P}$, separately. In particular, the number 0 in this table indicates existence of a $(\mathcal{P}, p)$-based nodal cubic with an empty finite loop. For the order of the numeration of points, see Figure 11.2.

APPENDIX A

THE MODIFICATIONS OF ELLIPTIC AND HYPERBOLIC LINES UNDER CREMONA TRASFORMATIONS

In all of the following figures, □ and ∘ show the corresponding hyperbolic and elliptic lines, respectively. The colors black and white of squares and circles show the dominant and subdominant points, respectively.

A.1 Elliptic and hyperbolic lines corresponding to a 6-configuration in QC^6

Figure A.1

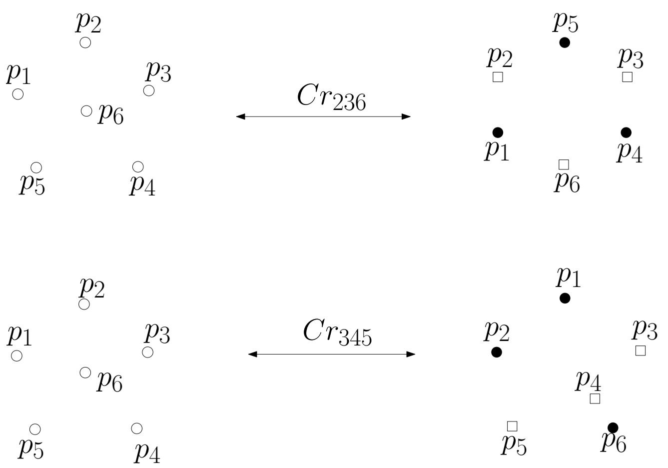

(a) The modifications of types of lines corresponding to a 6-configuration in QC_6^6.

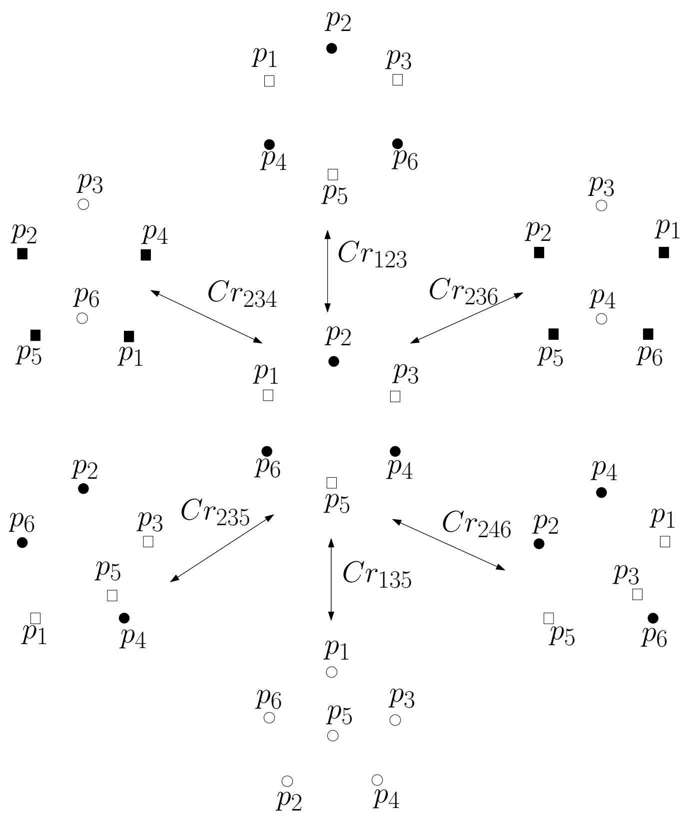

(b) The modifications of types of lines corresponding to a 6-configuration in QC_1^6.

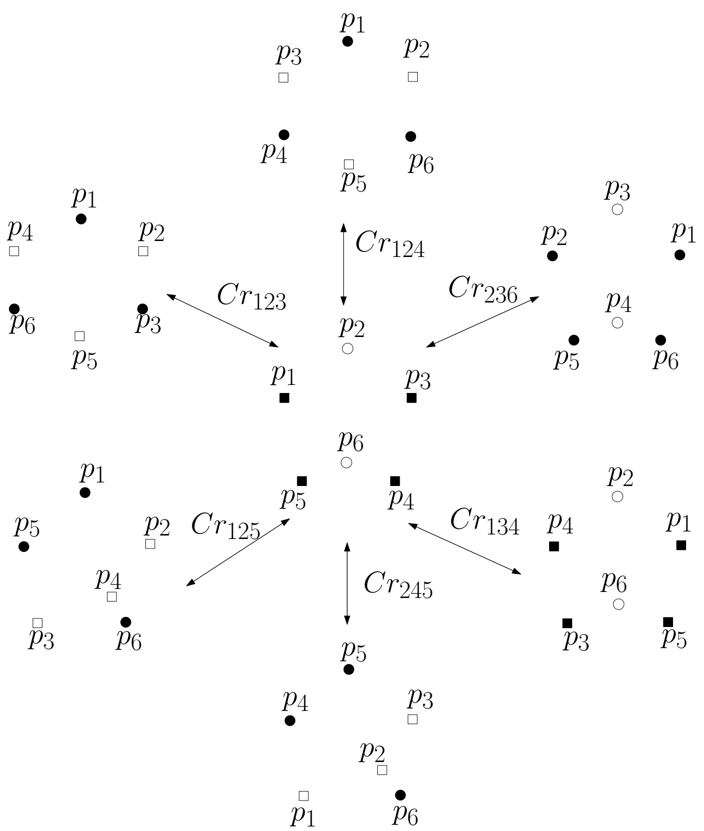

(c) The modifications of types of lines corresponding to a 6-configuration in QC_2^6.

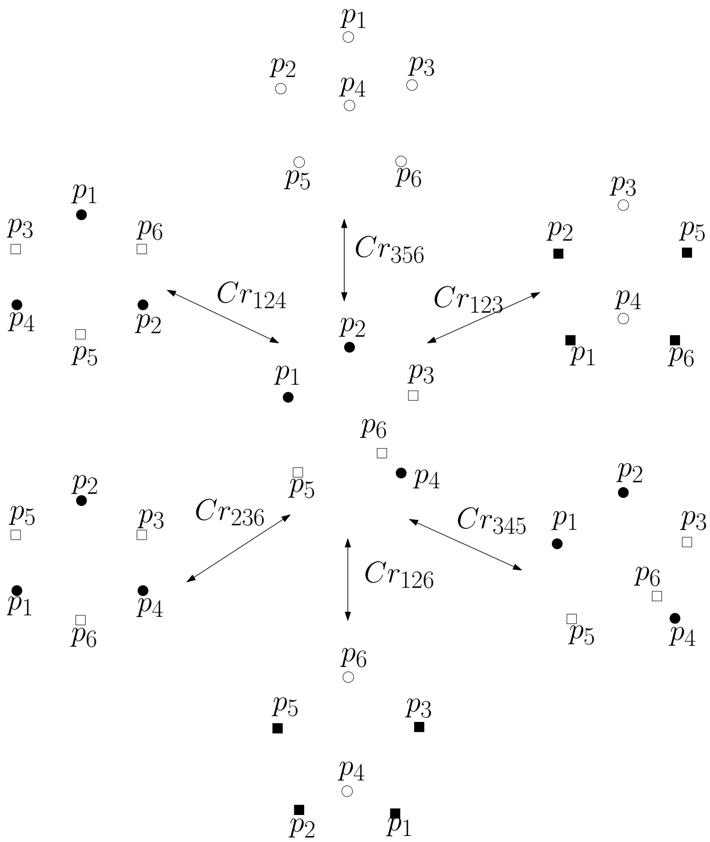

(d) The modifications of types of lines corresponding to a 6-configuration in QC_3^6.

APPENDIX B

ANTI-CANONICAL CORRESPONDENCE BETWEEN CONFIGURATIONS IN QC^7 AND ARONHOLD SETS

In the following figure, we indicate the colors of points in some cases, and do not do it in the other cases. (We do it if there is a hexagonal subconfiguration. And if there are several subconfigurations, then you take the principal one.)

B.1 Aronhold sets obtained by Cremona transformations based at triple of bitangent lines of the heptagonal Aronhold set

Figure B.1

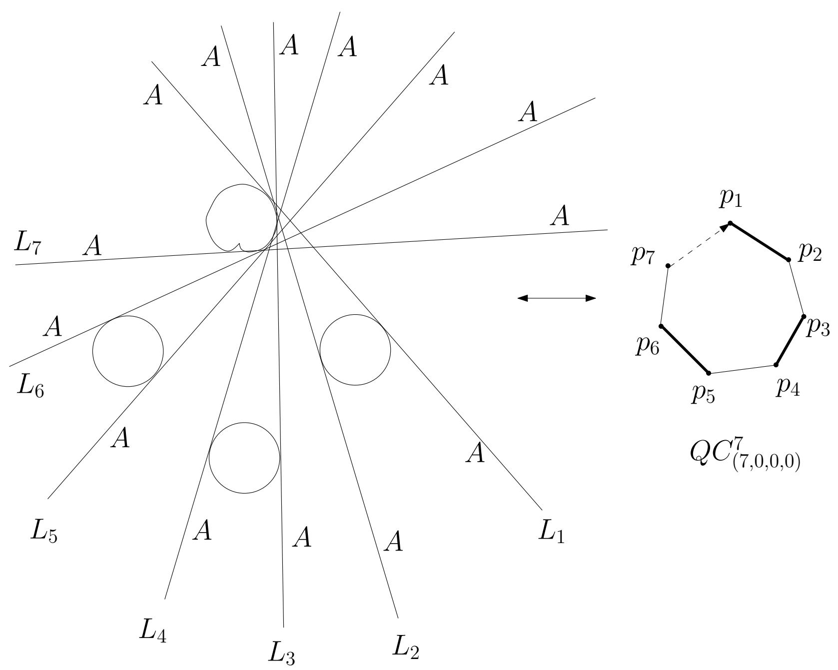

(a) The CAC-correspondence for the Q-deformation class $QC^7_{[7,0,0,0]}$

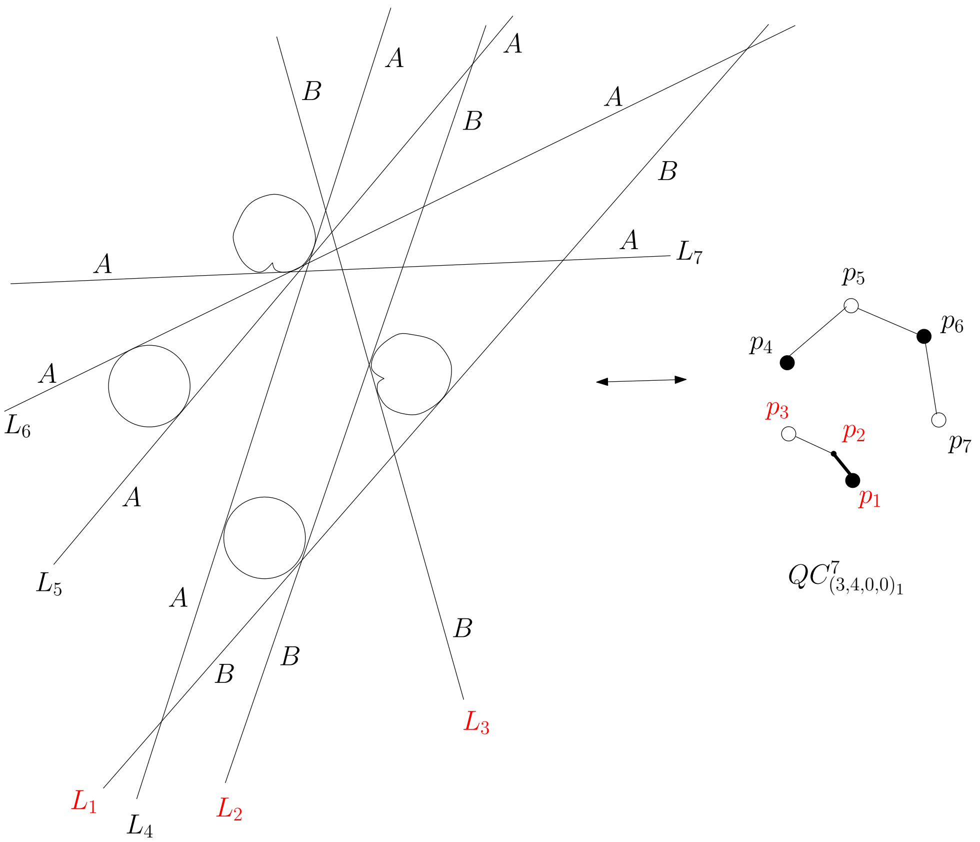

(b) Cr_{123}

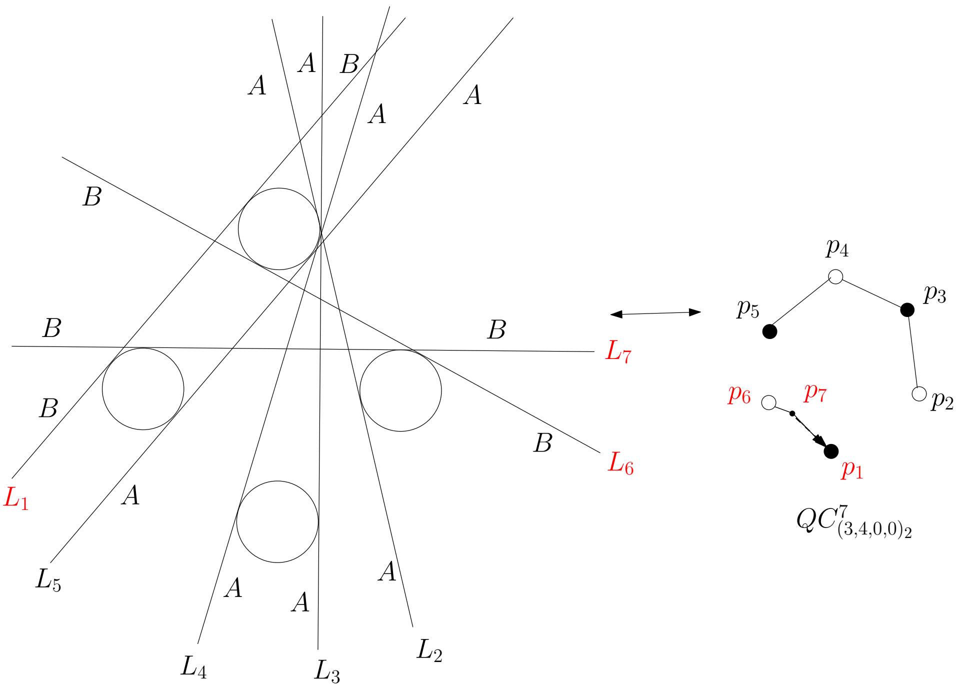

(c) Cr_{167}

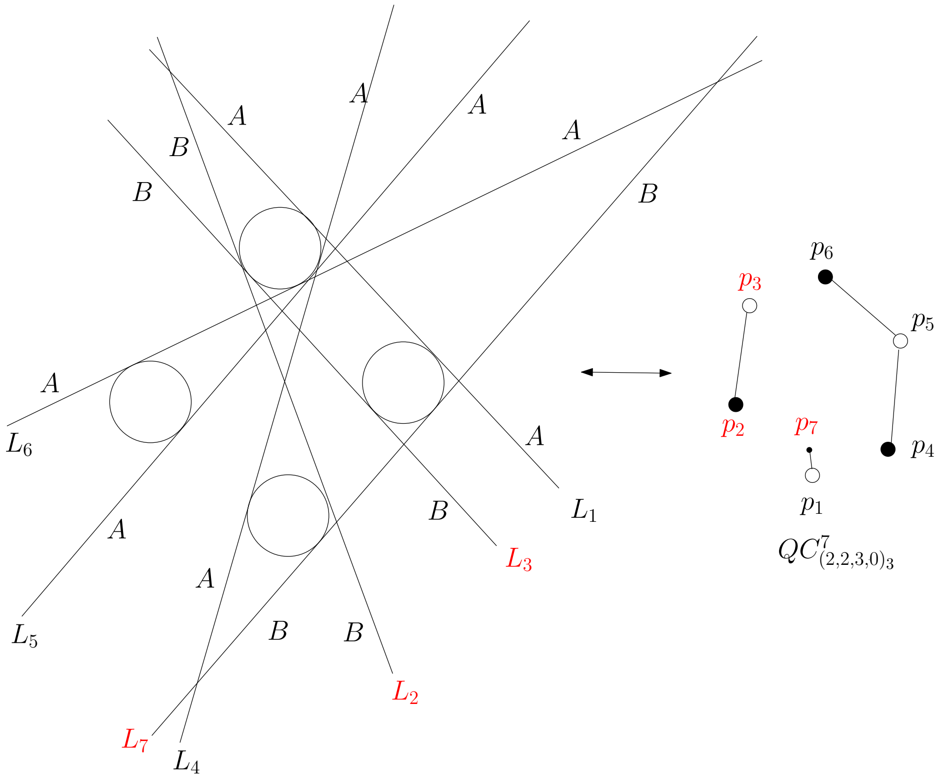

(d) Cr_{237}

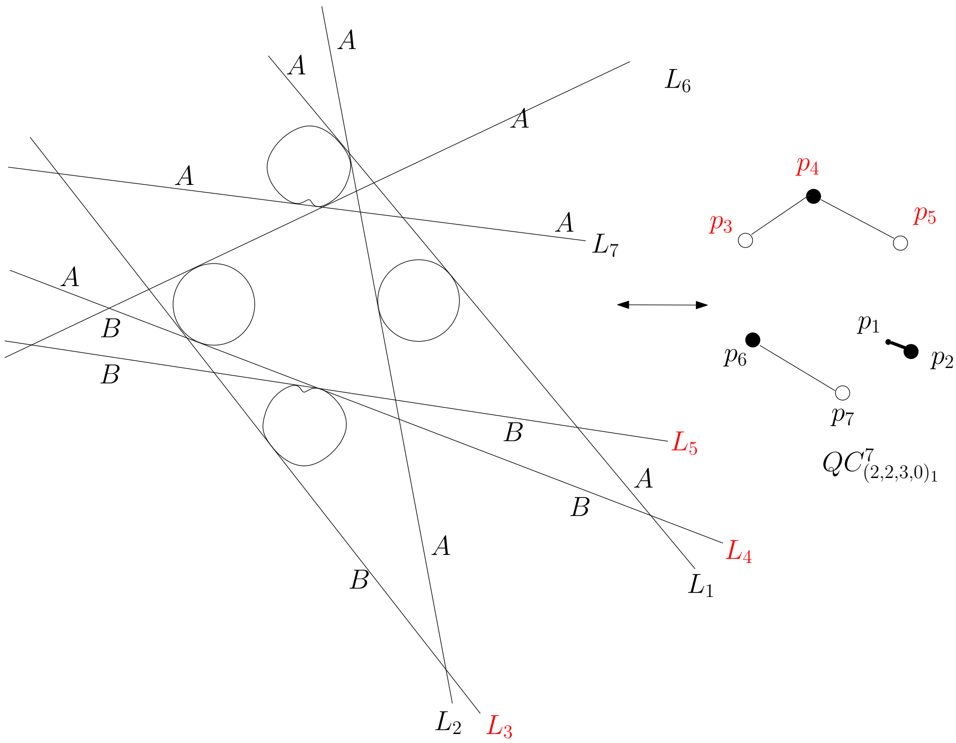

(e) Cr_{345}

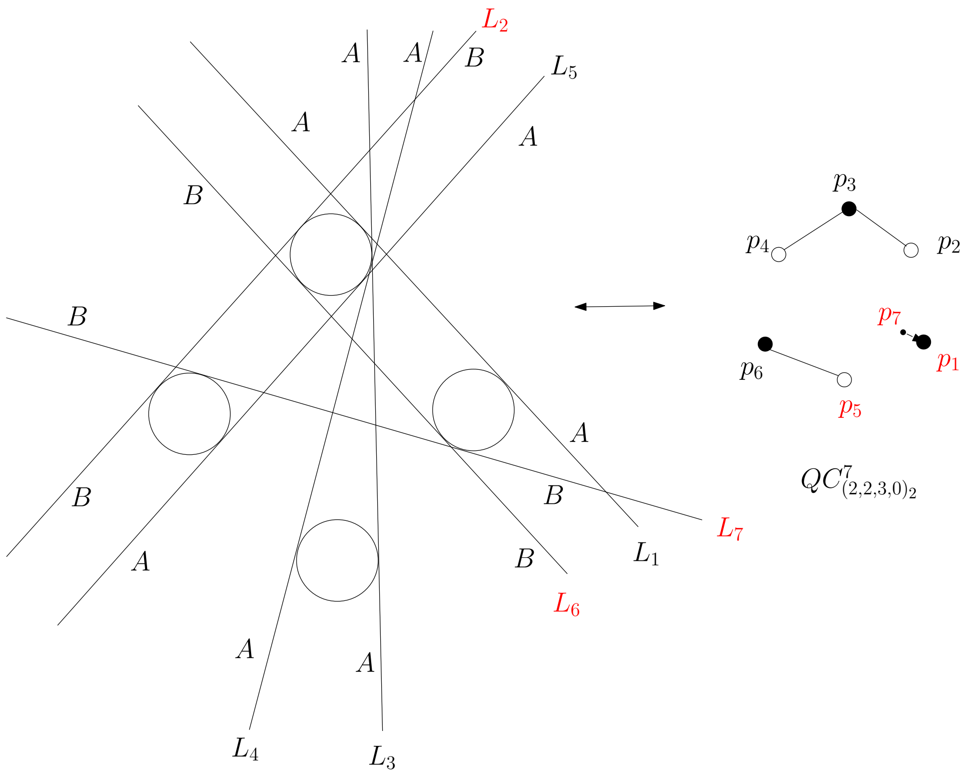

(f) Cr_{267}

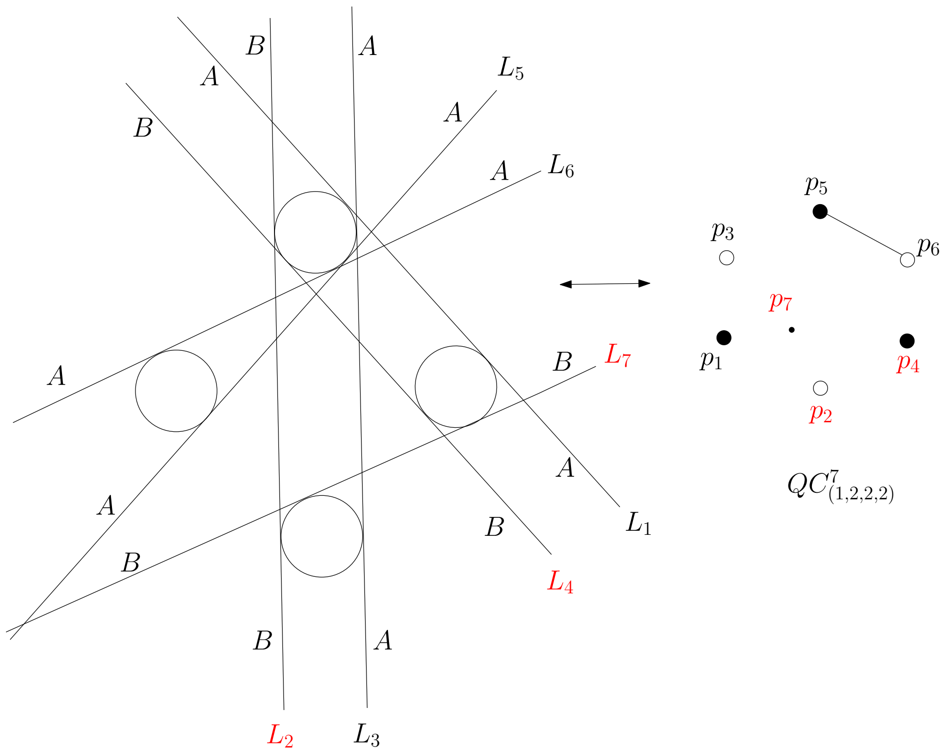

(g) Cr_{247}

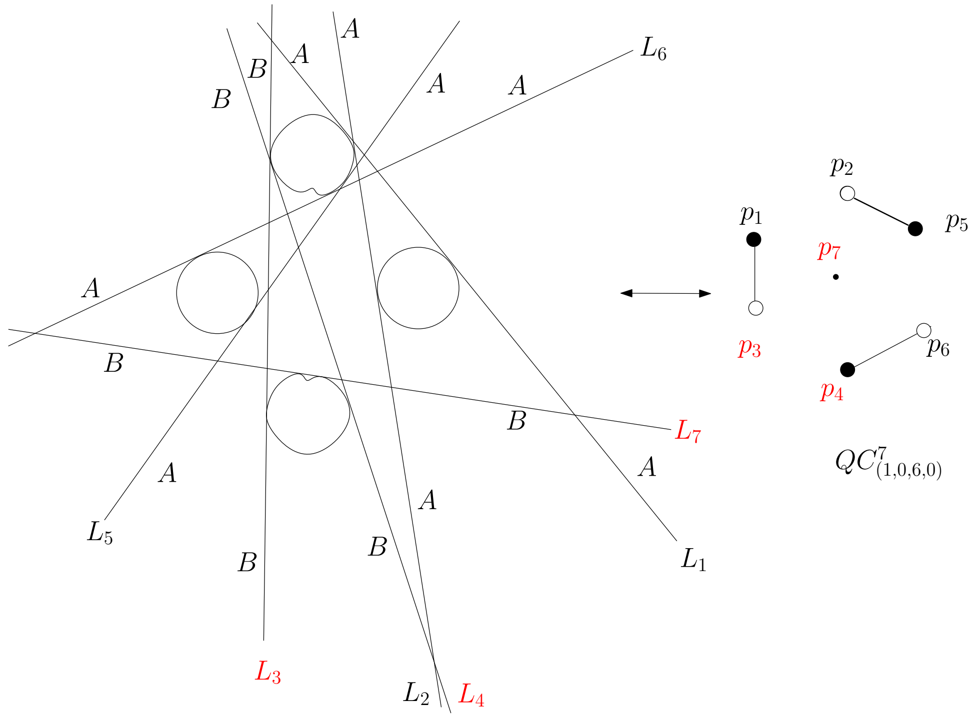

(h) Cr_{347}

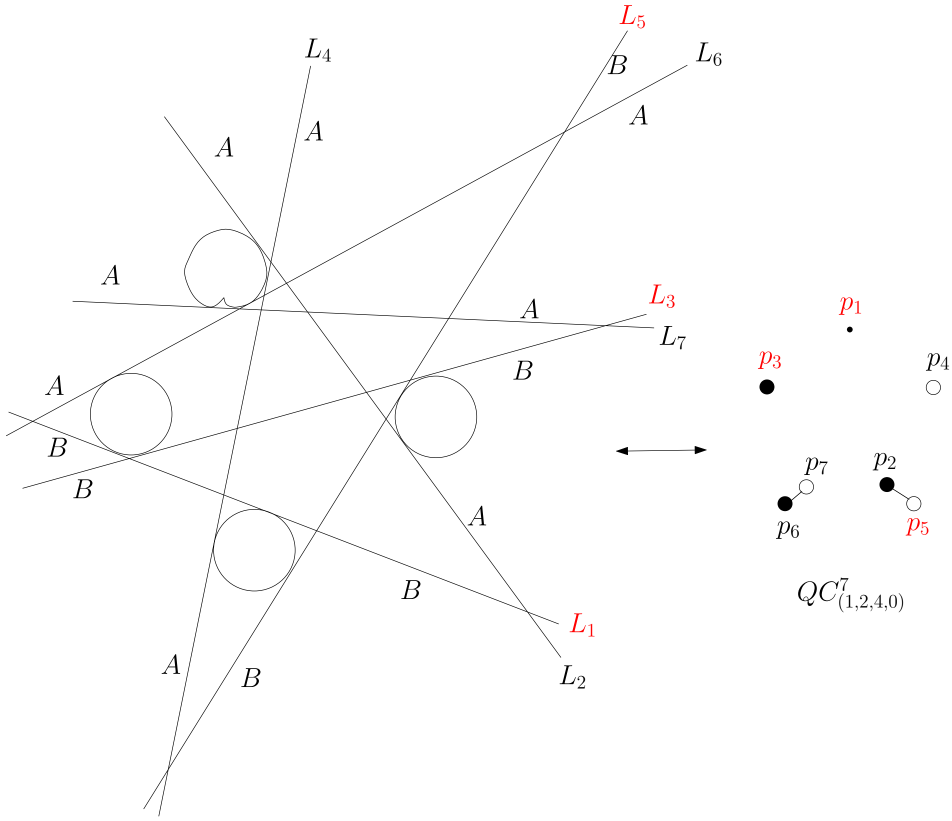

(i) Cr_{135}

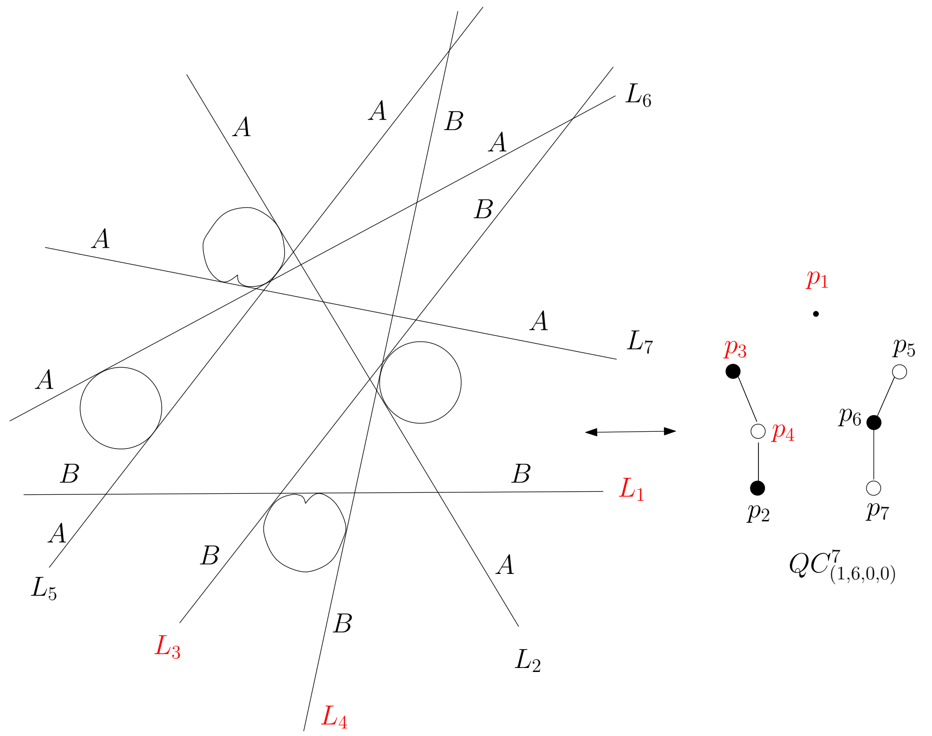

(j) Cr_{134}

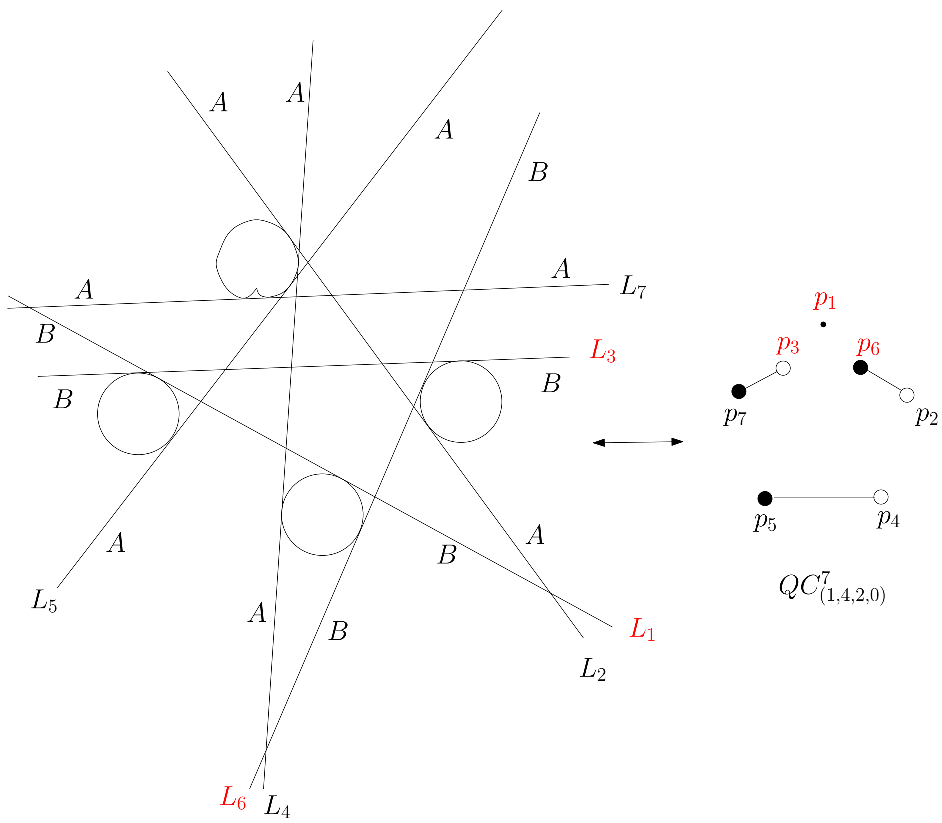

(k) Cr_{136}

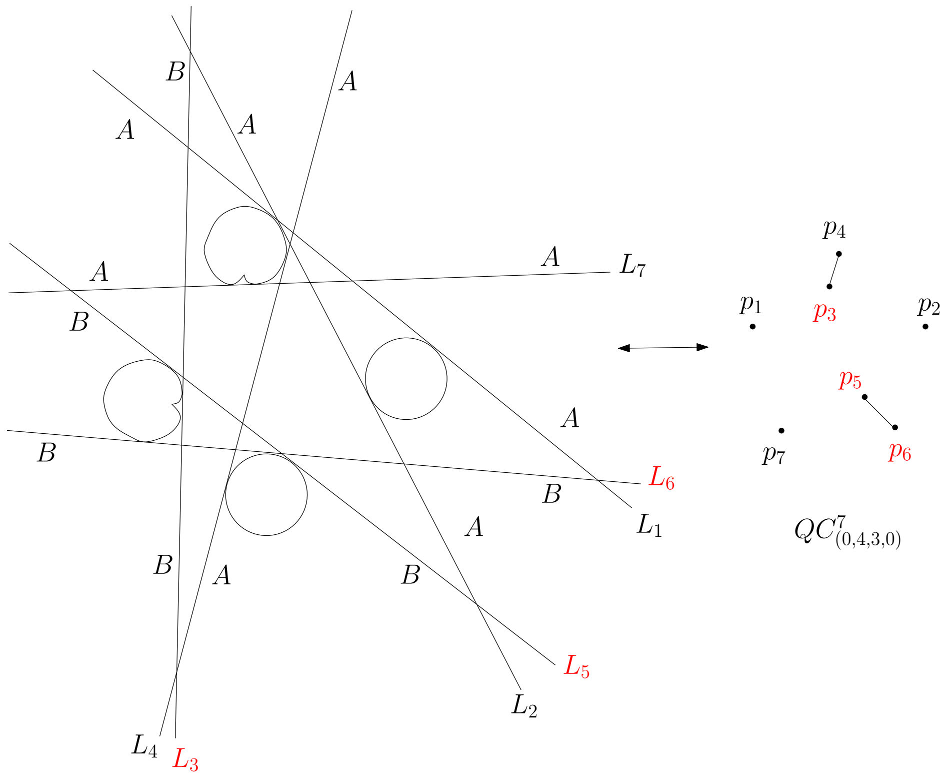

(l) Cr_{356}

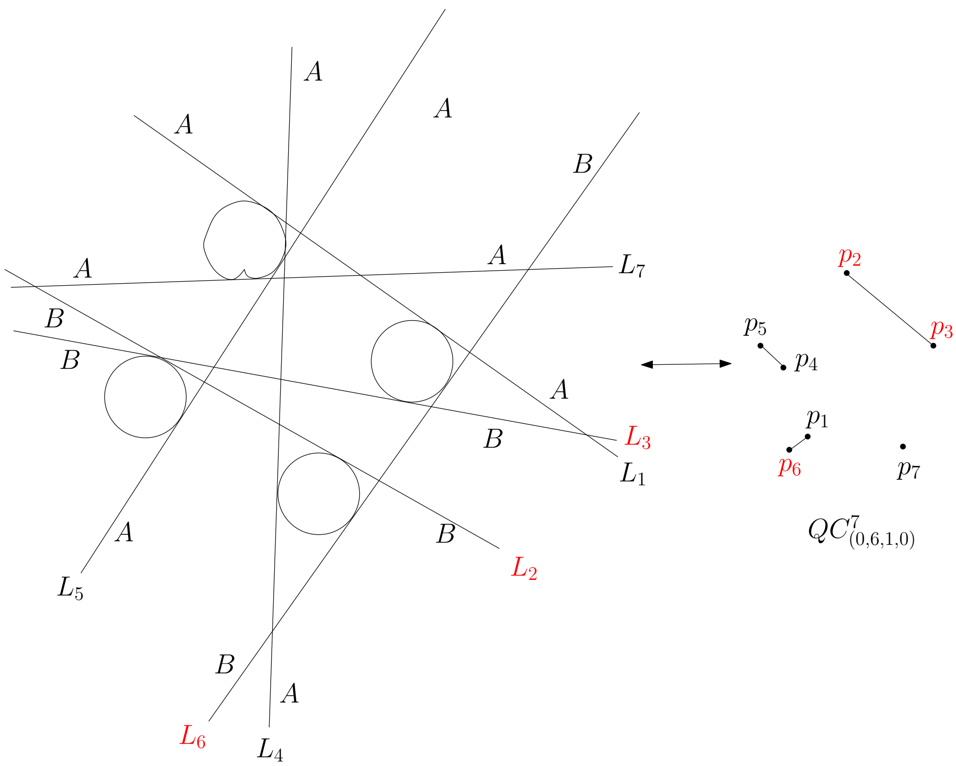

(m) Cr_{236}

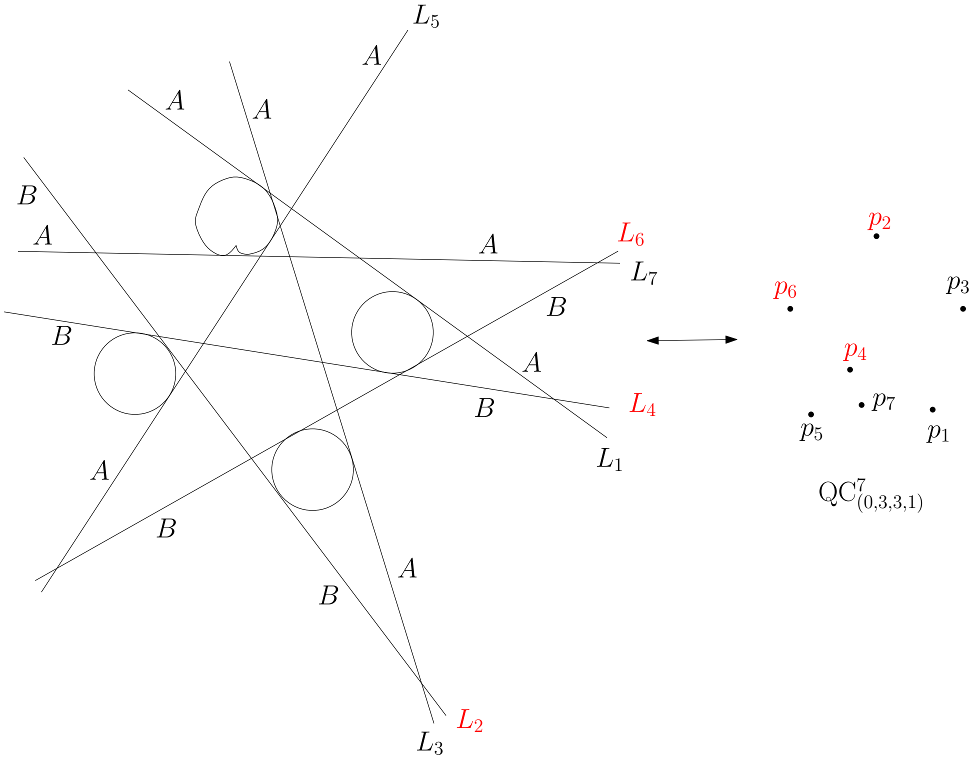

L_5
A
A
A
B
A
L_6
A
L_7
B
B
A
B
L_4
L_1
A
B
A
B
L_2
L_3
p_2
p_6
p_3
p_4
p_7
p_5
p_1
$\mathrm{QC}^7_{(0,3,3,1)}$

(n) Cr_{246}

REFERENCES

[GH] Griffiths P., Harris J. *Principles of Algebraic Geometry*. A Wiley-Interscience Publication, (1938).

[V1] Viro O. Ya. *Topological problems on lines and points of the three-dimensional space*. Doklady AN SSSR, 284 (1985), 1049-1052 (Russian); English translation in Soviet Math. Doklady 32, (1985), 528-531

[V2] Viro O. Ya. *Complex Orientations of Real Algebraic Surfaces*. (2006) ArXiv:math/0611396v1 [math.AG].

[F] Finashin S. *Configurations of Seven Points in* $\mathbb{R}P^3$. Topology and Geometry, Rokhlin Seminar, Lect. Notes Math., 1346 (1988), 501-526.

[VD] Viro O. Ya., Drobotukhina Yu. V. *Configurations of skew-lines*. Algebra i Analiz, 1:4 (1989), 222-246.

[M1] Mazurovskii V. F. *Configurations of six skew lines*. Zap. Nauchn. Semin. LOMI, 167 (1988), 121-134 .

[FK1] Finashin S., Kharlamov V. *Abundance of Real Lines on Real Projective Hypersurface*. International Mathematics Research Notices, (2012) ArXiv:1201.2897 [math.AG].

[FK2] Finashin S., Kharlamov V. *Topology of real cubic fourfolds*. J Topology (2010) 3 (1): 1-28. doi: 10.1112/jtopol/jtp034.

[M3] Mazurovskii V. F. *Configurations of at most* 6 *lines of* $\mathbb{R}P^3$. Lect. Notes Math., 1524 (1992), 354-371.

[T1] Fiedler-Le Touzé S. *Pencils of cubics as tools to solve an interpolation problem*. Applicable Algebra in Engineering, Communication and Computing, (2007), 18, 53-70.

[T2] Fiedler-Le Touzé S. *Pencils of cubics with eight base points lying in convex position in* $\mathbb{R}P^2$. ArXiv:1012.2679 [math.AG].

[T3] Fiedler-Le Touzé S. *Rational pencils of cubics and configurations of six or seven points in* $\mathbb{R}P^2$. ArXiv: 1210.7146 math.AG, Sept. 2013.

[H] Hartshorne R. *Algebraic Geometry*. Graduate Texts in Mathematics 52, Springer-Verlag., (1977).

[VV] Viro J., Viro O. Ya. *Configurations of skew lines*. ArXiv:math/0611374 [math.GT].

[M4] Mazurovskii V.F. *Configurations of at most Six* $(2n-1)$*- Dimensional Subspaces of* $\mathbb{R}P^{4n-1}$. American Mathematical Society (1994), 1051-8037.

[RD] Bacher R., Garber D. *Spindle Configurations of skew lines*. ArXiv:0205245v1 [math.GT].

[HA] Henderson A. *The Twenty-Seven Lines upon the Cubic Surface*. University of Michigan Historical Math Collection (1911).

[D1] Dolgachev Igor V. *Luigi Cremona and Cubic Surfaces*. Incontro di Studio 36, Istituto Lombardo di Scienze e Lettere (2005), 55–70.

[D2] Dolgachev Igor V. *Classical Algebraic Geometry: A Modern View*. Cambridge University Press (2012).

[DO] Dolgachev Igor V., Ortland D. *Points set in Projective spaces and Theta functions*. Société Mathématique de France (1988), 165.

[Se] Segre B. *The Non-Singular Cubic Surfaces*. Oxford Univ. Press, London (1942).

[Man] Manin Yu. I. *Cubic Forms*. Second ed., North-Holland Mathematical Library, North-Holland Publishing Co., Amsterdam, 4, (1986).

[CS] Caporaso L., Sernesi E. *Recovering Plane Curves from their Bitangents*. ArXiv:math/0008239v2 [math.AG].

[N] Nart E. *Bitangents and theta characteristic of plane quartics*.In the book: Corbes de génere 3, 2006, pp. 1-26.

[DZ] Degtyarev A. I., Zvonilov V. I. *Rigid Isotopy Classication of Real Algebraic Curves of Bidegree* $(3,3)$ *on Quadrics*. Mathematical Notes (1999), Vol. 66, No. 6.

[FK3] Finashin S., Kharlamov V. *Topology of real cubic hypersurfaces* (unpublished notes)

[PSV] Plaumann D., Sturnfels B.,and Vinzant C. *Quartic curve and their bitangents*. ArXiv:1008.4104v2 [math.AG].

[DIK] Degtyarev A., Itenberg I., Kharlamov V. *Real Enrique Surfaces*. Lect. Notes Math., 1746 (2000).

CURRICULUM VITAE

PERSONAL INFORMATION

Surname, Name: Zabun, Remziye Arzu

Nationality: Turkish (TC)

Date and Place of Birth: 28.08.1979, Koyulhisar/Sivas

Marital Status: Single

Phone: +905377879654

EDUCATION

Degree	Institution	Year of Graduation
Ph.D.	Middle East Technical University Department of Mathematics	expected September 2014
M.S.	Çukurova University Department of Mathematics	December 2005
B.S.	Çukurova University Department of Mathematics	May 2003
High School	Atatürk Lisesi	1998

PROFESSIONAL EXPERIENCE

Year	Place	Enrollment
2006-till now	Middle East Technical University	Research and Teaching Assistant

PUBLICATIONS

Title	Journal	Year
C^*-embedding and Stone-Cech Compactification	Fen ve Mühendislik Bilimleri Dergisi	2005